

Thesis for the Master's degree in Molecular Biosciences
Main field of study in Molecular Biology

**“Biofilm formation in *Bacillus cereus*
group bacteria – screening of strains
and initial molecular studies”**

Truls Johan Biørnstad

60 study points

Department of Molecular Biosciences
Faculty of mathematics and natural sciences

UNIVERSITY OF OSLO 06/2006



**Biofilm formation in *Bacillus cereus* group
bacteria – screening of strains and initial
molecular studies**

By

Truls Johan Biørnstad

Department of Molecular Biosciences

And

Department of Pharmaceutical Biosciences
School of Pharmacy

University of Oslo

Thesis for the degree of Master of Science in Molecular
Biology, Department of Molecular Biosciences, University of
Oslo, Norway, June 2006

ACKNOWLEDGMENTS

This work was performed at the Department of Pharmaceutical Biosciences, School of Pharmacy, University of Oslo, Norway, from August 2005 to June 2006, under external supervision of Professor Anne-Brit Kolstø and Associate professor Ole Andreas Økstad and under internal supervision of Associate professor William Davies, Department of Molecular Biosciences, University of Oslo.

I would like to thank my supervisors, especially Associate professor Ole Andreas Økstad, for excellent guidance through this degree, for inspiration and for expanding my interest in the microbiological world. Thank you all for an insight into the fascinating world of research and for your input during the entire process. I am also very grateful to Michel Gohar (INRA, France) for cooperation through this project and with the establishment of the screening method.

A big thank you to all the members of the *Bacillus*-group, especially Are, Fredrik, Kim, Nicolas and Lillian, and all the people at the Department of Pharmaceutical Biosciences. You have all helped me in some way to successfully complete my degree through being who you are, sharing good company and scientific input.

I am very grateful for my family and friends, without you I would not have had the time, money or support needed to complete my degree. And finally, I would like to thank my partner, Christine, for being there for me these past these years and for her love and support.

Oslo, June 29th, 2006

Johan Biørnstad

ABSTRACT

In this study we have established a method for screening a collection of strains, from the *Bacillus cereus* group of bacteria, for biofilm formation, including soil isolates, strains from culture collections, reference strains, dairy isolates, and clinical strains from different types of human infections. Certain strains from the *B. cereus* group, which includes the opportunistic human pathogen *B. cereus*, insecticidal *B. thuringiensis*, and the obligate human and animal pathogen *B. anthracis*, are known to have the ability to form biofilm, an attached state in which cells are closely packed and firmly attached to each other and usually a solid surface. In biofilm, microorganisms aggregate and excrete a protective and adhesive matrix of a polymeric, usually carbohydrate-containing, substance. The matrix may provide beneficial functions, such as protection from antibiotics and the immune system during infection and giving bacterial cells the ability to communicate during growth. Biofilm formation is known, at least for certain bacterial pathogens, to contribute to the aetiology of human disease, exemplified by *Pseudomonas aeruginosa* infections in cystic fibrosis patients.

In this study 81 strains have been screened for biofilm formation, resulting in the confirmation of 7 strains, which form biofilm. The ability to form biofilm has not been observed to specifically correlate with strain origin; however strains isolated outside their natural environment (soil and insect intestine) have shown a higher propensity to form biofilm.

We have also initiated gene disruption studies in a candidate regulatory gene, the pleiotropic transcriptional regulator *plcR*, to reveal its possible involvement in biofilm formation in *Bacillus cereus* ATCC 10987, a strain closely related to *B. anthracis*, isolated from spoiled cheese in the 1930s.

ABBREVIATIONS

~	approximately
°C	degrees Celsius
Δ	delta (indication for gene knock-out mutation)
%	percent (age)
ATCC	American Type Culture Collection
bp	base pairs
BSA	Bovine Serum Albumin
DNA	deoxyribonucleic acid
e.g.	<i>exempli gratia</i> (for the sake of example...)
EDTA	ethylenediaminetetraacetic acid
EMBOSS	The European Molecular Biology Open Software Suite
g	gram(s)
h	hour(s)
i.e.	<i>id est</i> (that is...)
kb	kilobasepair(s)
kg	kilogram(s)
l	litre(s)
LB	Luria Bertani
M	molar (mol/litre)
mg	milligram(s)
min	minute(s)
ml	millilitre(s)
mM	millimolar (millimol/litre)
μg	microgram
μl	microlitre
NCBI	National Centre for Biotechnology Information (U.S.A.)
NEB	New England Biolabs (U.S.A.)
ON	over night
PBS	phosphate-buffered saline
PCR	polymerase chain reaction
rpm	revolutions per minute
T _m	melting temperature
Tris	2-Amino-2-(hydroxymethyl)-1,3-propanediol
w/v	weight/volume

CONTENTS

Acknowledgements	iii
Abstract	iv
Abbreviations	v
Contents	vi
List of Figures, Tables and Pictures	x
1. Introduction	1
1.1 The <i>Bacillus</i> genus.....	1
1.2 The <i>Bacillus cereus</i> group of bacteria.....	1
1.2.1 <i>Bacillus anthracis</i>	2
1.2.2 <i>Bacillus thuringensis</i>	4
1.2.3 <i>Bacillus cereus</i>	5
1.2.4 <i>Bacillus mycoides/Bacillus pseudomycoides</i>	7
1.2.5 <i>Bacillus weihenstephanensis</i>	7
1.2.6 <i>Bacillus cereus</i> group and genetics.....	7
1.2.7 Sporulation.....	8
1.3 Biofilm formation.....	10
1.4 <i>Bacillus cereus</i> and biofilm formation.....	14
1.5 Screening for biofilm formation.....	15
1.6 Genetics of biofilm formation.....	16
1.7 The <i>plcR</i> regulon.....	18
1.8 <i>Bacillus cereus</i> ATCC 10987.....	20
1.9 Aim of the study	21

2. Materials and Methods	22
2.1 Materials	22
2.1.1 Bacterial strains.....	22
2.1.2 Reagents.....	23
2.1.2.1 Reagents and chemicals.....	23
2.1.2.2 Enzymes.....	24
2.1.2.3 Solutions.....	25
2.1.2.4 Growth media.....	26
2.2 Methods	27
2.2.1 Growth of bacteria.....	27
2.2.2 Growth curves.....	27
2.2.3 Biofilm screening method.....	28
2.2.4 Crystal violet staining of serial dilution of bacteria....	30
2.3 Genetic methods	30
2.3.1 <i>plcR</i> locus sequence extraction and primer design for gene deletion.....	30
2.3.2 Genomic DNA extraction.....	30
2.3.3 Polymerase chain reaction (PCR).....	31
2.3.4 Agarose Gel Electrophoresis.....	32
2.3.5 Purification.....	33
2.3.6 Plasmids and preparation.....	34
2.3.7 Restriction enzyme digest.....	34
2.3.8 Dephosphorylation of linearized vector 5' ends.....	36
2.3.9 Ligation and Transformation.....	36
2.3.10 Sequencing.....	37

2.3.11 Sequence Analysis.....	38
3. Results.....	39
3.1 Colony morphology of strains screened for biofilm.....	39
3.2 Growth curves.....	41
3.2.1 Standard growth curve for reference strains.....	41
3.2.2 Standard growth curve for selected biofilm strains.....	43
3.2.3 Crystal violet staining of serial dilution of bacteria.....	44
3.3 Biofilm screening.....	46
3.3.1 Establishing the biofilm screening method.....	46
3.3.2 Optimization of biofilm screening method.....	49
3.3.3 Screening for biofilm formation in <i>Bacillus cereus</i> group bacteria.....	54
3.3.4 Biofilm positive strain confirmation.....	68
3.3 Construction of a <i>plcR</i> knock-out of <i>Bacillus cereus</i> ATCC 10987..	72
3.3.1 Knock-out construct cloning and antibiotic resistance markers.....	73
3.3.2 <i>plcR</i> -locus sequence extraction and primer design...	74
3.3.3 Isolation of template DNA for PCR amplification....	76
3.3.4 PCR of <i>plcR</i> flanking regions and resistance cassettes.....	78
3.3.5 Isolation and verification of plasmid.....	77
3.3.6 Cloning of <i>plcR</i> upstream into pUC19.....	79
3.3.7 Cloning of <i>plcR</i> downstream into pUC19_ <i>plcR</i> upstream...	81
3.3.8 Cloning antibiotic resistance cassette into pUC19_ <i>plcR</i> upstream_ <i>plcR</i> downstream.....	83
3.4 Sequence analysis.....	86

3.4.1 Sequence analysis of resistance cassettes.....	86
3.4.2 Sequence analysis of constructs made for <i>plcR</i> knock-out ...	87
4. Discussion and Conclusions.....	90
4.1 The biofilm conundrum.....	90
4.2 Bacterial growth during biofilm screening.....	90
4.2.1 Colony morphology.....	90
4.2.2 Bacterial growth over time.....	91
4.3 Biofilm screening.....	92
4.3.1 Testing and optimisation of biofilm screening system....	92
4.3.2 Crystal violet staining – technical consideration.....	93
4.3.3 Biofilm screening.....	94
4.4 Knock-out construction of <i>plcR</i>.....	97
4.4.1 Biofilm formation and genetics.....	97
4.4.2 Cloning of <i>plcR</i> flanking regions.....	99
4.4.3 Cloning of resistance cassettes.....	99
4.5 Further studies.....	99
5. References.....	101
6. Appendix.....	115
6.1 Biofilm formation.....	115
6.2 Construction of a <i>plcR</i> knock-out of <i>Bacillus cereus</i> ATCC 10987..	129
6.2.1 pUC19 cloning vector.....	129
6.2.2 Sequence of resistance cassettes.....	130
6.2.3 Sequence of <i>plcR</i> knock-out constructs.....	131

List of Figures, Tables and Pictures

Figure 1.1 Hypothetical model of life cycles of <i>B. cereus</i> group bacteria.....	3
Figure 1.2 Pathogenic life cycle of <i>B. anthracis</i> , <i>B. cereus</i> and <i>B. thuringensis</i>	6
Figure 1.3 Model of biofilm development.....	11
Figure 1.4 Genome map of <i>B. cereus</i> ATCC 10987.....	21
Figure 2.1 Structure of crystal violet.....	29
Figure 2.2 Absorbance pattern of crystal violet.....	29
Figure 3.1 Standard growth curve for reference strains.....	42
Figure 3.2 Growth curve for selected strains used in biofilm screening.....	43
Figure 3.3 Crystal violet staining of bacterial serial dilution.....	45
Figure 3.4 Biofilm formation, as measured by crystal violet absorbance, of reference strains, after 24 hours incubation.....	47
Figure 3.5 Biofilm formation, as measured by crystal violet absorbance, of reference strains, after 48 hours incubation.....	48
Figure 3.6 Biofilm formation, as measured by crystal violet absorbance, of reference strains, after 72 hours incubation.....	48
Figure 3.7 Biofilm formations as measured by crystal violet absorbance after 24 hours of incubation, background signal deducted.....	55
Figure 3.8 Biofilm formations as measured by crystal violet absorbance after 48 hours of incubation, background signal deducted.....	56
Figure 3.9 Biofilm formations as measured by crystal violet absorbance after 72 hours of incubation, background signal deducted.....	56
Figure 3.10 Biofilm formations as measured by crystal violet absorbance after 24 hours of incubation, background signal deducted.....	57
Figure 3.11 Biofilm formations as measured by crystal violet absorbance after 48 hours of incubation, background signal deducted.....	57
Figure 3.12 Biofilm formations as measured by crystal violet absorbance after 72 hours of incubation, background signal deducted.....	58

Figure 3.13 Biofilm formations as measured by crystal violet absorbance after 24 hours of incubation, background signal deducted.....	58
Figure 3.14 Biofilm formations as measured by crystal violet absorbance after 48 hours of incubation, background signal deducted.....	59
Figure 3.15 Biofilm formations as measured by crystal violet absorbance after 72 hours of incubation, background signal deducted.....	59
Figure 3.16 Biofilm formations as measured by crystal violet absorbance after 24 hours of incubation, background signal deducted.....	60
Figure 3.17 Biofilm formations as measured by crystal violet absorbance after 48 hours of incubation, background signal deducted.....	60
Figure 3.18 Biofilm formations as measured by crystal violet absorbance after 72 hours of incubation, background signal deducted.....	61
Figure 3.19 Biofilm formations as measured by crystal violet absorbance after 24 hours of incubation, background signal deducted.....	61
Figure 3.20 Biofilm formations as measured by crystal violet absorbance after 48 hours of incubation, background signal deducted.....	62
Figure 3.21 Biofilm formations as measured by crystal violet absorbance after 72 hours of incubation, background signal deducted.....	62
Figure 3.22 Biofilm formations as measured by crystal violet absorbance after 24 hours of incubation, background signal deducted.....	63
Figure 3.23 Biofilm formations as measured by crystal violet absorbance after 48 hours of incubation, background signal deducted.....	63
Figure 3.24 Biofilm formations as measured by crystal violet absorbance after 72 hours of incubation, background signal deducted.....	64
Figure 3.25 Biofilm formations as measured by crystal violet absorbance after 24 hours of incubation, background signal deducted.....	64
Figure 3.26 Biofilm formations as measured by crystal violet absorbance after 48 hours of incubation, background signal deducted.....	65
Figure 3.27 Biofilm formations as measured by crystal violet absorbance after 72 hours of incubation, background signal deducted.....	65

Figure 3.28 Biofilm formations as measured by crystal violet absorbance after 24 hours of incubation, background signal deducted.....	66
Figure 3.29 Biofilm formations as measured by crystal violet absorbance after 48 hours of incubation, background signal deducted.....	66
Figure 3.30 Biofilm formations as measured by crystal violet absorbance after 72 hours of incubation, background signal deducted.....	67
Figure 3.31 Biofilm formations as measured by crystal violet absorbance after 24 hours of incubation, background signal deducted.....	69
Figure 3.32 Biofilm formations as measured by crystal violet absorbance after 48 hours of incubation, background signal deducted.....	69
Figure 3.33 Biofilm formations as measured by crystal violet absorbance after 72 hours of incubation, background signal deducted.....	70
Figure 3.34 Method and way of cloning knock-out construct.....	73
Figure 3.35 Multiple cloning cite of pUC19, showing selected restriction sites.....	74
Figure 3.36 pUC19 vector, showing MCS, replication site, resistance cassette and <i>lacZ</i> gene...	76
Figure 3.37 Placement of primers according to upstream and downstream region of <i>plcR</i>	78
Figure 3.38 Cloning of <i>plcR</i> upstream into pUC19.....	80
Figure 3.39 Cloning of the downstream region of <i>plcR</i> cloned into pUC19_plcRupstream.....	81
Figure 3.40 Cloning of resistance cassettes (<i>spc/ery</i>) into pUC19_plcRupstream _plcRdownstream.....	84
Figure 3.41 pUC19_plcRupstream_plcRdownstream construct aligned with known <i>plcR</i> upstream sequence, using Align.....	87
Figure 3.42 pUC19_plcRupstream_plcRdownstream construct aligned with known <i>plcR</i> downstream sequence, using Align.....	88
Figure 3.43 pUC19_plcRupstream_plcRdownstream_spectinomycin construct aligned with known spectinomycin cassette sequence, using Align.....	88
Figure 4.1 Multilocus Enzyme Electrophoresis (MLEE) phylogenetic tree.....	95

Figure 6.1 Biofilm formation as measured by crystal violet absorbance after 24 hours of incubation (background signal from negative control not deducted), with standard deviation from 16 parallels included...	115
Figure 6.2 Biofilm formation as measured by crystal violet absorbance after 48 hours of incubation (background signal from negative control not deducted), with standard deviation from 16 parallels included...	116
Figure 6.3 Biofilm formation as measured by crystal violet absorbance after 72 hours of incubation (background signal from negative control not deducted), with standard deviation from 16 parallels included...	116
Figure 6.4 Biofilm formation as measured by crystal violet absorbance after 24 hours of incubation (background signal from negative control not deducted), with standard deviation from 16 parallels included...	117
Figure 6.5 Biofilm formation as measured by crystal violet absorbance after 48 hours of incubation (background signal from negative control not deducted), with standard deviation from 16 parallels included...	117
Figure 6.6 Biofilm formation as measured by crystal violet absorbance after 72 hours of incubation (background signal from negative control not deducted), with standard deviation from 16 parallels included...	118
Figure 6.7 Biofilm formation as measured by crystal violet absorbance after 24 hours of incubation (background signal from negative control not deducted), with standard deviation from 16 parallels included...	118
Figure 6.8 Biofilm formation as measured by crystal violet absorbance after 48 hours of incubation (background signal from negative control not deducted), with standard deviation from 16 parallels included...	119
Figure 6.9 Biofilm formation as measured by crystal violet absorbance after 72 hours of incubation (background signal from negative control not deducted), with standard deviation from 16 parallels included...	119
Figure 6.10 Biofilm formation as measured by crystal violet absorbance after 24 hours of incubation (background signal from negative control not deducted), with standard deviation from 16 parallels included.	120
Figure 6.11 Biofilm formation as measured by crystal violet absorbance after 48 hours of incubation (background signal from negative control not deducted), with standard deviation from 16 parallels included.	120
Figure 6.12 Biofilm formation as measured by crystal violet absorbance after 72 hours of incubation (background signal from negative control not deducted), with standard deviation from 16 parallels included.	121
Figure 6.13 Biofilm formation as measured by crystal violet absorbance after 24 hours of incubation (background signal from negative control not deducted), with standard deviation from 16 parallels included.	121
Figure 6.14 Biofilm formation as measured by crystal violet absorbance after 48 hours of incubation (background signal from negative control not deducted), with standard deviation from 16 parallels included.	122
Figure 6.15 Biofilm formation as measured by crystal violet absorbance after 72 hours of incubation (background signal from negative control not deducted), with standard deviation from 16 parallels included.	122

Figure 6.16 Biofilm formation as measured by crystal violet absorbance after 24 hours of incubation (background signal from negative control not deducted), with standard deviation from 16 parallels included.	123
Figure 6.17 Biofilm formation as measured by crystal violet absorbance after 48 hours of incubation (background signal from negative control not deducted), with standard deviation from 16 parallels included.	123
Figure 6.18 Biofilm formation as measured by crystal violet absorbance after 72 hours of incubation (background signal from negative control not deducted), with standard deviation from 16 parallels included.	124
Figure 6.19 Biofilm formation as measured by crystal violet absorbance after 24 hours of incubation (background signal from negative control not deducted), with standard deviation from 16 parallels included.	124
Figure 6.20 Biofilm formation as measured by crystal violet absorbance after 48 hours of incubation (background signal from negative control not deducted), with standard deviation from 16 parallels included.	125
Figure 6.21 Biofilm formation as measured by crystal violet absorbance after 72 hours of incubation (background signal from negative control not deducted), with standard deviation from 16 parallels included.	125
Figure 6.22 Biofilm formation as measured by crystal violet absorbance after 24 hours of incubation (background signal from negative control not deducted), with standard deviation from 16 parallels included.	126
Figure 6.23 Biofilm formation as measured by crystal violet absorbance after 48 hours of incubation (background signal from negative control not deducted), with standard deviation from 16 parallels included.	126
Figure 6.24 Biofilm formation as measured by crystal violet absorbance after 72 hours of incubation (background signal from negative control not deducted), with standard deviation from 16 parallels included.	127
Figure 6.25 Biofilm formation as measured by crystal violet absorbance after 24 hours of incubation (background signal from negative control not deducted), with standard deviation from 16 parallels included.	127
Figure 6.26 Biofilm formation as measured by crystal violet absorbance after 48 hours of incubation (background signal from negative control not deducted), with standard deviation from 16 parallels included.	128
Figure 6.27 Biofilm formation as measured by crystal violet absorbance after 72 hours of incubation (background signal from negative control not deducted), with standard deviation from 16 parallels included.	128
Figure 6.28 pUC19 cloning vector.....	129
Figure 6.29 Sequence of spectinomycin-resistance cassette.....	130
Figure 6.30 Sequence of erythromycin-resistance cassette.....	130
Figure 6.31 Sequence of pUC19_plcRupstream clone insert.....	131
Figure 6.32 Sequence of pUC19_plcRupstream_plcRdownstream clone insert.....	131
Figure 6.33 Sequence of pUC19_plcRupstream_plcRdownstream_spectinomycin clone insert.....	131

Table 2.1 Bacterial strains used for biofilm screening.....	22
Table 2.2 Bacterial strains used for making genetic construct.....	23
Table 2.3 Double digest recommendations for restriction enzymes <i>KpnI</i> and <i>SacI</i>	35
Table 2.4 Double digest recommendations for restriction enzymes <i>BamHI</i> and <i>Sa I</i>	35
Table 2.5 Double digest recommendations for restriction enzymes <i>EcoRI</i> and <i>HindIII</i>	35
Table 3.1 Biofilm formation for the 81 tested strains.....	71
Table 3.2 Primers used in knock-out construction.....	75
Picture 2.1 Lambda DNA-BstE II Digest.....	33
Picture 3.1 Colony morphology of <i>B. cereus</i> AH 75, AH 183, AH 226, AH 405, AH 604 and AH 815.....	40
Picture 3.2 Colony morphology of <i>B. cereus</i> AH 884, AH 1248 and <i>B. thuringensis</i> AH 1031...	41
Picture 3.3 Falcon, PVC, round-bottom, 96-well microtiter plate.....	50
Picture 3.4 Microtiter plate containing 125 µl culture.....	53
Picture 3.5 Biofilm ring formation after staining with crystal violet.....	53
Picture 3.6 Wells after addition of acetone/ethanol.....	54
Picture 3.7 Biofilm formation for biofilm-positive and biofilm-negative strains.....	68
Picture 3.8 Solubilised crystal violet for biofilm-positive and biofilm-negative strains.....	68
Picture 3.9 Agarose gel electrophoresis of extracted DNA from <i>B. cereus</i> ATCC 10987.....	77
Picture 3.10 Agarose gel electrophoresis of linearized pUC19 plasmids.....	77
Picture 3.11 Agarose gel electrophoresis of PCR products of spectinomycin and erythromycin resistance cassette.....	79
Picture 3.12 Agarose gel electrophoresis of PCR products of upstream and downstream <i>plcR</i>	79
Picture 3.13 Agarose gel electrophoresis of pUC19_plcRupstream after cloning.....	81
Picture 3.14 Agarose gel electrophoresis of restriction enzyme digestion by <i>BamHI</i> and <i>SalI</i> of pUC19_plcRupstream_plcRdownstream and pAT113_plcRupstream_plcRdownstream constructs...	83
Picture 3.15 Agarose gel electrophoresis of restriction enzyme digestion of pUC19_plcRupstream_plcRdownstream_spectinomycin construct with <i>SmaI</i>	84
Picture 3.16 Agarose gel electrophoresis of restriction enzyme digestion of pUC19_plcRupstream_plcRdownstream_spectinomycin with <i>EcoRI</i> and <i>HindIII</i>	85

Picture 3.17 Agarose gel electrophoresis of restriction enzyme digestion of

pUC19_plcRupstream_plcRdownstream_spectinomycin with *EcoRI* and *HindIII*.....

86

1 INTRODUCTION

1. Introduction

1.1 The *Bacillus* genus

The *Bacillus* genus consist of gram-positive, facultative anaerobic, spore-forming, rod shaped, motile bacteria commonly found in soil and insect intestine, but also in dairy product, food and some species may cause infection in humans and animals. The vegetative cells range from 0.5 by 1.2 to 2.5 by 10 μm in diameter (Turnbull *et al.*, 1991). The genus is highly heterogeneous, certain species are psychrophilic or thermophilic, but optimal growth is seen in the temperature range between 25°C and 37°C. The G+C content of the DNA can vary from 32% to 69% between different species, and most strains are catalase positive, possess peritrichous flagella, and sporulate in air (Turnbull *et al.*, 1991; Turnbull *et al.*, 1990).

1.2 The *Bacillus cereus* group of bacteria

The *Bacillus cereus* group of bacteria, a cluster within the *Bacillus* genus, comprises six recognized species, namely *Bacillus anthracis*, *Bacillus cereus*, *Bacillus mycoides*, *Bacillus pseudomycoides*, *Bacillus thuringiensis* and *Bacillus weihenstephanensis* (Gordon *et al.*, 1973; Lechner *et al.*, 1998; Priest *et al.*, 1988; Turnbull *et al.*, 1991). A close genetic relationship has been observed between all members and it is therefore suggested that the entire group represents a single species (Helgason *et al.*, 2000; Patra *et al.*, 2002). DNA sequence variations in the 16S-23S internally transcribed spacers (Daffonchio *et al.*, 2000), Multilocus Enzyme Electrophoresis (MLEE) (Helgason *et al.*, 2000) and sequence analysis of house-keeping genes (Helgason *et al.*, 2002) suggest that *B. anthracis*, *B. cereus sensu stricto* and *B. thuringiensis* are members of a single species, *B. cereus sensu lato*. Characteristics

have been suggested to allow the differentiation and identification of the *B. cereus* group members (Drobniowski *et al.*, 1993; Granum *et al.*, 2001) and the key diagnostic feature used for identification of *B. cereus* strains, until now, has been their ability to provoke haemolysis and to hydrolyze lecithin, but an inability to ferment mannitol. This media-based-identification method is still the most commonly used method for identification of *B. cereus* (Holbrook *et al.*, 1980).

The *B. cereus* group bacteria, compared to other *Bacilli* group bacteria, are a group of bacteria, which carry a high amount of pathogenicity genes. The genes encoding for the pathogenicity in *B. anthracis* against mammals (including humans) and the pathogenicity in *B. thuringensis* against insects are coded for and present on plasmids. The presences of these plasmids are used as a method for differentiation of species within the *B. cereus* group. *B. cereus* is also seen to carry large plasmids, but their involvement in pathogenicity is still unclear. Emetic *B. cereus* does, however, carry emetic toxin genes on large plasmids, indicating that the plasmids do in all cases both define the sub species of the *B. cereus* group of bacteria and contribute to the pathogenicity of the strain.

1.2.1 *Bacillus anthracis*

Bacillus anthracis is the causative agent of anthrax, which is primarily a disease in mammals, including man (Mock and Fouet, 2001). Anthrax had been linked to endemic soil environments long before *B. anthracis* was identified as the causative agent (Rayer *et al.*, 1850; Davaine *et al.*, 1863). Virulence of *B. anthracis* is based on the presence of the two virulence plasmids, pXO1 (181, 7 kbp) and pXO2 (94, 8 kbp), present in all virulent strains. The plasmid pXO1 encodes three toxic factors: the protective antigen (PA), the lethal factor (LF) and the oedema factor (EF) (Bhatnagar and Batra, 2001), while the pXO2 plasmid encodes a poly-D-glutamic acid capsule enabling the bacterium to resist complement binding

and phagocytosis after initial phagocytosis of spores and germination. Both plasmids have been sequenced and functional studies are currently under way (Okinaka *et al.*, 1999 a and b). Models, available, of *B. anthracis* ecology, rely on its pathogenicity, i.e. how the spores are ingested by herbivores, how the animals become infected and how the bacteria proliferate in the lymphoid glands, expressing the exotoxins, which ultimately leads to the death of the animal (Figure 1.1). Once the animal is dead the bacteria will again form spores, a process directly linked to depletion of nutrients and presence of oxygen, and have an unknown fate in the environment (Jensen *et al.*, 2003).

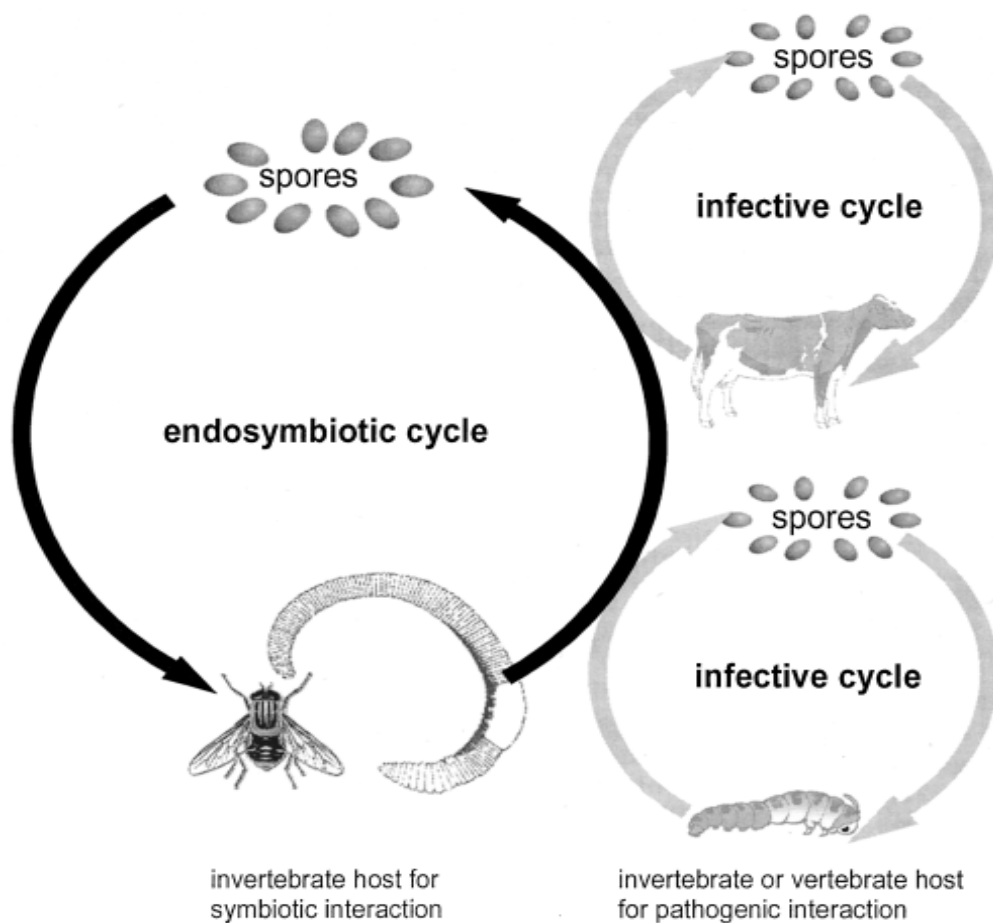


Figure 1.1: Hypothetical model in which the members of the *B. cereus* group experience two life cycles: one type (left figure) in which the bacteria live in a symbiotic relation with their invertebrate host(s) and another (right figure), more infrequent life cycle, in which the bacteria can multiply rapidly in another infected insect host or a mammal, from Jensen *et al.*, 2003.

1.2.2 *Bacillus thuringiensis*

Bacillus thuringiensis is generally regarded as an insect pathogen, because of its ability to produce large crystal protein inclusions (δ -endotoxins) during sporulation. These δ -endotoxins are seen to be encoded mainly on the plasmids as so-called *cry*-genes (Kronstad *et al.*, 1983; González and Carlton, 1984), where they are actively synthesised. As much as 20% of the proteins synthesised during sporulation are products of the *cry*-genes and result in depositions as intracellular, crystalline inclusions. Upon completion of sporulation and mother cell lyses, the spore and inclusions are released, and the inclusions and spores are able to be ingested by insects, resulting in the protoxin solubilising in the alkaline midgut and there be converted to toxins (Aronson, 2002). The toxin will be able to bind to the mid-gut epithelial cells, creating pores in the cell membrane. As a result, the gut is rapidly immobilized and the epithelial cells lyse. This is considered the only feature that can distinguish *B. thuringiensis* from *B. cereus* (Baumann *et al.*, 1984). These inclusions, which constitute up to 25% of the dry weight of the sporulated cells (Agaïsse and Lerecluse, 1995), are responsible for the biopesticide activity of the bacterium and its target specificity (van Rie *et al.*, 1990). The insecticidal spectrum varies within the 83 different serotypes reported (Lecadet *et al.*, 1999), and affects insects primarily from the orders *Lepidoptera*, *Diptera* and *Coleoptera*. There are also reports of *B. thuringiensis* isolates active against mosquitoes, which are vectors for diseases such as malaria and yellow fever (Orduz *et al.*, 1995). According to Martin and Travers (1989), *B. thuringiensis* is a ubiquitous soil microorganism, but it is also found in environmental niches, including phylloplane and insects. The bacteria have until now also been found in water mills, in corn crops and in mosquito breeding habitats (Vankova and Purrini, 1979; Porcar and Caballero, 2000; Damgaard, 2000). Other findings have shown that the ecological niches occupied by *B. thuringiensis* are several; i) *B. thuringiensis* does not originate from soil, but is deposited there by insects (Glare and O'Callaghan, 2000); ii) *B.*

thuringensis may grow in soil only when the nutrient conditions are correct (Saleh et al., 1970); iii) *B. thuringensis* occupies the same niche as *B. cereus* and iv) vegetative *B. thuringensis* proliferates in the gut of the earthworm, leather jacket larvae and in plant rhizospheres (Hendriksen and Hansen, 2002). These different possibilities are not mutually exclusive. It is conceivable that *B. thuringensis* is a natural inhabitant of the intestinal system of certain insects, with or without provoking disease and eventually death (Figure 1.1). Therefore, the bacterium is able to be released in the soil and subsequently to proliferate when conditions are naturally favourable. *B. thuringensis* is speculated to be a natural inhabitant of the digestion system of many invertebrates (Hansen and Salamiou, 2000) and can sporulate when nutrients become limited.

1.2.3 *Bacillus cereus*

Bacillus cereus is more or less ubiquitous in nature and an opportunistic pathogen. *B. cereus* was first recognized to be the causative agent of food-borne illness in the 1950's. The diarrhoeal type of illness was described following the consumption of highly contaminated vanilla sauce; Hauge isolated *B. cereus* from the vanilla sauce and consumed it. After 16 hours this resulted in abdominal pain, nausea and watery diarrhoea (Hauge, 1955). This led to the linking of *B. cereus* to diarrhoeal diseases and to a greater understanding of this group of bacteria. In recent years *B. cereus* has been recognized as a causative agent of gastrointestinal and nongastrointestinal diseases (Ehling-Sculz *et al.*, 2004 and references therein). Two types of gastrointestinal diseases caused by *B. cereus* can be distinguished: emetic and diarrhoeal. The diarrhoeal type, caused by heat-labile enterotoxins, is mainly associated with meat products, vegetables and milk products, whereas emetic outbreaks, associated with a smaller heat-stable peptide toxin, are mainly linked to carbohydrate rich sources, such as rice, noodles and pasta (Shinagawa *et al.*, 1990; Kramer *et al.*, 1989). The emetic syndrome is mainly

characterized by vomiting 0.5 – 6 hours after ingestion of the contaminated food, while in the diarrhoeal syndrome symptoms appear 8 – 16 hours after ingestion and include abdominal pain and diarrhoea. Both types of food-borne illness are relatively mild and usually do not last more than 24 hours. Nevertheless, more severe cases have occasionally been reported and deaths have been registered due to ingestion of food contaminated with a high amount of emetic toxin (Lund *et al.*, 2000; Mahler *et al.*, 1997). *B. cereus* has also been shown to be responsible for wound and eye infections, systemic infections and may be linked to periodontitis (Beecher *et al.*, 2000; Drobniowski *et al.*, 1993; Helgason *et al.*, 2000), and recently *B. cereus* has been identified as the cause of a series of serious or even life-threatening infections in neutropenic and immunosuppressed patients and premature neonates (Arnaout *et al.*, 1999; Hilliard *et al.*, 2003). Its natural niche is probably the gut micro flora of invertebrates, but colonisation of mosquito larvae and various soil-dwelling pests have also been observed (Feinberg *et al.*, 1999; Luxananil *et al.*, 2001; Wenzel *et al.*, 2002).

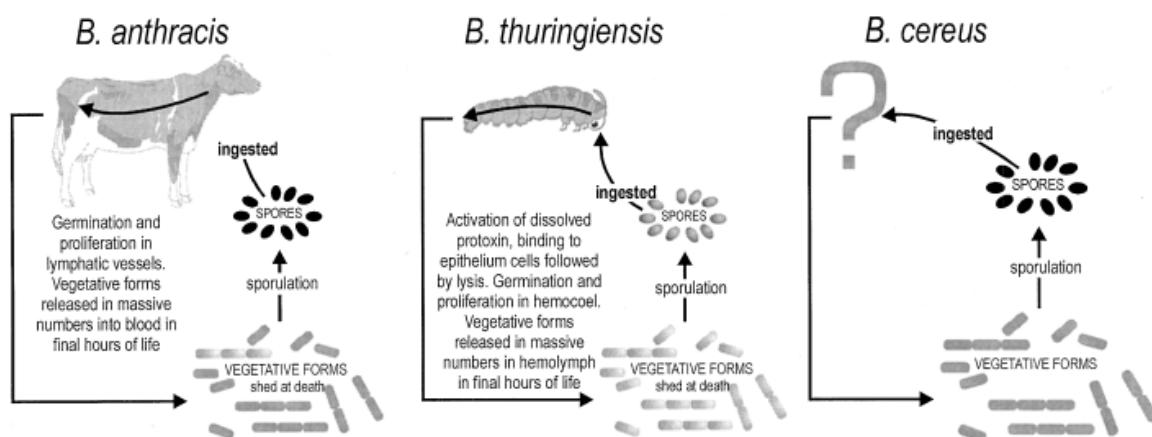


Figure 1.2: An illustration of the known pathogenic life cycles of *B. anthracis* and *B. thuringiensis*. Although a human pathogen, *B. cereus* has not been shown to enter a pathogenic life cycle similar to those of *B. anthracis* and *B. thuringiensis*, from Jensen *et al.*, 2003.

1.2.4 *Bacillus mycoides/Bacillus pseudomycoides*

Bacillus mycoides is distinguished from other members of the *Bacillus cereus* group by its rhizoid colony shape, made by curving filaments of bacterial cells and its lack of motility (Priest, 1993). *Bacillus pseudomycoides* is very similar to *B. mycoides*, however it does not have the long filaments of bacterial cells, hence the name *pseud.* *B. pseudomycoides* is distinguished from *B. mycoides* and *B. cereus* by difference in cell membrane fatty acid contents (Nakamura, 1998).

1.2.5 *Bacillus weihenstephanensis*

Bacillus weihenstephanensis is capable of growth below 7°C and shows characteristic differences in specific cold-shock-genes compared to *B. cereus* (Lechner *et al.*, 1998). However, there does also exist psychrotolerant strains of the *B. cereus* group, which not necessary are *B. weihenstephanensis* (Stenfors & Granum, 2001). It is not known if *B. weihenstephanensis* strains are capable of causing food poisoning as is the case with *B. cereus*, but the genetic composition of essential pathogenicity factors are seen to be present and thought to be expressed (Stenfors *et al.*, 2002), such as non-haemolytic enterotoxin Nhe.

1.2.6 *Bacillus cereus* group and genetics

Like many other bacteria, research on the *Bacillus cereus* group has benefited from the genomic revolution that started in 1995 with the publication of the first microbial genome sequence, that of *Haemophilus influenzae* (Fleischmann *et al.*, 1995). This has allowed for further research into the genetics, proteomics and transcriptomics of this group of bacteria. To date, the genome sequences of 15 isolates from the *B. cereus* group of bacteria are available in public databases and more are underway (www.genomesonline.org). Consequently, this group of bacteria provides one of the richest collections of near neighbour sequences, which will

impact future efforts due to the large amounts of data available for comparison between strains and genes. The *B. anthracis* A2012 strain (Florida strain), isolated from the victim of the bio terrorism attack in Florida (Pearson *et al.*, 2004), was the first draft genome to be published followed by the complete genome of *B. anthracis* Ames (Read *et al.*, 2003), and to date 10 *B. anthracis* strains have been sequenced (www.genomesonline.org). *B. cereus* ATCC 14579 was selected for whole genome sequencing as it is non-pathogenic and is the Type strain for *B. cereus* (Ivanova *et al.*, 2003; Sneath *et al.*, 1986). Whole-genome-based phylogenetic analysis done using *B. anthracis* Ames, *B. cereus* ATCC 14579 and *B. cereus* ATCC 10987, a dairy isolate, showed that *B. cereus* ATCC 10987 was phylogenetic more closely related to *B. anthracis* Ames than to *B. cereus* ATCC 14579 (Rasko *et al.*, 2004). While the genome sequence of *B. cereus* ATCC 14579 revealed a small extra chromosomal linear molecule (Ivanova *et al.*, 2003), *B. cereus* ATCC 10987 contained a large circular plasmid with homology to the *B. anthracis* plasmid pXO1 (Rasko *et al.*, 2004).

The isolates for which whole genome sequences are now available, do not properly represent the diversity observed in the *B. cereus* group of bacteria through methods such as Multilocus Sequence Typing (MLST; Helgason *et al.*, 2005) and Multilocus Enzyme Electrophoresis (MLEE; Helgason *et al.*, 2000). The choice of strains for sequencing up till now reflects bias driven by the need to understand rare pathogenic traits in some of these species (Rasko *et al.*, 2005). Only the future will, through new sequencing projects, allow an entire picture of this group of bacteria to form.

1.2.7 Sporulation

The *Bacillus cereus* group bacteria possess several complex development programs that drive environmental adaptation and morphological differentiation. These changes are seen to be quite elaborate and can result in major changes in cell appearance (Driks, 2002).

One of the best studied of these systems is spore formation, which is a characteristic feature in *Bacilli* and is well characterised in *Bacillus subtilis*. The spore is entirely distinct from the vegetative cell, possessing several molecules and structures unique to the spore (Kornberg *et al.*, 1968; Murell, 1967; Murrell, 1969 and Warth *et al.*, 1963), such as the molecules SpoA and σ -factors and structures as additional polysaccharides in the outer wall. Actively growing *Bacilli* are induced to differentiate into spores by starvation of carbon, nitrogen or, in some circumstances a phosphorus source, and spore formation is seen to take 7 hours at 37°C (Piggot *et al.*, 2004). Since *B. subtilis* is the best described spore forming Gram-positive bacterium, most genes related to spore formation are designated from *B. subtilis*, i.e. initiation signals resulting in activation of the master transcription regulator, Spo0A, which activates and triggers asymmetric sporulation division and transcription of the *spoIIA*, *spoIIIE* and *spoIIG* loci, which all encode for development regulators. This will result in the initiation and activation of sigma factors required for sequential mother cell and forespore gene transcription (Errington, 1993; Driks, 1999). These genes are also present in the *B. cereus* group bacteria, as identical or partially identical genes, and will presumably drive the same activation process and transcriptional control (Aronson, 2002). Sporulation division produces two distinct cells with different fates, the smaller prespore (forespore), which develops into the spore, and the mother cell, which will ultimately lyse and die. The surviving spore is able to survive for a long period of time, endure high temperatures, disinfection, UV-radiation and chemicals, and inhospitable environments such as soil and the ocean (Priest, 1993; Francis *et al.*, 1999), but can also sense the reappearance of even minute amounts of nutrients in the environment, and respond by converting back to a vegetative growing cell (Atrih *et al.*, 1999), in a separate developmental process called germination. Sporulation, used by *Bacilli* and many other Gram-positive bacteria, is seen as not only a way for survival, but also as a strategy for pathogenesis as the spore in many cases act as the infectious agent.

1.3 Biofilm formation

Microorganisms are often viewed as simple creatures when compared with other, more complex organisms, however studies of microbial development have shown that microorganisms are capable of complex differentiation and behaviour (O'Toole *et al.*, 2000). Examples include *Bacillus* spore formation, in which individual vegetative cells integrate multiple external and internal signals to successfully synthesize a new morphological structure that allows it to adapt for survival in a variety of harsh environments (1.2.7). Another excellent model system for study is the formation of surface-attached microbial communities, known as biofilms. Biofilms can be defined as communities of microorganisms that are attached to a surface. These communities consist of multiple layers of cells usually embedded in hydrated matrices of polysaccharides, either comprising single or multiple microbial species and can form on a range of biotic and abiotic surfaces. Although mixed-species biofilms predominate in most environments, such as teeth and gut, single-species biofilms exist in a large variety of infections, on surface of medical implants and on surfaces connected to the food industry (Adal *et al.*, 1996; Archibald *et al.*, 1997; Dickinson *et al.*, 1993). These single-species biofilms are the focus of most current research, which include gram-negative biofilm-forming bacteria *Pseudomonas aeruginosa* (O'Toole *et al.*, 2000), *Escherichia coli* and *Vibrio cholerae* (Yildiz *et al.*, 1999) and gram-positive biofilm-forming bacteria *Staphylococcus epidermidis* (Heilmann *et al.*, 1998), *Staphylococcus aureus*, *Bacillus lichienformis* (Ameur *et al.*, 2000), *Bacillus subtilis* (Branda *et al.*, 2004) and *Bacillus cereus* (1.4).

Biofilms are a stable point in a biological cycle that includes initiation, maturation, maintenance and dissolution (Figure 1.3). Bacteria seem to initiate biofilm development in response to specific environmental conditions, such as nutrient availability and/or the lack of it or the presence of other bacteria in the surrounding environment. Many examples indicate

that development of biofilms requires multicellular behavior and that the development of a biofilm is a complex process that requires collective bacterial behavior, many times involving more than one species.

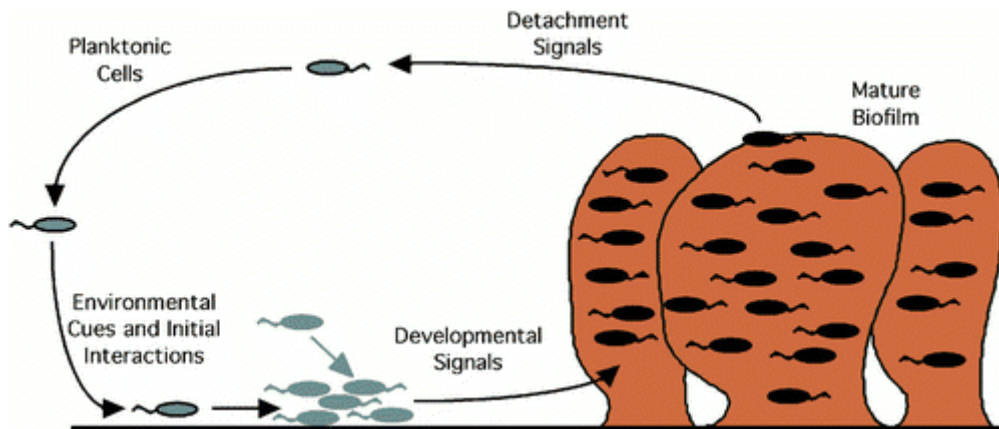


Figure 1.3: Model of biofilm development. Individual planktonic cells can form cell-to-surface and cell-to-cell contacts resulting in the formation of microcolonies and mature biofilms. Cells in the biofilm can return to a planktonic lifestyle to complete the cycle of biofilm development, from O’Toole *et al.*, 2000.

Prokaryotes can inhabit any environment suitable for higher life forms, as well as a variety of inhospitable settings that the majority of higher life forms find extreme (Madigan *et al.*, 1997). The one key element seen to affect biofilm formation is the ability of the bacteria to position themselves in niches where they can propagate. The common mechanisms for biofilm formation include flagellar based motility and different methods of surface translocation; e.g. twitching, gliding, darting and sliding motility (Henrichsen *et al.*, 1972). Bacterial communities in nature play a key role in the production and degradation of organic matter, which requires the combined effort of many species of bacteria with different metabolic capabilities, and are only able to perform this “expected” role in a community of several bacteria, often of different species. Bacteria are also thought to experience a certain degree of shelter and homeostasis when residing within a biofilm and one of the key components of this micro niche is the surrounding extrapolymeric substance matrix. This

matrix is often composed of a mixture of components, such as extracellular polysaccharides (EPS), proteins, nucleic acids, and many other substances present in the environment of biofilm formation. Bacteria are capable of producing polysaccharides themselves, either as wall polysaccharides (capsule) or as extracellular excretions into the surrounding environment (EPS in *S. aureus*, *E. coli*, *V. cholerae* and *P. aeruginosa*). EPS most likely play various roles in the structure and function of different biofilm communities and EPS may also play different roles in similar microbial communities under different environmental conditions (Dahlberg *et al.*, 1997; Watnick *et al.*, 1999; Yildiz *et al.*, 1999). The EPS matrix also has the potential to physically prevent access of certain antimicrobial agents into the biofilm by acting as an ion exchanger and thereby restricting diffusion of compounds from the surroundings into the biofilm (Gilbert *et al.*, 1997). The level of potential prevention, by the EPS matrix from antimicrobial agents, is totally dependant on the type, amount and properties (hydrophobicity and charge) of the antimicrobial agent in circulation. Furthermore, EPS can provide protection from a wide variety of environmental stress factors, such as UV radiation, pH shifts, osmotic shock and desiccation (Flemming, 1993).

Biofilms have been seen to have highly permeable water channels interspersed throughout the biofilm, and these have been compared to primitive circulation systems. They provide an effective means of exchange of nutrients and metabolites as well as removal of potentially toxic metabolites (Costerton *et al.*, 1995). The elaborate architecture provides the opportunity for metabolic cooperation and consequently provides for the improved growth and survival of most biofilms.

One of the greatest advances in modern medicine has been the fight against infectious diseases. There are, however, exceptions to this rule. The fight against bacteria, that form biofilm, is still not completely won. Bacteria in biofilm can be seen to be up to 1000-fold more resistant to antibiotic treatment than the same organism grown planktonically (Gilbert *et*

al., 1997) and survival rates are much higher in biofilm forming bacteria. Biofilm forming bacterial infections are more difficult to fight due to several elements such as, antibiotic resistance, protection from stress factors, the high recurrence frequency and the fact that biofilm infections are rarely resolved by the host's immune system. *P. aeruginosa* in patients with cystic fibrosis, chronic ear infections and periodontitis are examples of infections caused by biofilm forming bacteria seen to be difficult to combat and cure.

Biofilms do seem to play a role in adhesion to surfaces, both biotic and abiotic, and subsequently colonization of surfaces (O'Toole *et al.*, 2000). This is thought to be due to the higher levels of adhesion molecules present when cells group and the cooperation between cells growing in biofilm. Cell-surface interactions have been seen to be the initiating factor in biofilm formation (Heilmann *et al.*, 1996; Heilmann *et al.*, 1998). These interactions may be mediated through a number of factors, including uncharacterized surface proteins (Hussain *et al.*, 1997), extracellular proteins (Schumacher-Perdreau *et al.*, 1994), capsular polysaccharide/adhesion molecules on the surface of the bacteria (McKenney *et al.*, 1998) and cell surface-localized autolysins (Heilmann *et al.*, 1997), which aid in the movement of bacteria on a surface by making the surface smoother. The subsequent phase is the so-called "accumulative phase", which involves cell-cell interactions and the formation of cell aggregates on the surface. Numerous studies have been done to implicate polysaccharide intercellular adhesion (PIA) molecules in this process, but conclusive studies are still not done. The last stage of biofilm formation is the maturation of the bacterial community. This involves the production of extracellular polysaccharides ("slime") when the bacteria are growing on a surface. Little is known about how this extracellular polysaccharide affects the normal development of the biofilm and what role it plays in determining its architecture. Detachment of bacterial cells from the biofilm is seen after biofilm formation, but very little is

known about this and it is not a given that all biofilm forming bacteria, are able to detach, or how this process is mediated.

Biofilm formation does initiate a large amount of gene regulation, which is evident from the fact that organisms have multiple genetic pathways that control biofilm behavior (O'Toole *et al.*, 2000). Up-regulation of genes has been seen to occur during biofilm formation, such as the up-regulation of adhesion molecule genes in *V. cholerae* and up-regulation of pili-mediated movement in *P. aeruginosa*. Down-regulation, however, of specific genes in biofilm forming bacteria has been difficult to confirm, but is thought to happen (O'Toole *et al.*, 2000). The growth rate of bacteria in process of forming biofilm and when biofilm is formed is seen to be elevated compared to the growth rate during planktonic growth, but genetic background information is scarce and up-regulation of growth may only be the result of the general up-regulation of genes during biofilm formation.

1.4 *Bacillus cereus* and biofilm formation

Different *Bacillus* species (*B. subtilis*, *B. cereus* and *B. thuringensis*) are known to form biofilm on solid surfaces and at air-liquid interfaces, often depending on environmental conditions. In the natural environments of the *Bacillus* species, biofilm formation may be the first step in a complex developmental process that simultaneously or sequentially incorporates fruiting body formation (Branda *et al.*, 2001), sporulation (Stragier and Losick, 1996), natural competence (Busch and Saier, 2002; Dubnau, 1999; Solomon and Grossman, 1996; Saier, 2000), planktonic motile cell release (Sauer *et al.*, 2004) and cell raft swarming (Julkowska *et al.*, 2004/2005).

B. cereus can easily contaminate food production or processing systems (Kotiranta *et al.*, 2000) and some strains have the ability to form biofilms that are highly resistant to cleaning products (Peng *et al.*, 2002). Biofilm formation occurs in a manner similar to the

found in better characterized *B. subtilis*; however biofilm forming *B. cereus* are mostly seen in the food and milk industry. Further speculations have been made as to where *B. cereus* has the ability to form biofilm, on/between teeth, in surgical wound and in milk tanks, but no large scale study has been done. Some *Bacillus* species, isolated from alkaline wash solutions used for cleaning in dairy factories, were shown to attach to stainless steel surfaces and produce proteases and lipases (Lindsay *et al.*, 2000), and thought to be a source of post-pasteurization contamination of milk and milk products. Through proteomic investigation of dairy-associated *B. cereus* biofilm (Oosthuizen *et al.*, 2001; Oosthuizen *et al.*, 2002) and comparison of two-dimensional gel electrophoresis of proteins found in different states of growth, several potential genes involved in biofilm formation within *B. cereus* strains have been identified. However, these results have not given any definite indications of genes involved with biofilm formation.

1.5 Screening for biofilm formation

A concerted effort to study microbial biofilms began only 20 years ago with the rediscovery that, in natural aquatic systems, bacteria are found predominantly attached to surfaces (Geesey *et al.*, 1977). Although biofilm formation has been recognized and has been a scientifically documented aspect of microbial physiology for more than 100 years, the understanding of the molecular process is just underway. During the past years simple screening, of isolates of biofilm defective mutants, has been made possible, thus making genetic analysis of biofilm development possible (Heilmann *et al.*, 1996; Mack *et al.*, 1994).

A simple screening method has been implemented utilizing plastic (PVC or polystyrene) 96-well microtiter dishes as a substrate for biofilm development, allowing large-scale screening of bacterial strains for the ability to form biofilm. Biofilm formation is often visualized by staining cells attached to the surface with a variety of dyes (such as crystal

violet or safranin) followed with washing and solubilisation of cells. Many bacterial dyes are positively charged (cationic) and combine with negatively charged cellular components such as nucleic acids (DNA and RNA) and acidic polysaccharides. Methylene blue, crystal violet and safranin are such cationic dyes. Other bacterial dyes are negatively charged (anionic) and combine with positively charged cellular components, such as proteins. Eosin and acid fuchsin are anionic dyes. The simplicity of this screening method has made possible the screening of thousands of randomly generated mutants, giving an indication of the genetic background for biofilm formation. *B. cereus* has been shown to form biofilm more frequently on PVC 96-well microtiter plates instead of polystyrene, in fresh LB medium containing bactopectone instead of tryptone, and to be ideally stained with crystal violet (Auger *et al.*, 2006). These findings have allowed the simultaneous screening of many *B. cereus* strains (this thesis; Michel Gohar, personal communication).

1.6 Genetics of biofilm formation

In Gram-negative bacteria known to form biofilm (*E. coli*, *P. aeruginosa*, *P. fluorescens* and *V. cholerae*), defects in genes involved in flagellar-mediated motility hinder biofilm formation under certain conditions; in *E. coli*, flagellar-mediated motility is important in establishing cell-surface contacts during biofilm formation in Luria Bertani (LB) broth (Pratt *et al.*, 1998; Genevaux *et al.*, 1996). Similarly, mutant non-motile strains of *P. aeruginosa* and *P. fluorescens* have been isolated in screens searching for defects in biofilm formation (O'Toole *et al.*, 1998). Twitching motility, which refers to surface translocation mediated by type IV pili, appears to be widespread among Gram-negative bacteria (Wall *et al.*, 1999) and has also been shown to be important for initial biofilm structural development by *P. aeruginosa*. It is important to note that even though these studies assign motility a major

role in biofilm formation, formation is also observed in strains without any known form of motility.

Nutritional background can also be an important factor for biofilm formation, seen for instance by the *ompR* allele in *E. coli*, a member of the subfamily of response regulators that have fourteen homologues in *E. coli* alone (Mizuno, 1997). OmpR has been seen to aid the production of *curli* (type of fimbriae/pili) in non-motile strains by sensing low levels of nutrition and thereby allowing the formation of biofilm (Vidal *et al.*, 1998). It is thought that force-generating movement helps to overcome overall repulsive forces between bacteria and surface, thereby increasing the chances of bacteria making the initial interaction with the surface. Once initial contact has been made, production of adhesion molecules are established by outer-membrane proteins. Overproduction of *curli* is thought to make non-motile *E. coli* “stickier”, allowing biofilm to form in the absence of force-generating movement.

Essential attractive forces required for the establishment of stable interactions between bacteria and surfaces have been argued to be provided by specific outer-membrane proteins, such as genes encoding for the mannose-sensitive type I pilus, which are essential for *E. coli* biofilm formation in LB broth (Pratt *et al.*, 1998). Type I pili are required for biofilm formation by *E. coli* on many surfaces, including PVC, and FimH, an element of Type I pili, has been observed to have the ability to bind both specifically and nonspecifically to mannose and abiotic surfaces.

The potential role of extracellular factors in biofilm formation, have always been speculated to have an important role. In Gram-negative bacteria acylated homoserine lactones (acyl-HSLs), which are quorum-sensing signal molecules, have been demonstrated to be present both in aquatic biofilms grown on submerged stones (McLean *et al.*, 1997), and in biofilms formed on urethral catheters (Stickler *et al.*, 1998). The acyl-HSLs are synthesized and secreted in high levels in cultures in which cell density is high and are thought to have an

important role in late biofilm formation. Extracellular factors, such as Crc, can also have a sensing of the environment role. Crc plays a role, in *P. aeruginosa*, by sensing the availability of carbon sources, and has been shown to affect expression of the type IV *pilA* structural gene (O'Toole *et al.*, 2000; MacGregor *et al.*, 1991; Wolff *et al.*, 1991).

The story for Gram-positive bacteria, which are mostly non-motile, is different except for some motile species, such as *B. cereus* and *B. subtilis*. In biofilm formation among Gram-positive bacteria there is thought to be a more direct link between extracellular polysaccharides and adhesion to surfaces. In the Gram-positive bacterium *B. subtilis*, biofilm formation has been examined to some extent (Branda *et al.*, 2001; Hamon and Lazazzera, 2001), and several determinants of biofilm formation have been identified. Transcriptional regulators (AbrB, Spo0A, CcpA and σ H), signal peptidase (SipW), and proteins involved in extracellular matrix synthesis (YveQ, YveR and YhxB) (Branda *et al.*, 2004; Hamon and Lazazzera, 2001; Hamon *et al.*, 2004; Stanley *et al.*, 2003) are all required for biofilm formation. Recent results (Auger *et al.*, 2006) show a clear connection between *B. cereus* biofilm formation and autoinducer 2 (AI-2) production. AI-2 was originally discovered in *V. harveyi* as a signal molecule and is thought to be a universal signaling factor for intra- and interspecies communication in response to cell density. In *V. harveyi*, AI-2 acts in conjunction with AI-1, an acyl-homoserine lactone signal, to regulate the luminescence in response to cell density, while in *B. cereus* it is thought to be a factor in sensing cell density during biofilm formation (Auger *et al.*, 2006).

1.7 The *plcR* regulon

The PlcR transcriptional activator, originally discovered as a positive regulator involved in the expression of phosphatidylinositol-specific phospholipase C in *B. thuringensis* (Lereclus *et al.*, 1996), is a global regulator controlling the expression of several non-specific

extracellular virulence factors in *B. thuringensis*. The *B. thuringensis plcR* gene is also present in *B. cereus* and *B. anthracis* and PlcR has also been seen to be a positive pleiotropic regulator of several virulence factors in *B. cereus* (Agaisse *et al.*, 1999; Økstad *et al.*, 1999), but is non-functional in *B. anthracis*. PlcR controls the expression of a large regulon comprising at least 23 genes, which fall into three broad classes: (i) cell-surface proteins, (ii) degradative enzymes and (iii) toxins (Agaisse, *et al.*, 1999; Gohar *et al.*, 2002). Thus PlcR controls the transcription of several extracellular proteins, including phospholipases, proteases and haemolysins, in *B. cereus* and *B. thuringiensis* (Agaisse *et al.*, 1999; Økstad *et al.*, 1999).

A nonsense mutation in the *plcR* gene has been shown to be responsible for the non-haemolytic phenotype of *B. anthracis* (Agaisse *et al.*, 1999). Recent reports have indicated that distinct mutations in *plcR*, which are observed in some *B. cereus* group strains, result in a haemolysis-negative and lecithinase-negative phenotype (Slamti *et al.*, 2004). Mutations in the pleiotropic regulator PlcR thus might be a reason for some atypical characteristics when using the media-identification method (based on lecithinase-activity), and is also speculated to have a role in biofilm formation. Preliminary studies of the effect of PlcR on biofilm formation show that PlcR is expressed in biofilm forming cells of the strong biofilm former *B. thuringiensis* 407, and that biofilm cells can excrete enterotoxins normally regulated by PlcR (Michel Gohar, personal communication). Furthermore, for another biofilm forming strain, *B. cereus* ATCC 10987, the culture supernatant has been shown to be able to confer biofilm formation properties to strains that are otherwise not able to form biofilm in experimental conditions (Michel Gohar, personal communication). It would therefore be of interest to construct a *plcR* knock-out strain of *B. cereus* ATCC 10987, to investigate a possible role of PlcR in biofilm formation in this strain, and the possible effect on the ability to induce biofilm formation in non-biofilm formers.

1.8 *Bacillus cereus* ATCC 10987

Bacillus cereus ATCC 10987 was isolated from a study on cheese spoilage in Canada in 1930 (Smith, 1952; Herron, 1930) and has been used as a model strain in our group for many years. This strain had been observed to have all the characteristics of a *B. cereus* strain, but did also have unknown pathogenic properties enabling the strain to colonise cheese production facilities. Recent studies have also shown that this strain has the ability to form biofilm (Auger *et al.*, 2006; this thesis) and to produce proteins, which may have an effect on surrounding cells.

Initial genome research resulted in the production of a genome map from a *B. cereus* ATCC 10987 pUC18 plasmid DNA library (Figure 1.4; Økstad *et al.*, 1999), which indicated important markers and genes in the genome, but whose identity was unknown. This resulted in the entire genome being sequenced (Rasko *et al.*, 2004) and allowed for the further use of this strain in both phylogenetic and molecular studies.

The genome of *B. cereus* ATCC 10987 has now been demonstrated, through sequence analysis, to contain the *plcR* locus and *plcR* regulated putative virulence factors such as phosphatidylinositol-specific phospholipase C (PI-PLC), phosphatidylcholine-preferring phospholipase C (PC-PLC), sphingomyelinase, non-haemolytic enterotoxin and proteases (Økstad *et al.*, 1999; Lindbäck *et al.*, 1999), and to also express a high level of phospholipase C. *B. cereus* ATCC 10987 contains a single large plasmid that is similar to the *B. anthracis* pXO1 plasmid and encodes a number of unique factors and conserved regulatory proteins (Rasko *et al.*, 2004). Based on overall protein and nucleotide similarity, phylogeny and shared novel genes, *B. cereus* ATCC 10987 is more closely related to *B. anthracis* Ames (Read *et al.*, 2003) than it is to another dairy-isolated *B. cereus* strain, the type strain ATCC 14579.

All this combined makes *B. cereus* ATCC 10987 a very interesting and exciting strain to work with and research will be continued in the future.

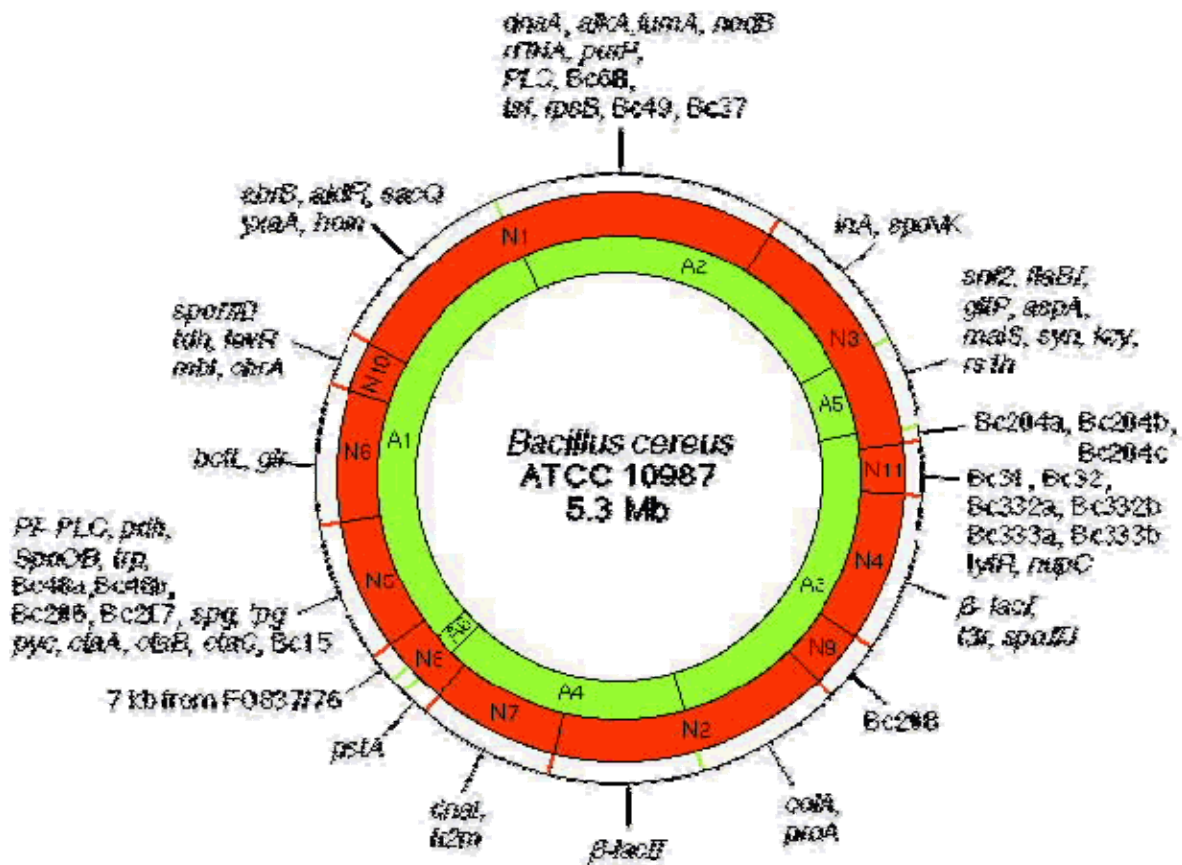


Figure 1.4: Genome map of *Bacillus cereus* ATCC 10987, N1-N11 indicating *NotI* fragments and A1-A6 indicating *AsdI* fragments. Restriction fragments are ordered according to size with lowest number corresponding to the largest fragment. From Økstad *et al.*, 1999.

1.9 Aim of the study

The aim of this study was to establish a method for screening a collection of more than 81 strains from the *B. cereus* group for biofilm formation, including soil isolates, strains from culture collections, reference strains, dairy isolates, and clinical strains from different types of human infections. The ability to form biofilms would then be compared with strain origin, to investigate the frequency of biofilm formation in the *B. cereus* group of bacterial pathogens, and whether the propensity to form biofilm could be correlated with the source of isolation or with the strain phylogeny. We also aimed to initiate gene disruption studies in a candidate regulatory gene, *plcR*, to reveal its possible involvement in biofilm formation in *B. cereus* ATCC 10987.

2 MATERIALS AND METHODS

2.1 Materials

2.1.1 Bacterial strains

Table 2.1: Bacterial strains used for biofilm screening

Strain	Origin
AH 75	<i>Bacillus cereus</i> ATCC 10987 (dairy, cheese spoilage, Canada)
AH 181	<i>Bacillus cereus</i> ATCC 10876 (<i>B.c</i> 569) (NRRL, Agriculture Research Service, Peoria, U.S.A.)
AH 183	<i>Bacillus cereus</i> ATCC 14579 (dairy)
AH 186	<i>Bacillus cereus</i> F4433/73 (diarrhoea, patient, Central Public Health Laboratory, London, U.K.)
AH 187	<i>Bacillus cereus</i> F4810/72 (vomit, patient, Central Public Health Laboratory, London, U.K.)
AH 188	<i>Bacillus cereus</i> F837/76 (Central Public Health Laboratory, London, U.K.)
AH 189	<i>Bacillus cereus</i> F2038/78 (Central Public Health Laboratory, London, U.K.)
AH 226	<i>Bacillus cereus</i> ATCC 4342 (dairy)
AH 248	<i>Bacillus thuringensis</i> , subsp. <i>kurstaki</i> 4D1
AH 249	<i>Bacillus thuringensis</i> , subsp. <i>kurstaki</i> 4D4
AH 252	<i>Bacillus thuringensis</i> , subsp. <i>kurstaki</i> 4H2
AH 257	<i>Bacillus thuringensis</i> , subsp. <i>israelensis</i> 4Q1
AH 258	<i>Bacillus thuringensis</i> , subsp. <i>israelensis</i> 4Q5
AH 259	<i>Bacillus cereus</i> 6A1
AH 265	<i>Bacillus thuringensis</i> 4A4
AH 338	<i>Bacillus mycoides</i> (soil)
AH 401	<i>Bacillus cereus</i> 181 (dairy, Sweden)
AH 404	<i>Bacillus cereus</i> 3048 (dairy, Valio, Finland)
AH 405	<i>Bacillus cereus</i> 1230 (dairy, Nurmes, Norway)
AH 407	<i>Bacillus cereus</i> 3122 (dairy, Valio, Finland)
AH 513	<i>Bacillus cereus</i> s1-2 (soil, Moss, Norway)
AH 535	<i>Bacillus cereus</i> s2-21 (soil, Moss, Norway)
AH 543	<i>Bacillus cereus</i> s3-1 (soil, Moss, Norway)
AH 546	<i>Bacillus cereus</i> s3-5 (soil, Moss, Norway)
AH 560	<i>Bacillus cereus</i> s4-3 (soil, Moss, Norway)
AH 580	<i>Bacillus cereus</i> s4-24 (soil, Moss, Norway)
AH 584	<i>Bacillus cereus</i> s4-28 (soil, Moss, Norway)
AH 588	<i>Bacillus cereus</i> s4-32 (soil, Moss, Norway)
AH 595	<i>Bacillus cereus</i> vet-1 (dairy, Norwegian College of Veterinary Medicine, Oslo, Norway)
AH 597	<i>Bacillus cereus</i> vet-3 (dairy, Norwegian College of Veterinary Medicine, Oslo, Norway)
AH 599	<i>Bacillus cereus</i> vet-5 (dairy, Norwegian College of Veterinary Medicine, Oslo, Norway)
AH 601	<i>Bacillus cereus</i> vet-8 (dairy, Norwegian College of Veterinary Medicine, Oslo, Norway)
AH 603	<i>Bacillus cereus</i> vet-10 (dairy, Norwegian College of Veterinary Medicine, Oslo, Norway)
AH 604	<i>Bacillus cereus</i> vet-11 (dairy, Norwegian College of Veterinary Medicine, Oslo, Norway)
AH 605	<i>Bacillus cereus</i> vet-17 (dairy, Norwegian College of Veterinary Medicine, Oslo, Norway)
AH 607	<i>Bacillus cereus</i> vet-59 (dairy, Norwegian College of Veterinary Medicine, Oslo, Norway)
AH 608	<i>Bacillus cereus</i> vet-61 (dairy, Norwegian College of Veterinary Medicine, Oslo, Norway)
AH 609	<i>Bacillus cereus</i> vet-68 (dairy, Norwegian College of Veterinary Medicine, Oslo, Norway)
AH 611	<i>Bacillus cereus</i> vet-87 (dairy, Norwegian College of Veterinary Medicine, Oslo, Norway)
AH 612	<i>Bacillus cereus</i> vet-131 (dairy, Norwegian College of Veterinary Medicine, Oslo, Norway)
AH 613	<i>Bacillus cereus</i> vet-132 (dairy, Norwegian College of Veterinary Medicine, Oslo, Norway)
AH 623	<i>Bacillus cereus</i> (soil, Tromsø, Norway)
AH 631	<i>Bacillus cereus</i> (soil, Tromsø, Norway)
AH 648	<i>Bacillus cereus</i> (soil, Tromsø, Norway)
AH 652	<i>Bacillus cereus</i> (soil, Tromsø, Norway)
AH 656	<i>Bacillus cereus</i> (soil, Tromsø, Norway)
AH 681	<i>Bacillus cereus</i> (soil, Tromsø, Norway)

Strain	Origin
AH 691	<i>Bacillus cereus</i> (soil, Tromsø, Norway)
AH 699	<i>Bacillus subtilis</i> 168
AH 724	<i>Bacillus cereus</i> (urine, patient, Skien, Norway)
AH 810	<i>Bacillus cereus</i> (periodontitis, patient, Faculty of Dentistry, University of Oslo, Oslo, Norway)
AH 811	<i>Bacillus cereus</i> (periodontitis, patient, Faculty of Dentistry, University of Oslo, Oslo, Norway)
AH 812	<i>Bacillus cereus</i> (periodontitis, patient, Faculty of Dentistry, University of Oslo, Oslo, Norway)
AH 813	<i>Bacillus cereus</i> (periodontitis, patient, Faculty of Dentistry, University of Oslo, Oslo, Norway)
AH 814	<i>Bacillus cereus</i> (periodontitis, patient, Faculty of Dentistry, University of Oslo, Oslo, Norway)
AH 815	<i>Bacillus cereus</i> (periodontitis, patient, Faculty of Dentistry, University of Oslo, Oslo, Norway)
AH 816	<i>Bacillus cereus</i> (periodontitis, patient, Faculty of Dentistry, University of Oslo, Oslo, Norway)
AH 818	<i>Bacillus cereus</i> (periodontitis, patient, Faculty of Dentistry, University of Oslo, Oslo, Norway)
AH 819	<i>Bacillus cereus</i> (periodontitis, patient, Faculty of Dentistry, University of Oslo, Oslo, Norway)
AH 820	<i>Bacillus cereus</i> (periodontitis, patient, Faculty of Dentistry, University of Oslo, Oslo, Norway)
AH 831	<i>Bacillus cereus</i> (periodontitis, patient, Faculty of Dentistry, University of Oslo, Oslo, Norway)
AH 874	<i>Bacillus cereus</i> SIC (clinical, patient, U.S.A.)
AH 884	<i>Bacillus cereus</i> (blood, patient, Rikshospitalet, Oslo, Norway)
AH 892	<i>Bacillus cereus</i> (wound after insect bite, patient, Regional Hospital, Tromsø, Norway)
AH 1031	<i>Bacillus thuringensis</i> 407 (soil, Paris, France)
AH 1091	<i>Bacillus cereus</i> ATCC14579 (dairy, cured of linear 15kb-plasmid)
AH 1123	<i>Bacillus cereus</i> 9823 (clinical, France)
AH 1127	<i>Bacillus cereus</i> 9843 (clinical, France)
AH 1129	<i>Bacillus cereus</i> Bc004 (clinical, post-traumatic endophthalmitis, Univ. Oklahoma, U.S.A.)
AH 1134	<i>Bacillus cereus</i> Bc006 (clinical, post-traumatic endophthalmitis, Univ. Oklahoma, U.S.A.)
AH 1143	<i>Bacillus weihenstephanensis</i> WSBC 10201
AH 1146	<i>Bacillus weihenstephanensis</i> WSBC 10205
AH 1248	<i>Bacillus thuringensis</i> subsp. <i>konkukian</i> str. 97-27 (leg wound infection, French soldier, Bosnia)
AH 1270	<i>Bacillus cereus</i> 0001+31175 (cervix, patient, Landsspítali, Reykjavík, Iceland)
AH 1271	<i>Bacillus cereus</i> 9903+02049 (secretary lamp, Landsspítali, Reykjavík, Iceland)
AH 1273	<i>Bacillus cereus</i> 9708+03060 (blood, patient, Landsspítali, Reykjavík, Iceland)
AH 1295	<i>Bacillus cereus</i> (veterinary, Norwegian College of Veterinary Medicine, Oslo, Norway)
AH 1297	<i>Bacillus cereus</i> (veterinary, Norwegian College of Veterinary Medicine, Oslo, Norway)
AH 1353	<i>Bacillus cereus</i> (food poisoning, diarrhoeal outbreak, Larvik, Norway)
AH 1363	<i>Bacillus cereus</i> ATCC14579 (dairy, Δ plcR mutant)
AH 1369	<i>Bacillus cereus</i> 9901+17036 (amniotic fluid, patient, Landsspítali, Reykjavík, Iceland)

Table 2.2: Bacterial strains used for making genetic construct

Strain	Origin
AH 617	<i>Escherichia coli</i> (containing pAT113 plasmid)
AH 1337	<i>Escherichia coli</i> (containing pUC19/spc-cassette plasmid)
AH 1352	<i>Escherichia coli</i> (containing pUC19 plasmid)
AH 1363	<i>Escherichia coli</i> (containing pUC19/ery-cassette plasmid)

2.1.2 Reagents

2.1.2.1 Reagents and chemicals

NR. 1 bacterial agar	Oxoid
Acetone	J.T.Baker
Agarose	Sigma

Ampicillin	Sigma
Bactopeptone	Oxoid
Boric acid	Sigma
Crystal violet	Sigma
EDTA	M&B
Erythomycin	Sigma
Ethidiumbromide	Sigma
Ethanol	Arcus
Hydrochloric acid	Prolab
Isopropanol	Arcus
KCl	Merck
KH ₂ PO ₄	Merck
Methanol	Prolab
NaCl	Merck
Na-citrate	J.T.Baker
Orange G	BDH
Spectionmycin	Sigma
Seakem-GTG	FMC
Tris-base	Sigma
Tryptone	Oxoid
Yeast Extract	Oxoid

2.1.2.2 Enzymes

<i>HincII</i>	NEB
<i>SacI</i>	NEB

<i>SalI</i>	NEB
<i>KpnI</i>	NEB
<i>HindIII</i>	NEB
<i>EcoRI</i>	NEB
Alkaline phosphatase (CIP)	NEB
DynAzyme II DNA polymerase	Finnzymes

2.1.2.3 Solutions

10 x TBE (TRIS/Borate Buffer)

108.0 g Tris Base

55.0 g Boric acid

9.3 g EDTA

Dissolved in 950 ml distilled water.

Volume adjusted to 1 l with water. Not autoclaved. Stored at room temperature.

TE-buffer, pH 7.6

10 ml 1M Tris-HCl pH 7.6

2 ml 0.5M EDTA pH 8.0

Volume adjusted to 1 l with water. Autoclaved. Stored at 4 °C.

Orange mix

20 g Ficoll

0.25 g Orange G

4 ml 0.5M EDTA

Dissolved in 100 ml of distilled water, sterile filtered and stored at - 20°C.

50 x TAE (TRIS/acetat buffer)

2.0 M Tris Base

1.0 M cons. acetic acid

50 mM 0.5 M EDTA pH 8.0

Dissolved in 1 l distilled water. Not autoclaved. Stored at room temperature.

PBS, pH 7.4

136.9 mM NaCl

2.7 mM KCl

10.1 mM Na₂HPO₄·2H₂O

1.8 mM KH₂PO₄

Dissolved in 5 l distilled water. PH adjusted to 7.4 with approximately 5.8 M HCL.

Autoclaved, stored at room temperature.

2.1.2.4 Growth media

LB medium

10 g Tryptone

5 g Yeast Extract

10 g NaCl

Dissolved in 950 ml of distilled water. pH adjusted to 7.0 with 5.8 M HCl and volume adjusted to 1 l with water. Autoclaved and stored at + 4°C.

Bactopeptone medium

10 g Bactopeptone

5 g Yeast Extract

10 g NaCl

Dissolved in 950 ml of distilled water. pH adjusted to 7.0 with 5.8 M HCl and volume adjusted to 1 l with water. Autoclaved and stored at + 4°C.

LB agar plates

10 g Tryptone

5 g Yeast Extract

10 g NaCl

15.0 g NR. 1 bacterial agar

Dissolved in 950 ml of distilled water. pH adjusted to 7.0 with 5.8 M HCl and volume adjusted to 1 l with water. Autoclaved, plated out at 20 ml per plate and stored at + 4°C.

All agar and broth preparations were prepared following manufacturers instructions. All media was sterilized by autoclaving at 0.35 kg cm⁻² for 20 minutes at 121° C.

2.2 Methods

2.2.1 Growth of bacteria

All strains used were picked from the strain collection held at the Department of Pharmaceutical Biosciences, University of Oslo, which contains more than 300 different *Bacillus cereus* group strains. These stock strains were originally produced by growing a single colony of each strain in LB medium over night (~16 hours) at 30°C with shaking at 225 rpm. Culture was then reinoculated in fresh medium, and grown aerobic to an optical density at 600nm of 0.6 (OD₆₀₀ = 0.6). Cell suspension (0.8 ml) was then mixed with 0.2 ml 87% (w/v) glycerol and stored at -70°C until use. Optical density was measured using an Eppendorf BioPhotometer, following manufacturer's guidelines.

2.2.2 Growth curves

Stock strains were picked from single colonies and grown in 10 ml LB medium over night at 30°C and with shaking at 225 rpm. Inoculation of over night cultures (100 µl of

overnight culture) into 10 ml fresh LB medium was performed to give cultures used in bacterial growth curve determination. At each time point 100 µl of culture was extracted and diluted with 900 µl pure LB medium in a 1 ml plastic cuvette. Measurements of the optical density of the culture were done at 600nm, using Eppendorf BioPhotometer and following manufactures guidelines. All growth experiments were performed in 30 ml sterilin tubes, at 30°C and with shaking at 225 rpm.

2.2.3 Biofilm screening method

Bacillus cereus group bacteria are seen to form biofilm at the air-liquid interface if biofilm forming abilities are present in isolate. Biofilm formation is also seen to be stronger on PVC surface and to form a multilayer of cells in bactopectone medium. Staining with crystal violet (Figure 2.1) of cells is seen to be efficient due to the ability of crystal violet to bind to the membrane of the cells and colour the cells a dark blue/violet. The crystal violet molecules bind between the outer membrane molecules and become permanently attached to the cells until solubilised, which may result in cell destruction.

Stock strains were grown and picked from single colonies, inoculated in 10 ml LB medium and grown over night. Inoculation of over night cultures (100 µl) into fresh 10 ml LB medium was performed to produce exponential growth phase culture. The precultures, in exponential growth phase, after 3 hours of growth, were diluted in 10 ml of fresh bactopectone medium (2.1.2.4) and transferred to 96-well polyvinylchloride microtiter plates in two parallel plates. Culture (125 µl) was inoculated in each well. After growth for 24, 48 and 71 hours of incubation at 30° C, the biofilm density was measured as follows: i) the microtiter plate wells were washed once with PBS (130 µl), ii) bound cells were stained with 1% (w/v) crystal violet solution (130 µl) at room temperature for 20 min (Hamon *et al.*, 2001; Michel Gohar, personal communication; Auger, *et al.*, 2006).

Crystal violet has the structure:

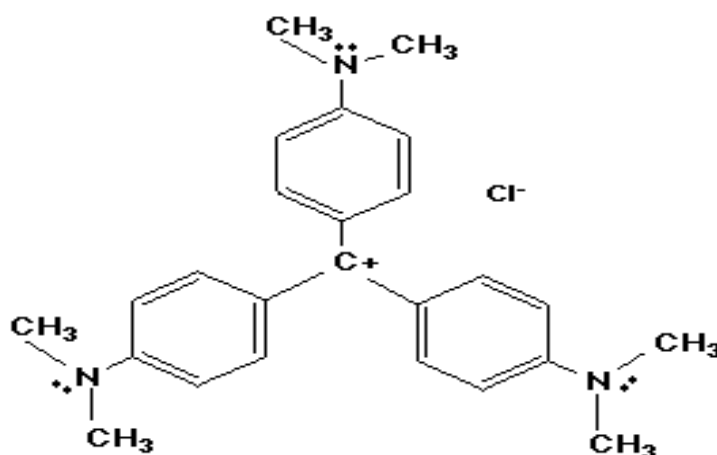


Figure 2.1: Structure of crystal violet, from www.DoChem.com.

iii) Wells were then washed three times with PBS (180 μ l), and remaining crystal violet attached to cells was solubilised with acetone/ethanol mixture (1:4) (150 μ l). The absorbance of the solubilised dye at 590 nm (Figure 2.2) was subsequently determined. Absorbance was measured in HTS 7000 Plus, Bio Assay Reader (Perkin Elmer) using Perkin Elmer HTSoft Wizard 2.0.

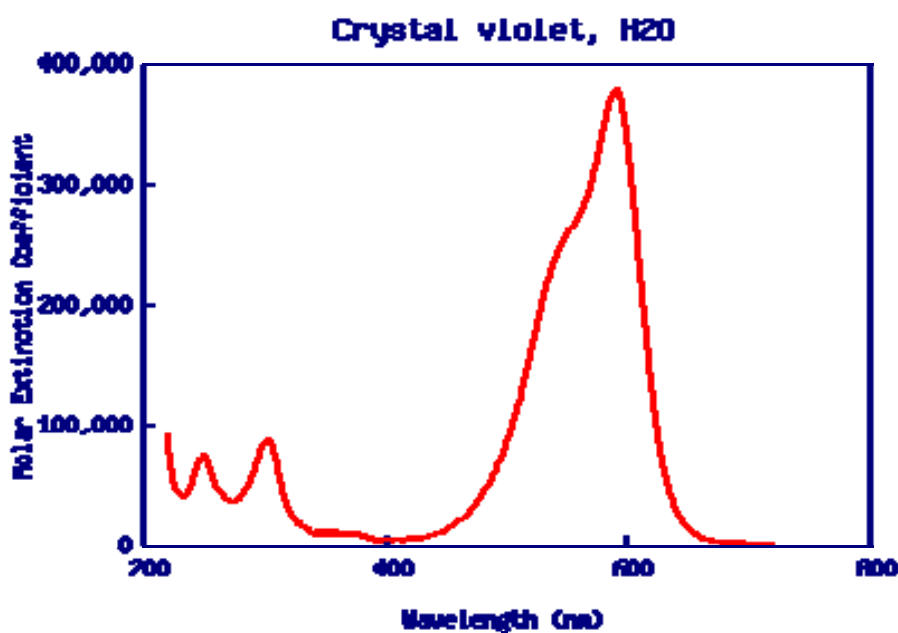


Figure 2.2: Absorbance pattern of crystal violet dissolved in water, from Du *et al.*, 1998.

2.2.4 Crystal violet staining of serial dilution of bacteria

To be able to show the correspondence between amount of bacterial cells and crystal violet staining a serial dilution of a culture, grown for 5 hours at 30°C and with shaking at 225 rpm, was stained by crystal violet and absorbance at 590nm was measured: In short, 1ml of overnight culture was pelleted at 13000 rpm for 1 minute, and resuspended in 100 µl PBS. This dilution was used to prepare an x2 serial dilution to a final dilution of 1/32 and stained with 1% (w/v) crystal violet (100 µl) for 20 minutes at room temperature. Stained cells were washed three times with PBS (1 ml) and solubilised with acetone/ethanol (1:4) (100 µl) solution. Absorbance was then measured at 590nm (2.2.3).

2.3 Genetic methods

2.3.1 *plcR* locus sequence extraction and primer design for gene deletion

plcR locus sequence extraction was performed using programs available through EMBNET (www.uio.no/EMBNET) and primer design was performed using *Primer3* software available on the internet (<http://frodo.wi.mit.edu>). *plcR* locus sequence extraction and primers design was performed to allow the amplification of fragments of the upstream and downstream regions of the *plcR* gene through PCR, for use in *plcR* knock-out construct construction (Section 3.1).

2.3.2 Genomic DNA extraction

An LB agar plate was inoculated with a stock strain (stored at -70°C) and incubated aerobically over night at 30°C. A single colony from this plate was resuspended in 10 ml LB medium in 30 ml tubes and incubated aerobically over night at 30°C and shaking (225 rpm). Overnight culture (100 µl) was inoculated in 10 ml LB medium in 30 ml tubes and grown for 3 hours at 30°C and shaking (225 rpm). Genomic DNA was isolated from the culture using

the Qiagen Genomic DNA 100 tip kit, which uses alkaline based lyses of bacterial cell, extraction of DNA via column (Qiagen anion-exchange resin) under low-salt and pH conditions, removal of RNA, proteins, dyes and low-molecular-weight impurities by a medium-slat wash, elution in a high-salt buffer and concentration and desalted by isopropanol precipitation of DNA. Manufacturer's guidelines were followed.

2.3.3 Polymerase chain reaction (PCR)

The development and amplification of synthetic DNA has been made possible by polymerase chain reaction (PCR), a reaction that can multiply DNA molecules by up to a billion fold in a test tube. PCR requires that nucleotide sequence of desired gene is known, due to the necessity of primers complementary to the sequence in the gene. PCR also requires the presence of the 4 nucleic acids, cytosine, thymine, adenine and guanine, a DNA polymerase and a DNA polymerase buffer.

PCR reactions were performed using ~50 ng chromosomal DNA, 32 pmol of each primer, 0.2 mM of each dNTP and 2 U DynAzyme II DNA polymerase (Finnzymes) in 1 x Dynazyme reaction buffer, in a 50 µl reaction volume. Reaction mixture was performed on ice to hinder unspecific primer binding and primer dimerisation. All primers had a calculated optimal melting point of 57°C.

PCR reaction in each tube (total volume of 50 µl):

5 µl dNTP-mix (2 mM each dNTP)

5 µl DynAzyme II polymerase buffer (10x)

1 µl DynAzyme II polymerase (Finnzymes) (2U/µl)

1 µl primer 1 (20 µM stock)

1 µl primer 2 (20 µM stock)

1 μ l template DNA (~50 ng)

MilliQ-water to 50 μ l

The reactions were carried out on a GeneAmp 2700 PCR machine (AppliedBiosystems) with an initial denaturation step at 94° C for 5 minutes, followed by 30 cycles of 94° C for 1 minute, annealing at 57°C for 1 minute and polymerisation at 72°C for 1 minute, finishing with a final extension step at 72°C for 7 minutes.

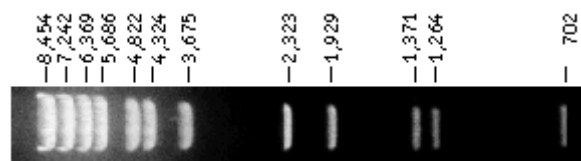
2.3.4 Agarose Gel Electrophoresis

Agarose gel electrophoresis is used to separate DNA fragments according to their size, in a network-like gel structure and the migration is based on the uniform negative charge of DNA forcing the molecules towards the positive pole in an electric field. DNA fragments are loaded in wells in the agarose gel and run through an electric field from negative charge to positive charge. Visualisation of DNA fragments is possible by ethidium bromide addition to the gel and UV illumination. Ethidium bromide has the ability to bind in between the base pairs of DNA molecules and fluoresce in UV light. Size determination of fragments run on gel is done by comparison with size marker lambda/*BstE* II (NEB). *BstE* II digest of lambda DNA yields 14 fragments suitable for use as molecular weight standards for agarose gel electrophoresis (Picture 2.1). The approximate mass of DNA in each of the bands is provided for approximating the mass of DNA in comparably intense samples of similar size.

Electrophoresis grade agarose at a concentration of 1% (w/v) in 1xTBE buffer was used for agarose gel electrophoresis, with ethidium bromide added to a final concentration of 0.5 μ g/ml in the gel. Sample DNA (10 μ l) was mixed with 3 μ l Orange mix loading dye and loaded on to the gel. Gels were run at 60-120V (2-4 V/cm) for 60 minutes and DNA patterns

were visualised using a UV transilluminator (BioRad). A 1kb DNA ladder, λ /BstEII, were used as size marker (NEB).

Agarose gel electrophoresis can also be used as a preparative tool, i.e. use electrophoresis to separate DNA fragments by their size and afterwards cut the DNA, corresponding to fragment size of sample, out of the gel for further use. This is preformed by using a scalpel, a UV transilluminator and gel purification kits.



Picture 2.1: Lambda DNA-BstE II Digest visualized by ethidium bromide staining. 1.0% agarose gel, from www.NEB.com

2.3.5 Purification

PCR products were purified directly from the PCR mixture by QIAquick PCR purification kit (Qiagen). Alternatively, preparative agarose gel electrophoresis was used to separate PCR products (2.3.4), and gel bands were purified by QIAquick Gel extraction kit (Qiagen). The QIAquick system combines spin-column technology with selective binding properties of a silica-gel membrane. DNA is absorbed to the silica-gel membrane in the presence of high salt while contaminants pass through the column. Special buffers provided with kit are optimized for efficient recovery of DNA and removal of contaminants. When gel purification was preformed 0.8% Seakem GTG agarose gel (1x TAE buffer) was used to give narrow bands more easily extracted from the gel. Manufacturer's guidelines were followed.

2.3.6 Plasmids and preparation

pUC19 was used as a cloning vector in this project (Figure 6.2.1). pUC19 vector was isolated from an *E. coli* strain in our strain collection (AH 1352), using the QIAprep Midiprep kit (Qiagen) following manufacturers guidelines. QIAprep midiprep kit is based on alkaline lyses of bacterial cells followed by absorption of DNA onto silica in presence of high salt. Elution is done in low-salt buffers. Manufactures guidelines were followed.

2.3.7 Restriction enzyme digest

Restriction enzymes were used to digest *plcR* upstream and *plcR* downstream PCR products, as well as vector pUC19. Manufacturer's guidelines were followed for temperature during digestion, concentrations of reactants and the use of bovine serum albumin (BSA). Enzymes were allowed to incubate for three hours.

Restriction enzyme digestion (30 µl volume per tube):

5 µl Buffer (corresponding to manufacturers guidelines for the given enzyme)

0.5 µl BSA (corresponding to manufacturers guidelines for the given enzyme)

1 µl enzyme 1

1 µl enzyme 2 (if double digest)

1-5 µl template

MiliQ-water to 30 µl

For the double digests performed in this thesis, the following recommended guidelines were followed:

Enzyme	Cat#	Temp	Supplied NEBuffer	Supplements		% Activity in NEBuffer			
				BSA	SAM	1	2	3	4
<i>Kpn</i> I	R0142	37°C	NEBuffer 1	Yes	No	100	75	0	50
<i>Sac</i> I	R0156	37°C	NEBuffer 1	Yes	No	100	50	10	100
<p>Double Digest Recommendation(s) for <i>Kpn</i> I + <i>Sac</i> I:</p> <p>Digest in NEBuffer 1 + BSA at 37 °C.</p>									

Table 2.3: Double digest recommendations for restriction enzymes *Kpn* I and *Sac* I, used to cut the plcR-upstream PCR product (www.neb.com)

Enzyme	Cat#	Temp	Supplied NEBuffer	Supplements		% Activity in NEBuffer			
				BSA	SAM	1	2	3	4
<i>Bam</i> H I	R0136	37°C	NEBuffer BamH I	Yes	No	75	100	50	75
<i>Sal</i> I	R0138	37°C	NEBuffer 3	Yes	No	0	0	100	0
<p>Double Digest Recommendation(s) for <i>Bam</i>H I + <i>Sal</i> I:</p> <p>Digest in NEBuffer BamH I + BSA at 37 °C.</p>									

Table 2.4: Double digest recommendations for restriction enzymes *Bam*H I and *Sal* I, used to cut the plcRdownstream PCR product (www.neb.com)

Enzyme	Cat#	Temp	Supplied NEBuffer	Supplements		% Activity in NEBuffer			
				BSA	SAM	1	2	3	4
<i>Eco</i> R I	R0101	37°C	NEBuffer EcoR I	No	No	100	100	100	100
<i>Hind</i> III	R0104	37°C	NEBuffer 2	No	No	50	100	10	50
<p>Double Digest Recommendation(s) for <i>Eco</i>R I + <i>Hind</i> III:</p> <p>Digest in NEBuffer <i>Eco</i>R I at 37°C.</p>									

Table 2.5: Double digest recommendations for restriction enzymes *Eco*R I and *Hind* III, used to cut the entire plcRupstream_plcRdownstream_resistance-cassette insert out of the pUC19 clone (www.neb.com)

2.3.8 Dephosphorylation of linearized vector 5' ends

In some instances, when using only one restriction enzyme in cutting reactions, treatment with calf alkaline phosphatase (CIP) was used to remove phosphate groups at the 5' end of the vector to prevent religation of plasmid without insert.

CIP reaction mixture:

2 µl CIP (NEB) (diluted 10 times with MilliQ-water)

4 µl DNA template

The reaction mixture was incubated at 37°C for 1 hour.

2.3.9 Ligation and Transformation

After PCR product and cloning vector were cut with corresponding restriction enzymes, the PCR product was ligated into the cloning vector (pUC19) and transformed into competent *E. coli* cells. Amounts of PCR product and plasmid vector in the ligation reaction were determined from agarose gel visualisation and the principal that there was to be a 1:5 molar ratio of plasmid to insert was followed.

Ligation mixture (total volume 20 µl):

1-5 µl insert

10-15 µl plasmid

2 µl T4 DNA ligase (NEB)

2 µl T4 DNA ligase buffer (NEB)

MilliQ-water to 20 µl

Ligation mixture was incubated overnight at 16°C.

To transform, 5 µl of ligation mixture was added to 50 µl One Shot TOP10 Competent cells (Invitrogen). One Shot TOP10 competent cells are cells made competent, i.e. able to take up foreign DNA via plasmids transformed to requirements. One Shot TOP10 competent cells have a transformation efficiency of $\sim 1 \times 10^9$ cfu/µg DNA. Manufacturer's guidelines were followed. Transformed competent cells (50-200 µl) were plated on LB agar containing 100 µg/ml ampicillin and grown over night at 37°C. Self-ligated pUC19 was always used as ligation and transformation control and showed that manufacturer's transformation efficiency concurred with our results. The subsequent single colonies were picked and grown overnight in 10 ml LB-medium at 37°C and shaking (225 rpm). 3 ml of over night culture was used for plasmid purification, using QIAprep Miniprep kit (Qiagen). QIAprep miniprep kit is based on alkaline lyses of bacterial cells followed by absorption of DNA onto silica in presence of high salt. Elution is done in low-salt buffers. Manufactures guidelines were followed.

The presence and product size of insert in plasmid was checked by corresponding restriction enzyme digestion (2.3.7) and agarose gel electrophoresis (2.3.4) to visualise presence or absence of plasmid containing the expected insert.

2.3.10 Sequencing

Sequencing of constructs was performed at the Institute of Molecular Bioscience, University of Oslo, Oslo, Norway, on plasmids (pUC19) containing inserts of different origin. Sequencing of plasmid vector clones (pUC19) containing resistance cassettes was done by GATC Biotech (Germany). All sequencing was done using M13forward and M13reverse primers.

2.3.11 Sequence Analysis

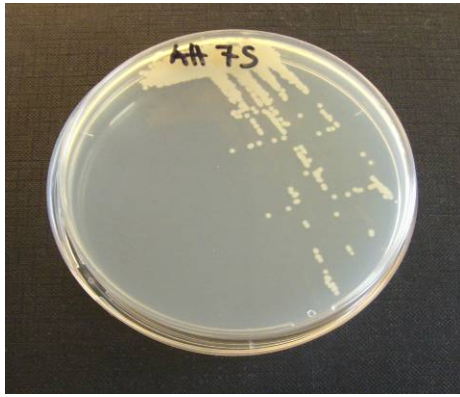
DNA sequences were viewed using GATCViewer 1.00 sequence analysis software (GATC Biotech, Germany), aligned using Vector NTI Suite 9 (Contig Express Project) and analysed using BLAST (<http://www.ncbi.nih.gov/>).

3 RESULTS

3.1 Colony morphology of strains screened for biofilm

The morphology and the bacterial colony structure was speculated to be linked to a strains ability to form biofilm and strains were therefore grown on LB agar at 30°C, over night, for use in growth experiments, for use in biofilm screening and to investigate whether colony morphology could be correlated to the strains ability to form biofilm. Strain colonies depicted (Picture 3.1 – 3.2) are both biofilm-positive (+) and biofilm-negative (-) strains and did, in reference to results of biofilm screening, show that the colony morphology of the strains is independent of their biofilm formation ability. For the *Bacillus cereus* group bacteria the morphology of the colonies are somewhat different, but differences are seen mainly in the size of the colonies and the general shape of the colonies. Some strains, e.g. AH 183 and AH 1031, form larger colonies with a somewhat jagged outline, while other strains, e.g. AH 75 and AH 1248, form smaller colonies with a smooth outline.

The only strain with uncharacteristic colony morphology for *B. cereus* or *B. thuringensis* was AH 884. This strain showed a “slime-like” growth, with no presence of single colonies, and came especially to our attention because it was seen to be a very strong biofilm former (3.3.4). AH 884 is a clinical isolate, isolated from patient blood (Rikshospitalet, Oslo, Norway), and was originally characterised *B. cereus*. However, 16S rRNA sequencing performed during this study (Erlendur Helgason, personal communication), identified AH 884 as *Bacillus licheniformis*, which are known for their abilities to form biofilm (Ameur *et al.*, 2005).



Picture 3.1: Colony morphology of biofilm-positive (+) and biofilm-negative (-) strains; *Bacillus cereus* AH 75 (+), AH 183 (-), AH 226 (+), AH 405 (+), AH 604 (+) and AH 815 (+) grown on LB agar, ON, at 30°C.



Picture 3.2: Colony morphology of biofilm-positive (+) and biofilm-negative (-) strains; *Bacillus cereus* AH 884 (+), AH 1031 (+) and AH 1248 (-) grown on LB agar, ON, at 30°C.

3.2 Growth curves

3.2.1 Standard growth curve for reference strains

Standard growth curve experiments (2.2.2) were done to see and to verify the ability for the strains to reach exponential phase at approximately the same time point (Figure 3.1). To produce this standard growth curve, the three reference strains (*B. cereus* ATCC 10987 (biofilm-positive), *B. cereus* ATCC 14579 (biofilm-negative) and *B. thuringensis* 407 (biofilm-positive)) were used and results used as indicative for all 81 strains throughout the biofilm screening.

For this experiment were strains grown for 5 hours, at 30°C and shaking at 225 rpm, in a total volume of 200 ml LB medium, in a 1 l flask. Every half hour, 1 ml samples were taken and measured (OD₆₀₀).

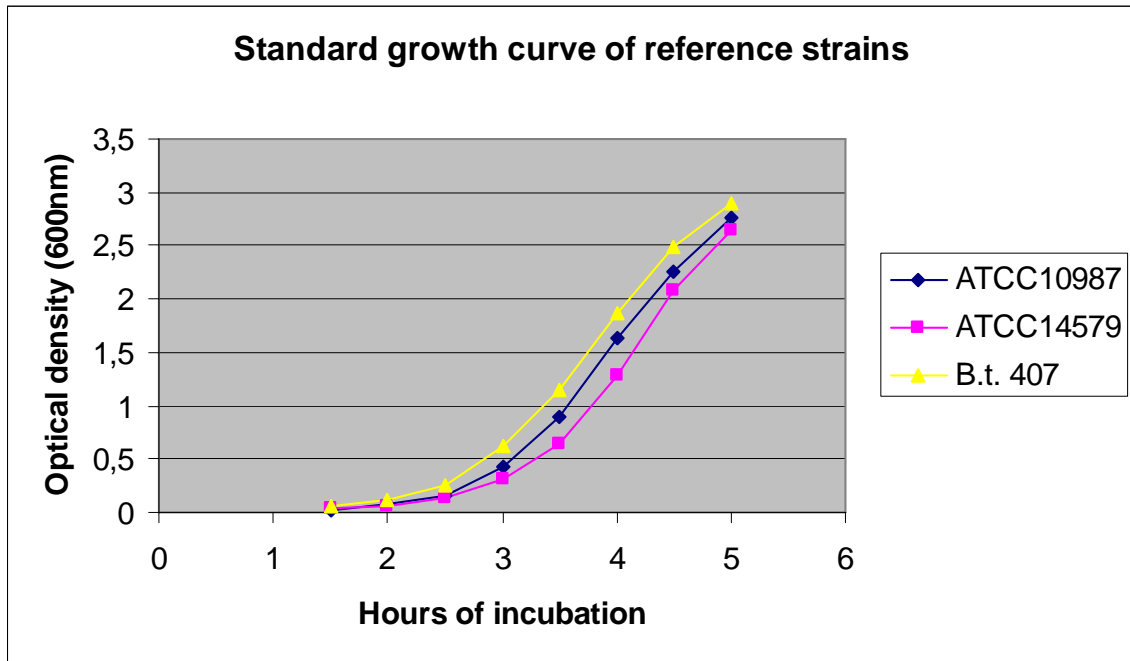


Figure 3.1: Standard growth curve for reference strains *Bacillus cereus* ATCC 10987, *Bacillus cereus* ATCC 14579 and *Bacillus thuringiensis* 407, grown in LB medium at 30°C and 225 rpm.

The standard growth curve for reference strains (Figure 3.1) indicated that the different strains grow with similar speed and reach exponential growth phase at approximately the same time point, 3 hours into incubation at 30 °C and 225 rpm. No difference between strains forming biofilm and those that do not, in the rate of growth, could be indicated or observed. This time point was therefore used consequently as time point for the extraction of samples for use during growth in microtiter plates.

3.2.2 Standard growth curves for selected biofilm screened strains

Standard growth curve experiments (2.2.2) were done using a group of selected strains, which were used during screening for biofilm formation. This was done to see and to verify, such as with the reference strains, if the ability for the strains to reach exponential growth phase at approximately the same time point was certain. To produce this standard growth curve, five strains, both biofilm-positive (+) and biofilm-negative (-), used during the biofilm screening were picked (Figure 3.2).

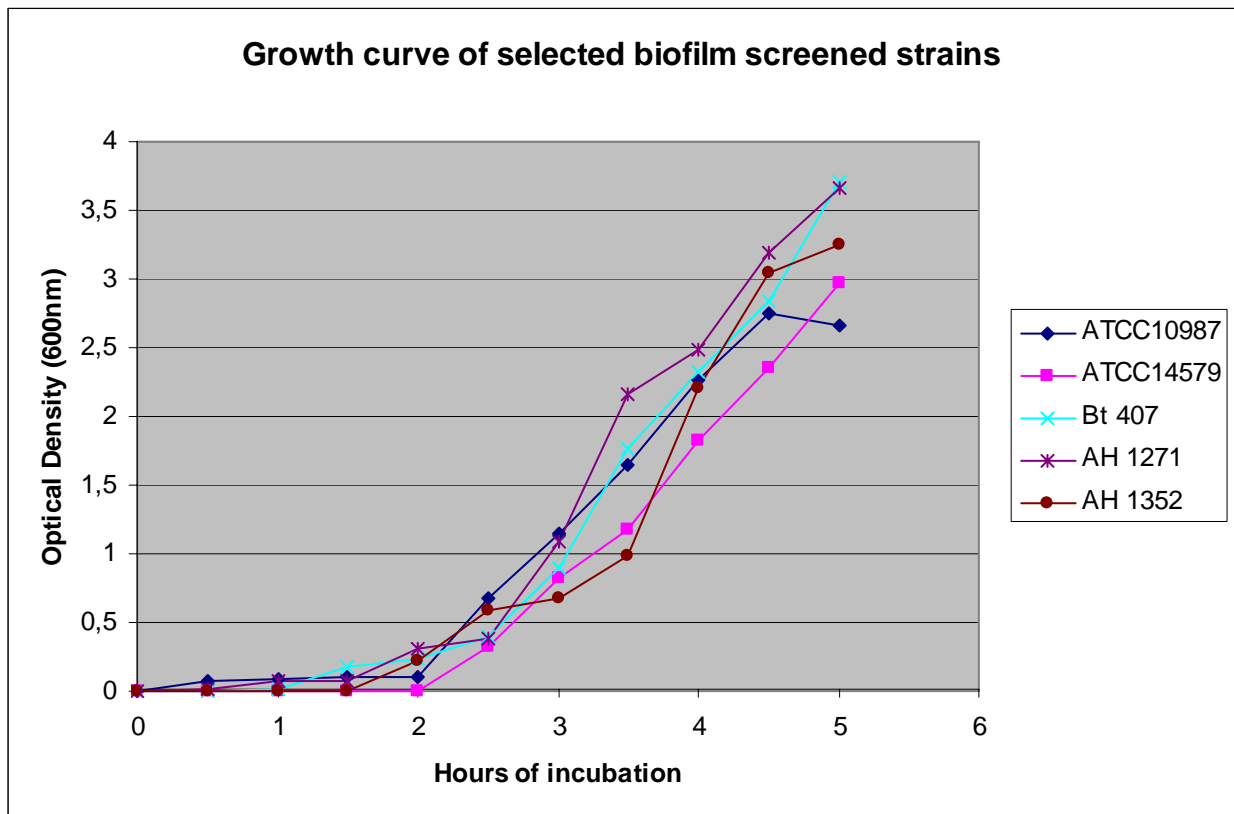


Figure 3.2: Growth curve of selected biofilm screened strains; *B. cereus* ATCC 10987 (+), *B. cereus* ATCC 14579 (-), *B. cereus* AH 1271 (-), *B. cereus* AH 1352 (-) and *B. thuringensis* 407 (+), grown in LB medium, at 30°C and 225 rpm.

The standard growth curve for selected biofilm screened strains (Figure 3.2) indicated that the different strains grow with similar speed and reach exponential growth phase at approximately the same time point, 3 hours into incubation at 30 °C and 225 rpm. No difference is observed between strains known to form biofilm and those strains known not to form biofilm. This again indicated that cultures, after 3 hours of growth, could be used consequently as time point for the extraction of samples for use during growth in microtiter plates.

3.2.3 Crystal violet staining of serial dilutions of bacterial strains

Crystal violet was used in the biofilm screening procedure as a dye to indicate the presence of cells left in the microtiter plate wells after incubation and wash, and therefore also used to indicate the level of biofilm formed by the strain. A serial dilution of bacteria, which would be subsequently dyed with crystal violet, allowed us to observe the relationship between the amount of cells dyed and the absorbance of crystal violet measured.

Reference strains *Bacillus cereus* ATCC 10987, *Bacillus cereus* ATCC 14579 and *Bacillus thuringensis* 407 were picked and used for this comparison.

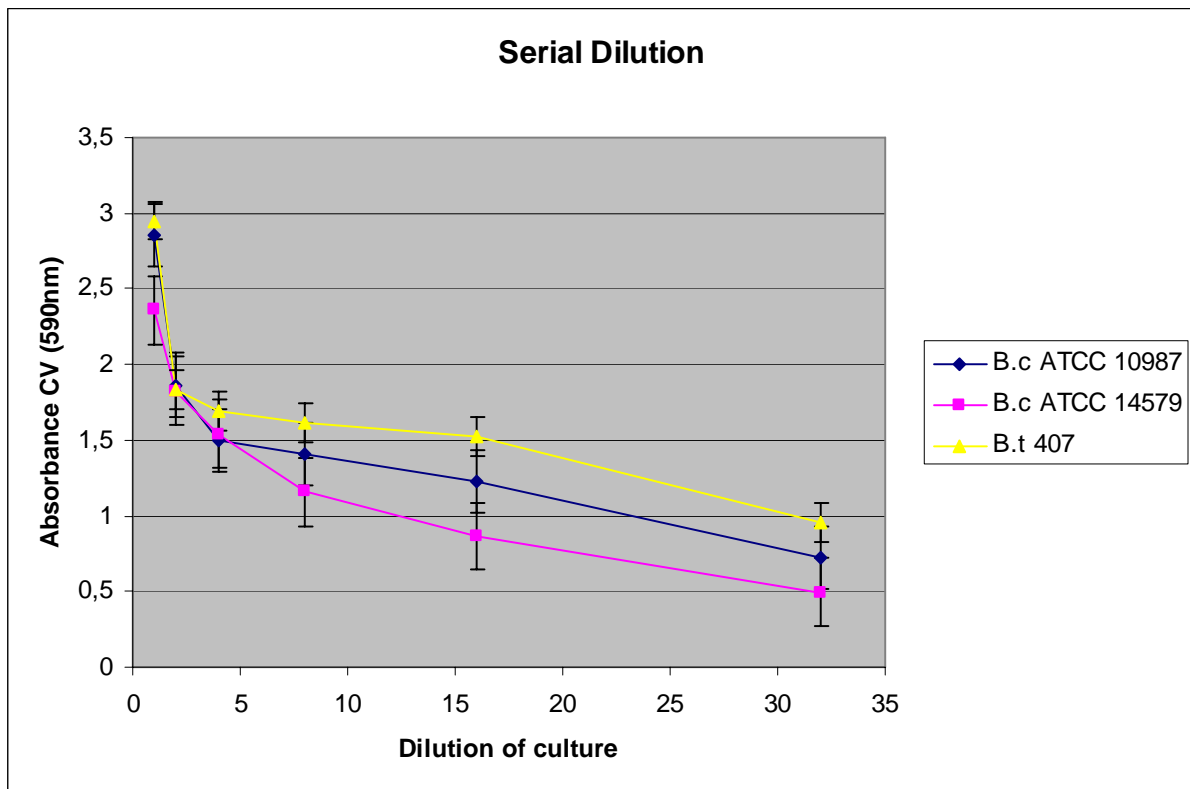


Figure 3.3: Crystal violet staining of bacterial serial dilution using *B. cereus* ATCC 10987, *B. cereus* ATCC 14579 and *B. thuringensis* 407, serially diluted and stained with crystal violet. The data represents the mean of four independent experiments, and error bars indicate standard deviation.

The results (Figure 3.3) indicated that the amount of bacterial cells present in the sample corresponded roughly to the absorbance of crystal violet at 590 nm. This is clearly linked with the biofilm screening procedure in the way that the amount of bacterial cells left in the wells after incubation and have formed a biofilm, will be stained by the crystal violet, and furthermore indicated that the amount of crystal violet measured at 590nm is linked to the amount of bacterial cells present in the wells, i.e. have bound to the wells and formed a biofilm.

3.3 Biofilm screening

The screening of strains for the formation of biofilm was preformed, due to the aims of this project, to be able to collect information on a strains ability to form biofilm.

3.3.1 Establishing the biofilm screening method

To establish the method for biofilm screening, four strains were selected. These four strains were selected due to background knowledge (Michel Gohar, personal communication) of their ability to form biofilm (+) or of not to form biofilm (-). The establishment of the biofilm screening method, using strains of known biofilm forming abilities, was done to make sure that the method used in our laboratory gave the same result as other laboratories. The following strains were selected for the establishment of the biofilm screening method in our laboratory:

- *Bacillus cereus* ATCC10987 (AH 75) (+)
- *Bacillus cereus* ATCC14579 (AH 183) (-)
- *Bacillus cereus* AH 812 (-)
- *Bacillus thuringensis* 407 (AH 1031) (+)

Strains were plated from -70°C stock on LB agar and grown over night at 30°C, a single colony was picked and inoculated in 10 ml LB medium, and grown over nigh at 30°C and 225 rpm. Over night culture (100µl) was grown for 3 hours in 10 ml LB medium, at 30°C and 225 rpm. After 3 hours of growth, 50µl of the culture was added to 10 ml Bactopeptone medium and 125 µl of this suspension was transferred to each well of three 96-well microtiter plates. For initial experiments, Costar flat well, 96-well microtiter plates were used. Microtiter plates were incubated for 24, 48 and 72 hours respectively, at 30°C, washed with PBS

(150µl), stained with crystal violet (130µl) and washed with PBS (180µl) three times.

Attached cells were resuspended in acetone/ethanol (1:4) (150µl) and absorbance measured at 590nm (2.2.3).

The results are shown in figure 3.4, 3.5 and 3.6:

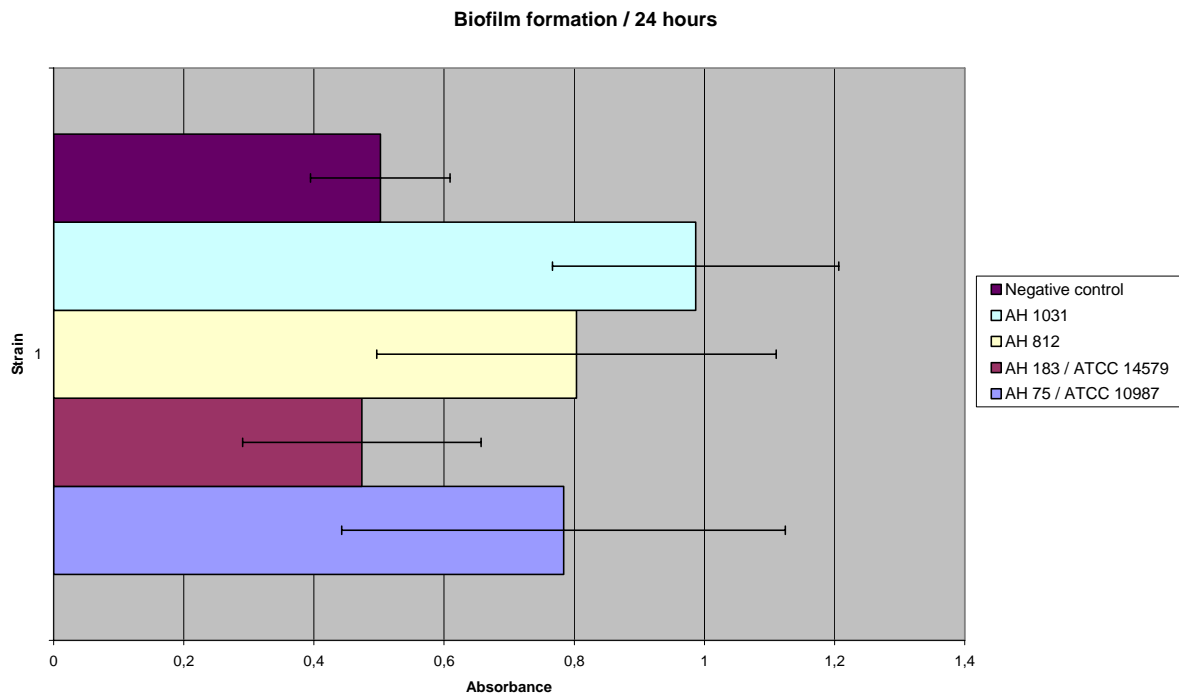


Figure 3.4: Absorbance (590nm) after 24 hours growth for *B. cereus* ATCC 10987, *B. cereus* ATCC 14579, *B. cereus* AH812 and *B. thuringensis* 407. Negative control is Bactopeptone medium incubated in the same conditions as the other samples.

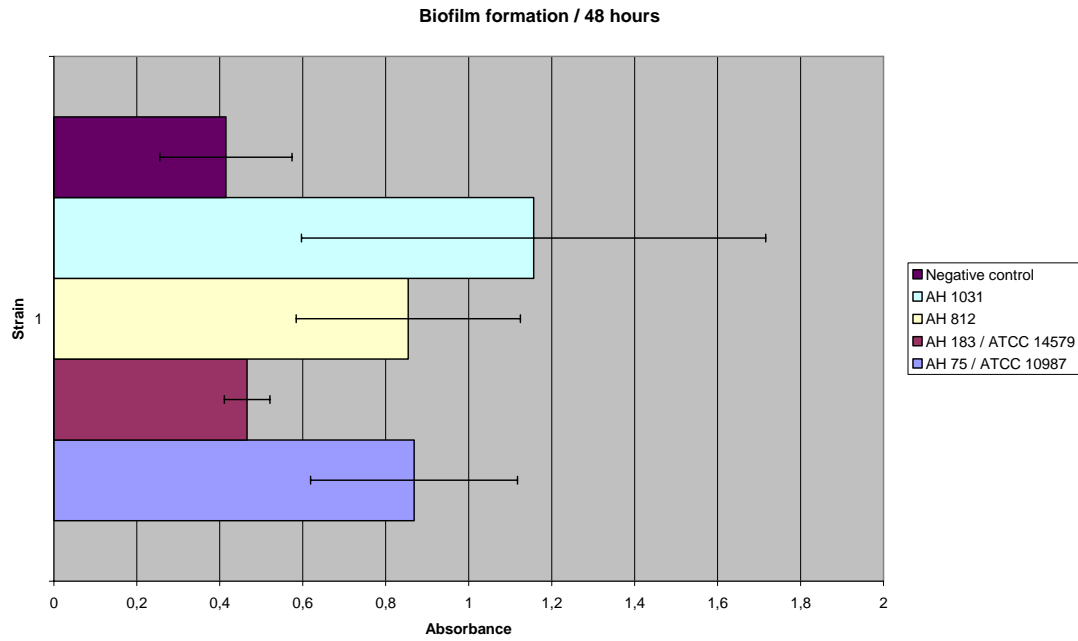


Figure 3.5: Absorbance (590nm) after 48 hours growth for *B. cereus* ATCC 10987, *B. cereus* ATCC 14579, *B. cereus* AH812 and *B. thuringensis* 407. Negative control is Bactopeptone medium incubated in the same conditions as the other samples.

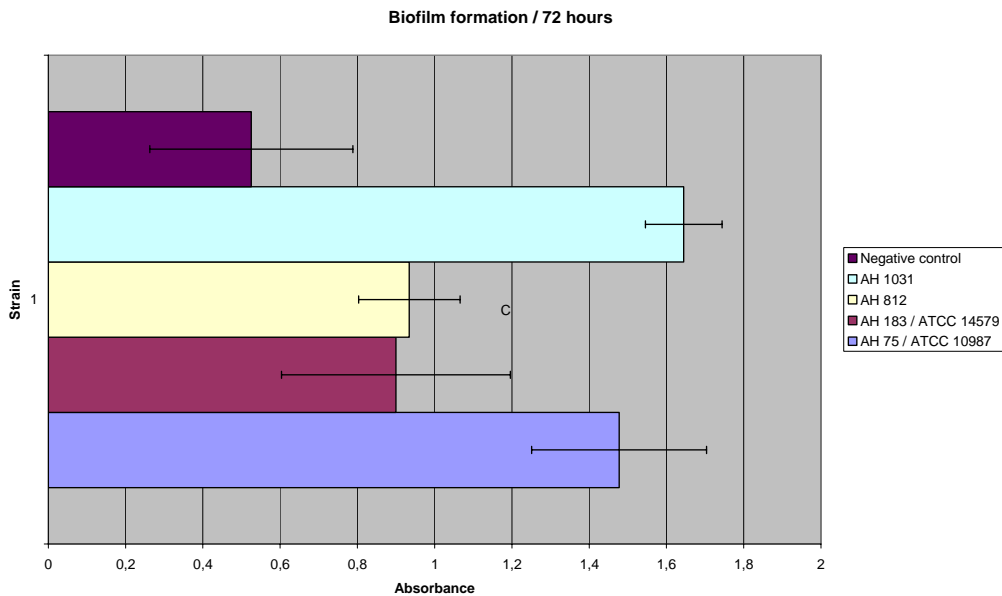


Figure 3.6: Absorbance (590nm) after 72 hours growth for *B. cereus* ATCC 10987, *B. cereus* ATCC 14579, *B. cereus* AH812 and *B. thuringensis* 407. Negative control is Bactopeptone medium incubated in the same conditions as the other samples.

The results showed that the known biofilm forming strains, *B. cereus* ATCC 10987 and *B. thuringensis* 407 were positive in this assay, while the known non biofilm forming strain, *B. cereus* ATCC 14579 was negative in this assay after 24 and 48 hours of incubation, but positive after 72 hours of incubation. *B. cereus* AH 812 gave a positive result at all three time points, but values were somewhat lower than *B. cereus* ATCC 10987 and *B. thuringensis* 407. Standard deviation and background signal was however relatively high for this set of experiments.

These test experiments did show that there are clear differences in the degree of attachment of bacterial cells, the retention of crystal violet by those cells and the absorbance of crystal violet at 590 nm between a biofilm forming strains, such as *B. thuringensis* 407, and non biofilm forming strains, such as *B. cereus* ATCC 14579. These test experiments also verified that the method used in our laboratory gave the same results as in other laboratories, indicating that our method is viable and useful. As seen, the negative control (pure bactopectone medium), did give some background signal, which could be seen due to retention of unspecific bound crystal violet in the wells. This background signal was later subtracted from the final absorbance measured for the 81 strains tested.

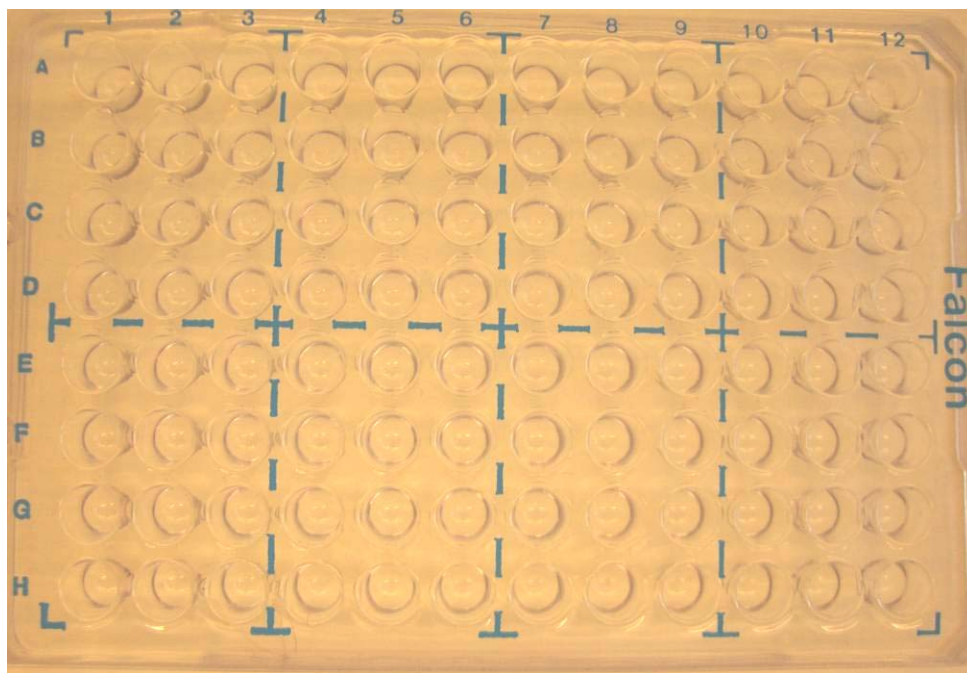
3.3.2 Optimization of biofilm screening method

Optimization of the biofilm screening method was preformed to be able to establish a method, which could be reproducible, reliable and give certain results through measurement of absorption and visualization of the biofilm ring formation after staining with crystal violet. When growing bacteria in such conditions, in a microtiter plate, there are many factors, which can possibly have an effect on the growth of the bacteria and the formation of biofilm, and there were these uncertainties, which were wished to be removed. Several different

parameters of the biofilm screening method were varied to control and to optimize the method.

For the optimization of the biofilm screening method, four strains, same four as used for establishment of the method (3.3.1), were picked and used under all the different conditions tested. These parameters were tested, first individually and later in combination to see if they had any effect on the screening method:

- i) The first parameter to be examined was the microtiter plates used in the screening. Earlier studies (Michel Gohar, personal communication) had shown that PVC based microtiter plates gave the best conditions for *B. cereus* group bacteria to form biofilm and that microtiter plates with round-bottomed wells allowed the bacteria to form a better and stronger biofilm. This resulted in the switch from flat-bottomed microtiter plates (Costar 2595 96-well flat bottomed PVC microtiter plates) to round-bottomed microtiter plates (Falcon 353911 96-well round bottomed PVC microtiter plates, picture 3.3).



Picture 3.3: Falcon, PVC, round-bottom, 96-well microtiter plate.

- ii) The use of bactopectone medium, i.e. medium where tryptone had been replaced with bactopectone, for the incubation in the microtiter plates, had been seen to increase the ability of *B. cereus* strains to form biofilm and was therefore used when cultures were grown in the microtiter plates (Michel Gohar, personal communication).
- iii) From immunological studies, the positioning of samples, the amount of culture in each well and the use of buffers in a microtiter plates have been seen to have an effect, e.g. when labelling with antibodies. This was therefore tested for to be able to exclude as an interfering variation. The four tested strains were placed in different positions on the microtiter plate, incubated with different volumes (100µl-200 µl) in each well and buffer (PBS and H₂O) was added in surrounding wells. The positioning of the samples in different places on the microtiter plates and the amounts of culture in each well showed no effect on the ability to form biofilm. However, the incubation with water present in the surrounding wells was seen to give stronger biofilm formation for biofilm-positive strains. This, most likely, due to the effect moisture had to hinder the cultures from drying during incubation. The incubation of the microtiter plates on top of a moist filter paper was therefore seen to give better growth conditions. The use of lids for the microtiter plates (Falcon 353913) and the incubation of the microtiter plates inside a closed (with lid) container also allowed the cultures in the microtiter plates to experience better growth conditions (results not shown).
- iv) During initial experiments (3.3.1), the unspecific binding of crystal violet to PVC in the wells was seen to give a high level of background signal and to increase the level of standard deviation. Sterile filtration of the dye, crystal violet, (using a 0.45 µm filter) was therefore performed and seen to reduce unspecific binding of crystal

violet to PVC. This resulted in the reduction of background signal, the subsequent reduction of standard deviation and allowed clearer positives and negatives to be observed.

The optimized screening method was as followed: For each time point, 24, 48 and 72 hours, two Falcon 353911 96-well round bottomed PVC microtiter plates were inoculated identically, with the same strain inoculated in 8 wells on each plate, giving a total of 16 parallel samples for each strain screened, for which the mean value gave the final score. Strains were inoculated in bactopectone and microtiter plates were incubated with lid and on moist filter paper.

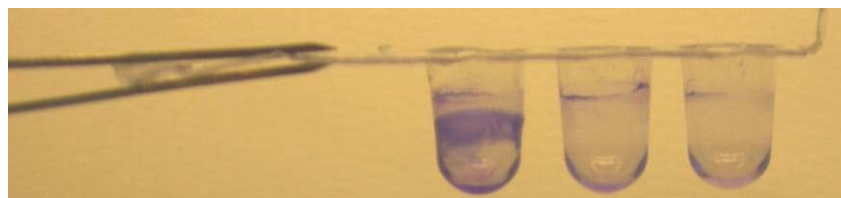
Even in the optimized screening method was a high level of background signal observed, resulting in high standard deviation. This indicated that crystal violet did, by itself, bind to the wells. Unspecific binding of crystal violet was observed in some wells in each parallel, which in turn gave high levels of absorbance and subsequently aided to the rise of the standard deviation. The unspecific binding of crystal violet was not seen to be affected by the time of incubation of the microtiter plate (24, 48 or 72 hours), but somewhat affected by the time the crystal violet was allowed to stain the well. 20 minutes of staining was seen to give the best result, i.e. cells were stained properly and unspecific binding was reduced as much as possible.

For every microtiter plate screened, the positive control *Bacillus thuringensis* 407, the negative control *B. cereus* ATCC 14579 and pure bactopectone medium were added to the plate to use as control of test systems consistency (Picture 3.4).

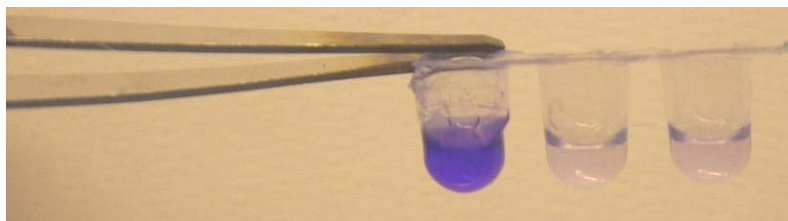


Picture 3.4: Microtiter plate containing 125 μ l culture in first three rows, *Bacillus thuringiensis* 407, *Bacillus cereus* ATCC14579 and pure bactopectone medium.

As observed in picture 3.5 the positive control, *B. thuringiensis* 407, produces a ring of crystal violet in the air-liquid interface of the well. This ring indicated that the cells have attached to the well wall and further indicates that a biofilm has been formed. The well of the negative control, *B. cereus* ATCC 14579, and the well incubated with pure bactopectone did show some ring formation, but this is however where the air-liquid interface was when the wells were stained with crystal violet and indicated unspecific binding. After ring had been dissolved with acetone/ethanol (1:4) (Picture 3.6), colour absorbance gave indication to the amount of crystal violet bound to the well wall.



Picture 3.5: Biofilm ring formation after staining with crystal violet, right to left; *Bacillus thuringiensis* 407, *Bacillus cereus* ATCC14579 and pure bactopectone medium.



Picture 3.6: Wells after addition of acetone/ethanol (1:4), left to right; *Bacillus thuringiensis* 407, *Bacillus cereus* ATCC14579 and pure bactopectone medium.

3.3.3 Screening for biofilm formation in *Bacillus cereus* group bacteria

To screen 81 strains from a *B. cereus* group strain collection available in the research group, the optimized biofilm method was used (3.3.2). Screening results are presented as mean absorbance for each strain with background signal deducted. The results presented (3.7 - 3.30) do therefore not include standard deviation. Please see appendix (6.1) for raw data, including standard deviation for each experiment.

To be able to determine biofilm-positive strains and biofilm-negative strains, some criteria were set. The ability to form biofilm was determined through two linked analysis methods; i) the presence of the ring after staining the well with crystal violet, and, ii) the level of crystal violet absorbance. The presence of the ring after crystal violet staining was easy to observe and to document (Picture 3.5) and equally easy was the measurement of crystal violet absorbance (590 nm) after crystal violet solubilisation (Picture 3.6). However, the level of absorbance after solubilisation had to be compared to the negative control used, background signal deduction and standard deviation. When ring was observed, absorbance of crystal violet was high and standard deviation was low, the strain was marked positive for biofilm formation. When no ring was observed, absorbance of crystal violet was low and standard deviation was high, the strain was marked negative for biofilm formation. As with all scientific experiments, some strains came in between these criteria and were dismissed as

biofilm positive strains due to lack of ring formation or re-checked (3.3.4). These criteria did result in the confirmation of 7 biofilm forming strains for future studies (Table 3.1).

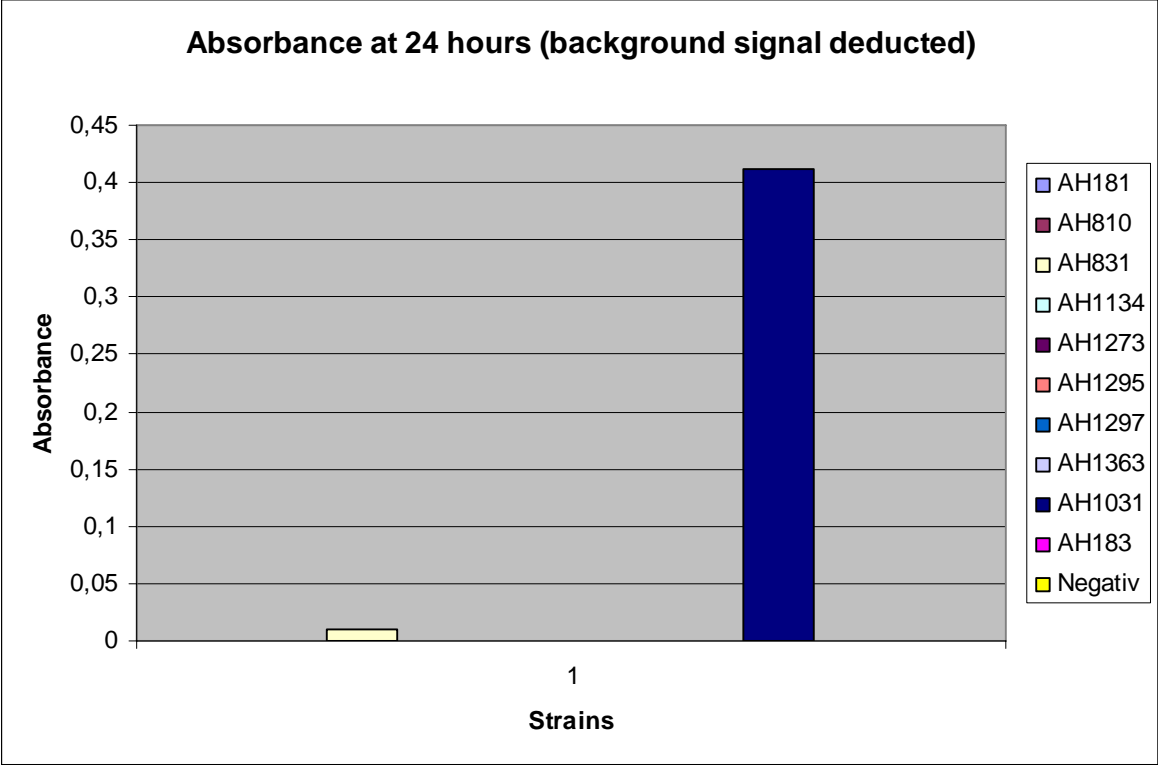


Figure 3.7: Biofilm formation as measured by crystal violet absorbance after 24 hours of incubation (background signal from negative control deducted)

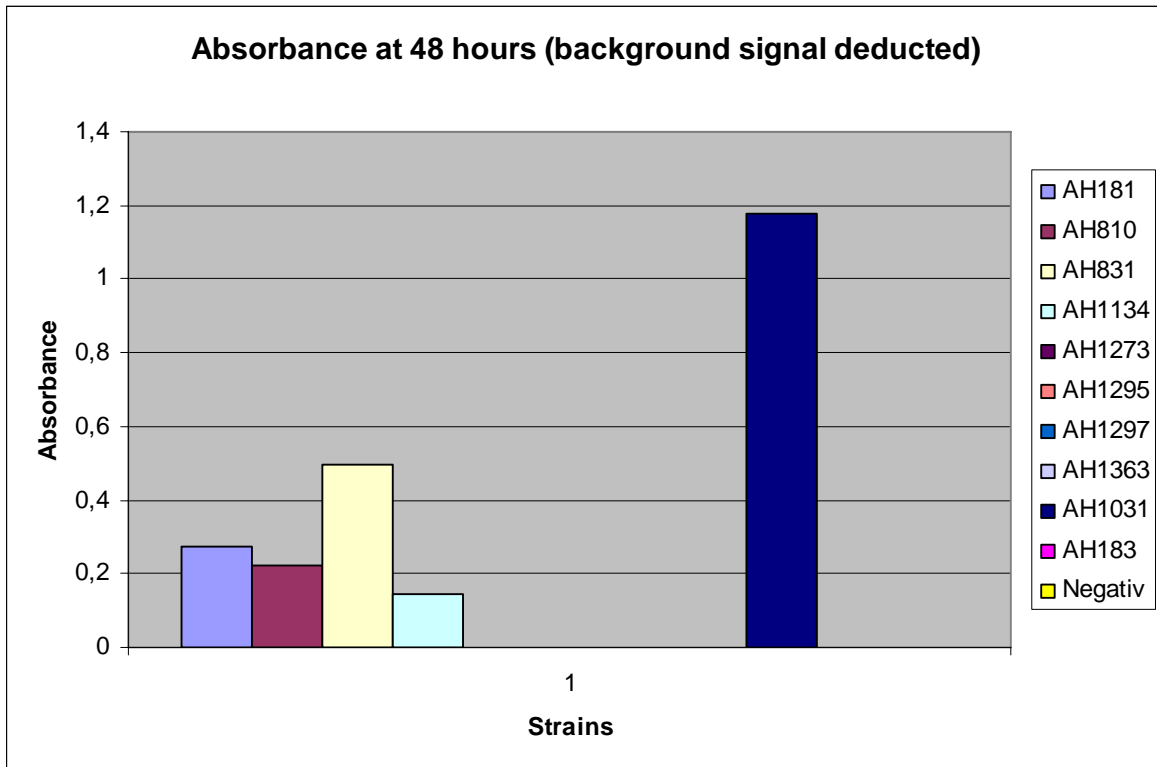


Figure 3.8: Biofilm formation as measured by crystal violet absorbance after 48 hours of incubation (background signal from negative control deducted)

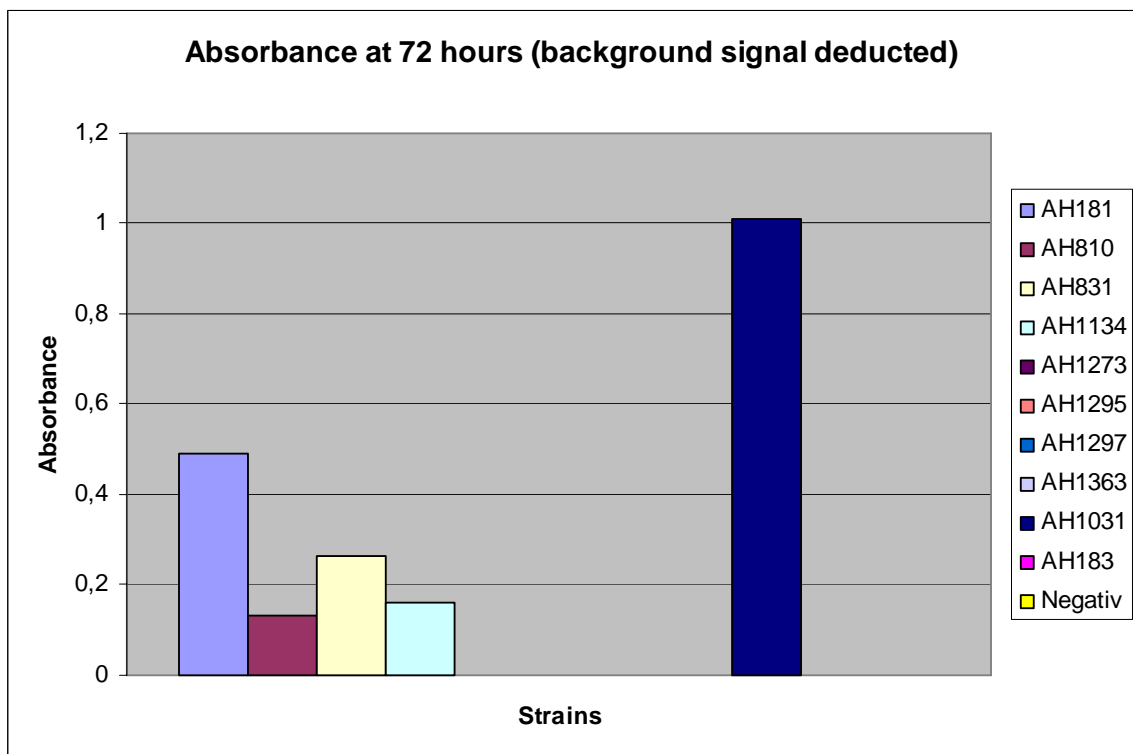


Figure 3.9: Biofilm formation as measured by crystal violet absorbance after 72 hours of incubation (background signal from negative control deducted)

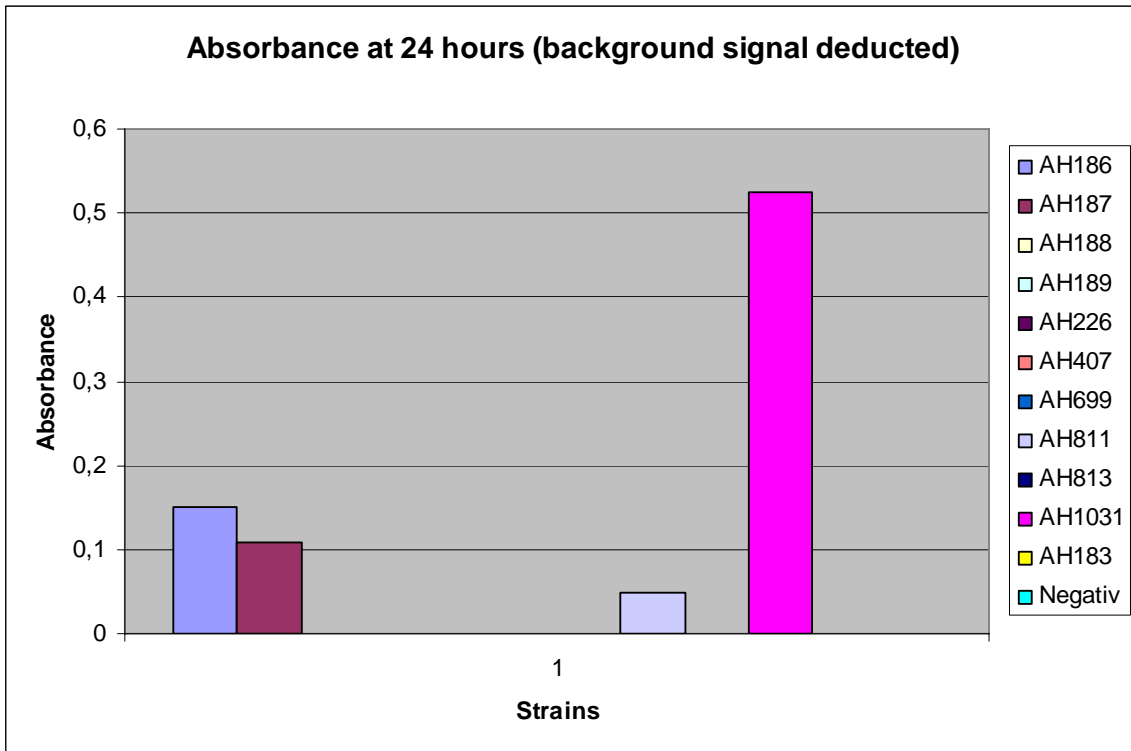


Figure 3.10: Biofilm formation as measured by crystal violet absorbance after 24 hours of incubation
(background signal from negative control deducted)

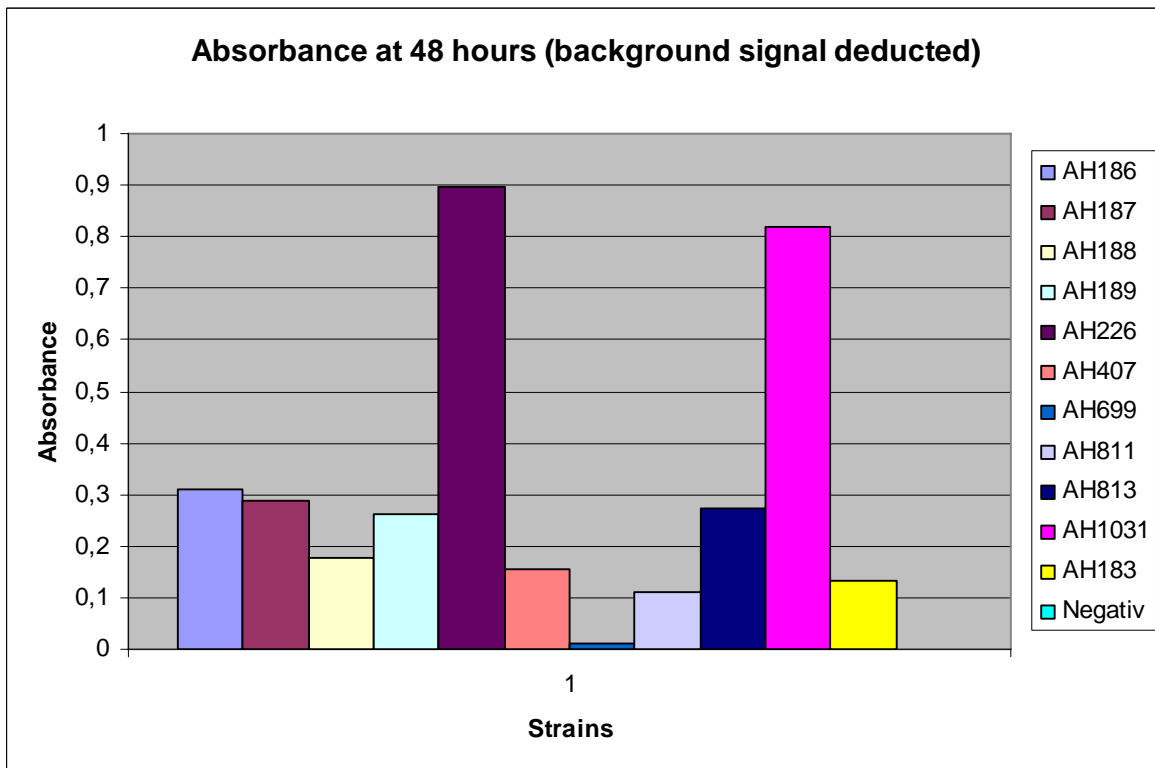


Figure 3.11: Biofilm formation as measured by crystal violet absorbance after 48 hours of incubation
(background signal from negative control deducted)

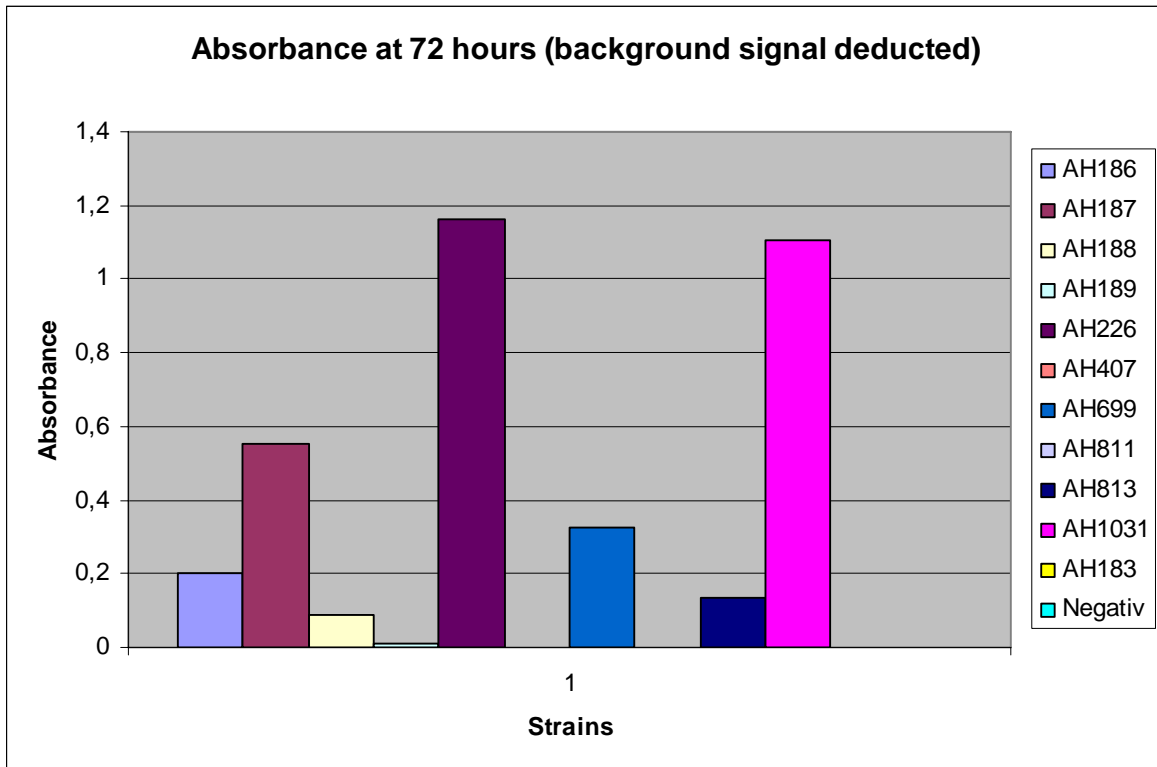


Figure 3.12: Biofilm formation as measured by crystal violet absorbance after 72 hours of incubation
(background signal from negative control deducted)

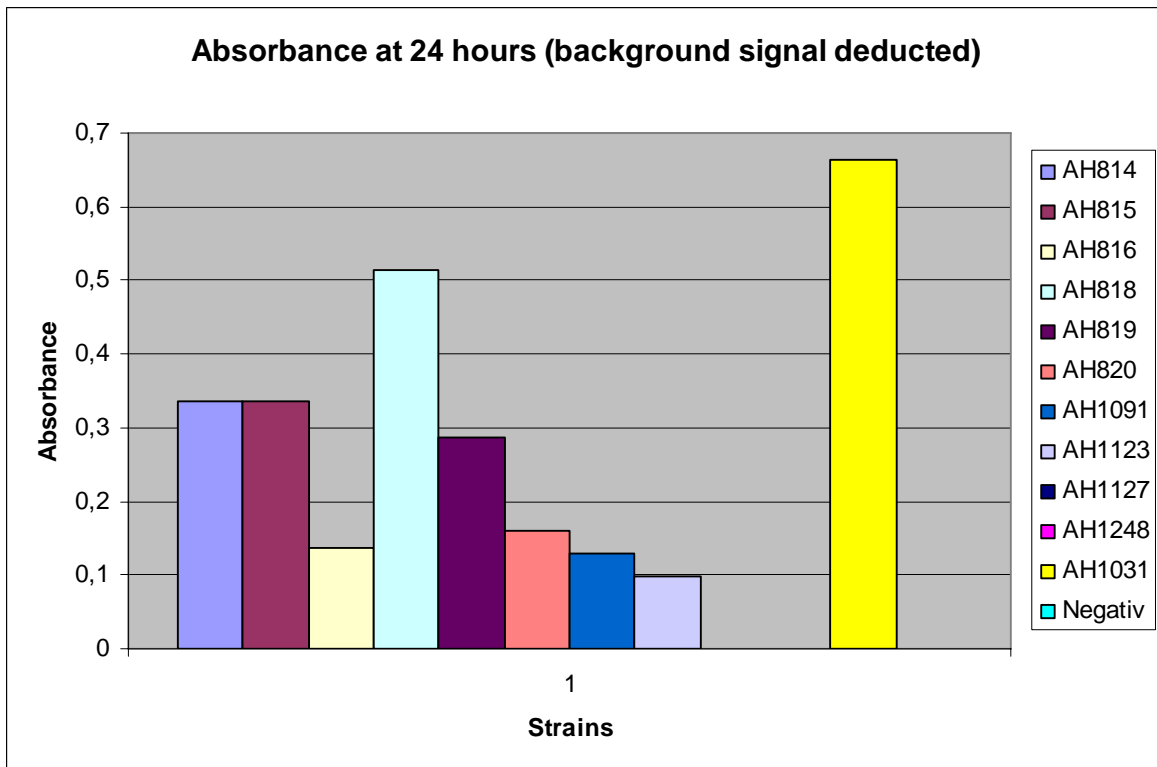


Figure 3.13: Biofilm formation as measured by crystal violet absorbance after 24 hours of incubation
(background signal from negative control deducted)

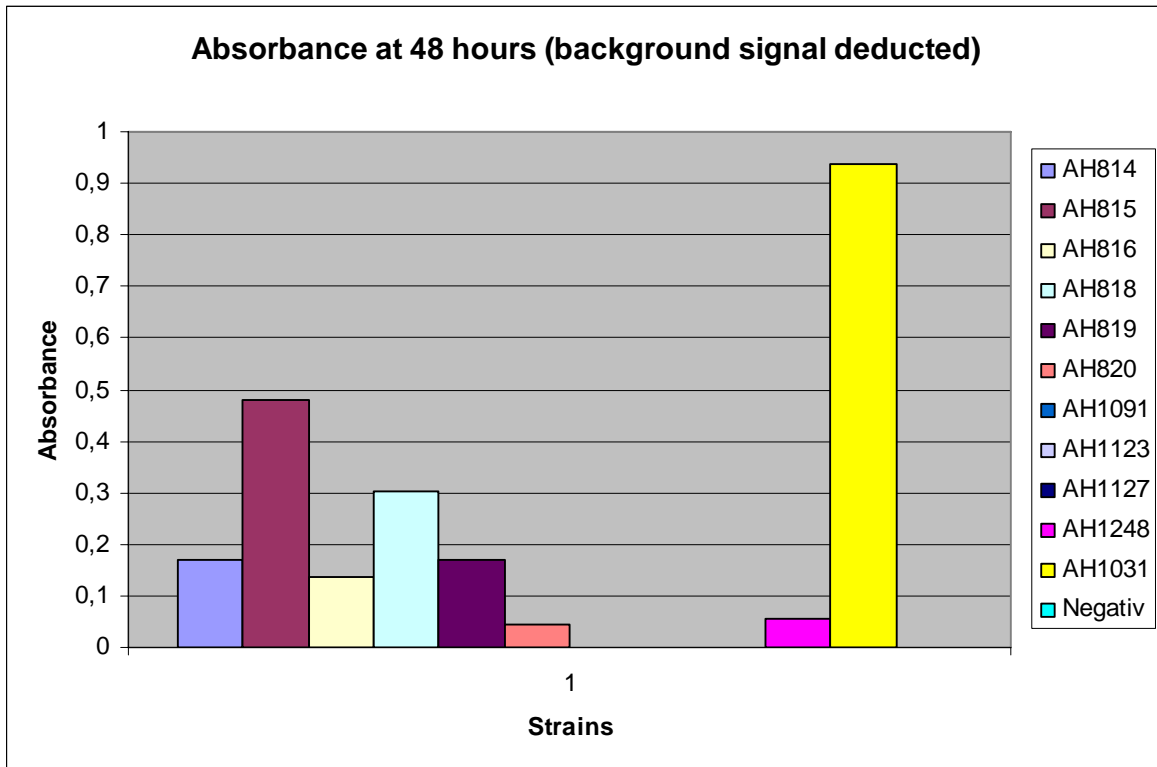


Figure 3.14: Biofilm formation as measured by crystal violet absorbance after 48 hours of incubation
(background signal from negative control deducted)

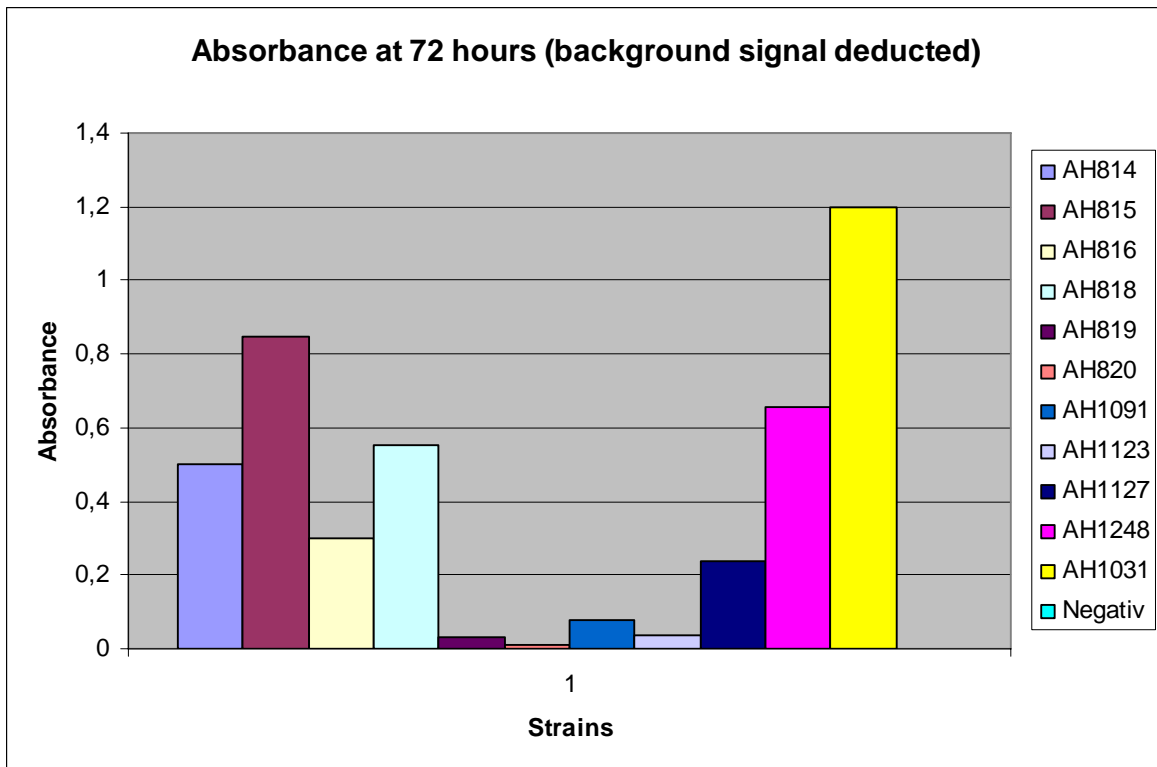


Figure 3.15: Biofilm formation as measured by crystal violet absorbance after 72 hours of incubation
(background signal from negative control deducted)

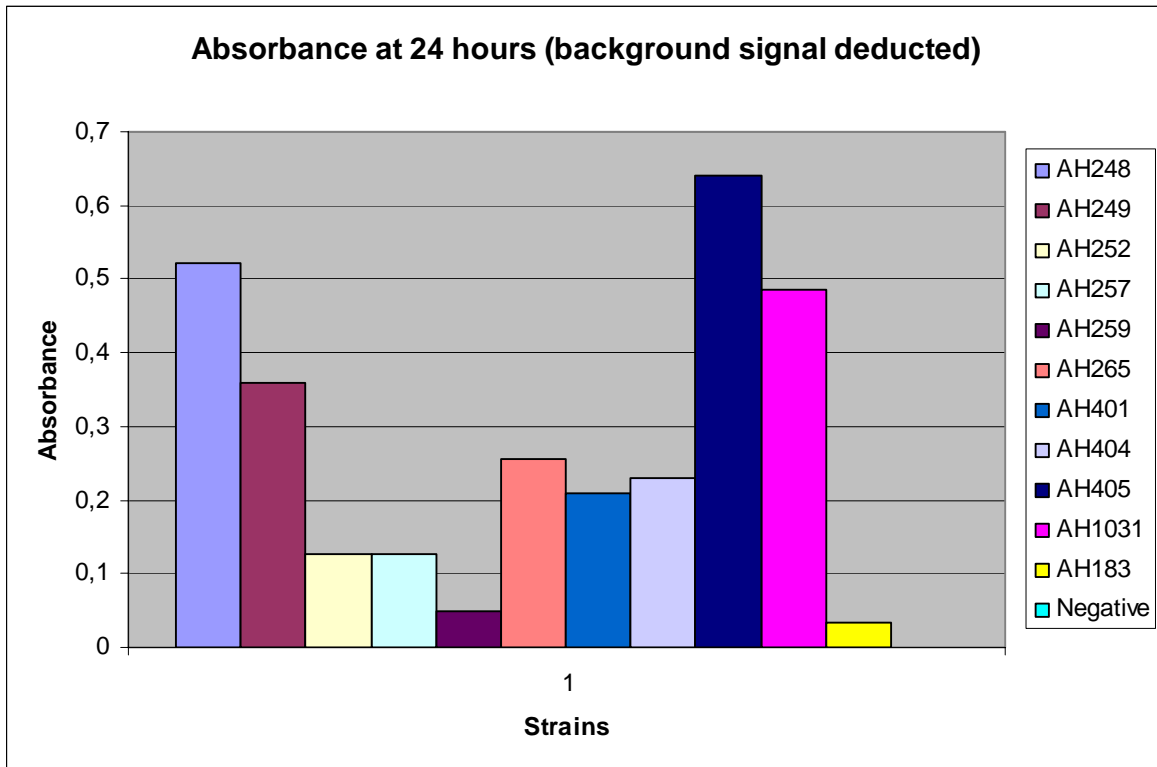


Figure 3.16: Biofilm formation as measured by crystal violet absorbance after 24 hours of incubation
(background signal from negative control deducted)

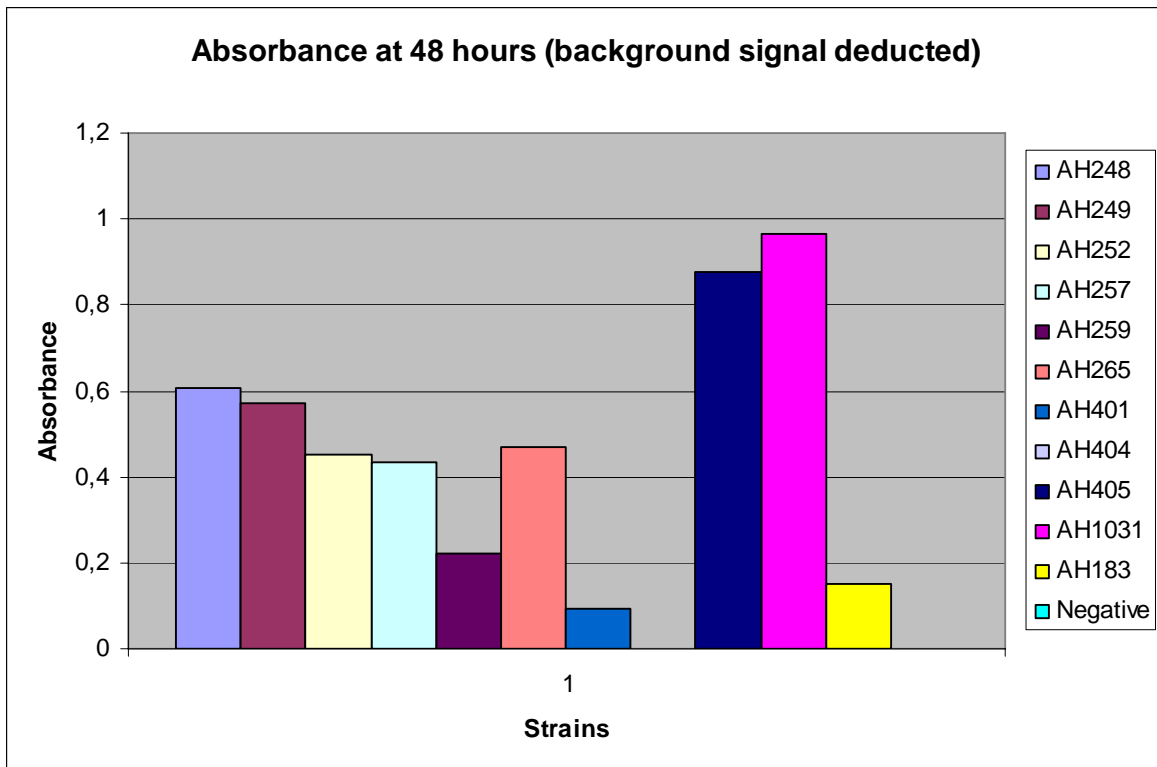


Figure 3.17: Biofilm formation as measured by crystal violet absorbance after 48 hours of incubation
(background signal from negative control deducted)

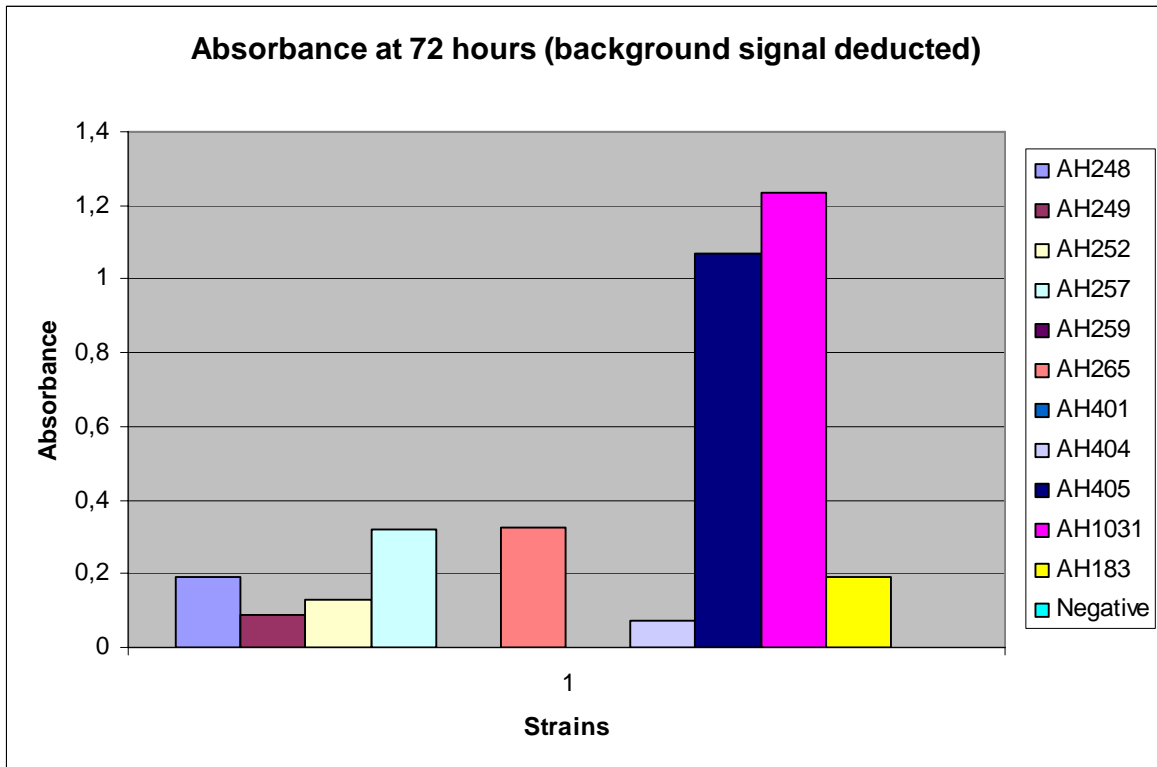


Figure 3.18: Biofilm formation as measured by crystal violet absorbance after 72 hours of incubation (background signal from negative control deducted)

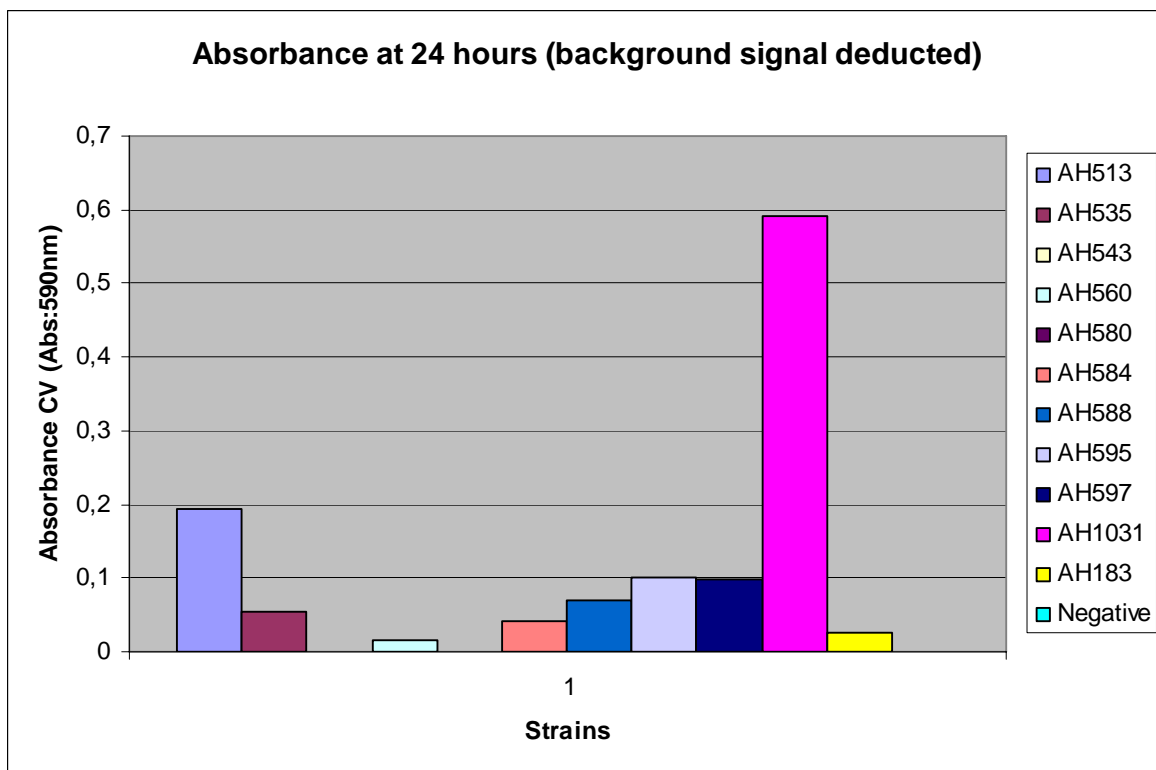


Figure 3.19: Biofilm formation as measured by crystal violet absorbance after 24 hours of incubation (background signal from negative control deducted)

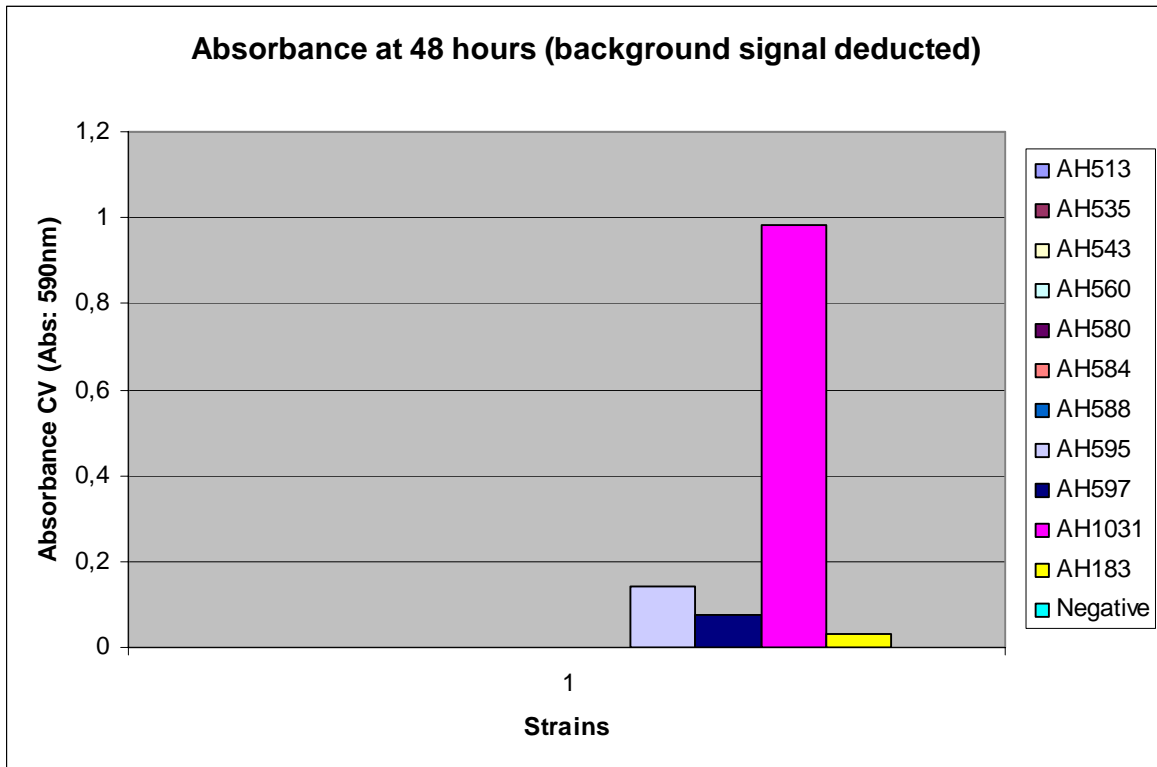


Figure 3.20: Biofilm formation as measured by crystal violet absorbance after 48 hours of incubation (background signal from negative control deducted)

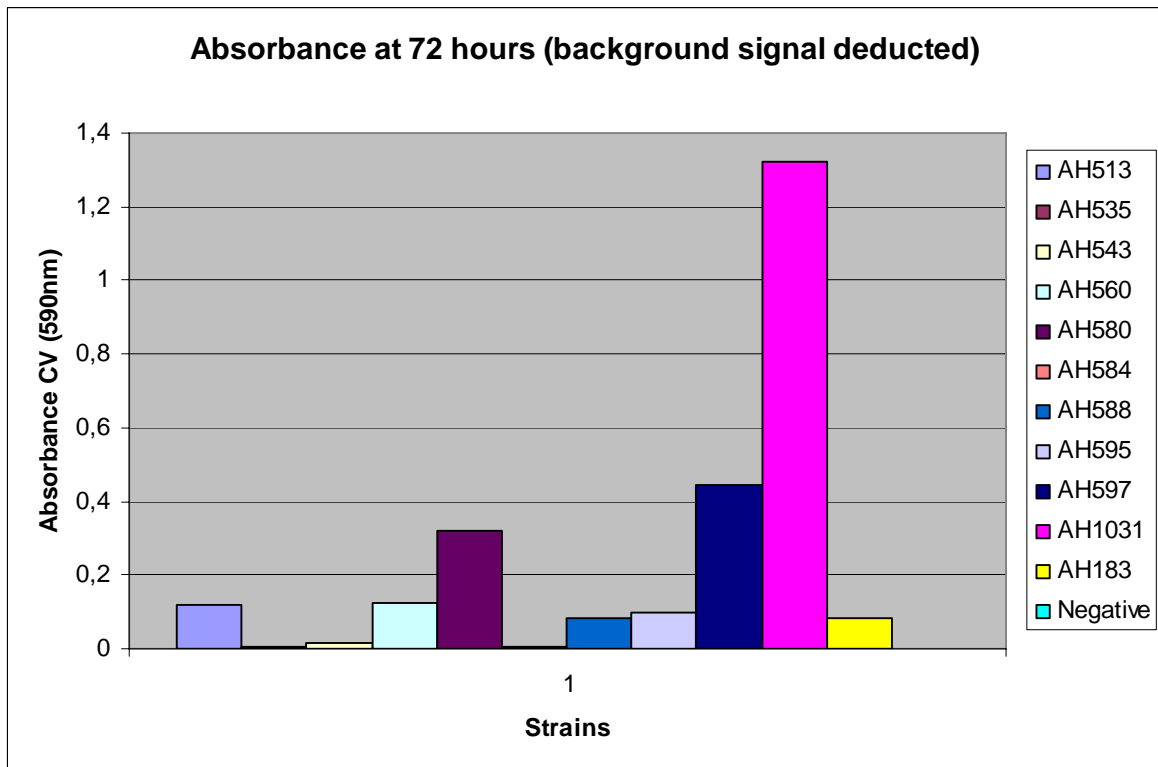


Figure 3.21: Biofilm formation as measured by crystal violet absorbance after 72 hours of incubation (background signal from negative control deducted)

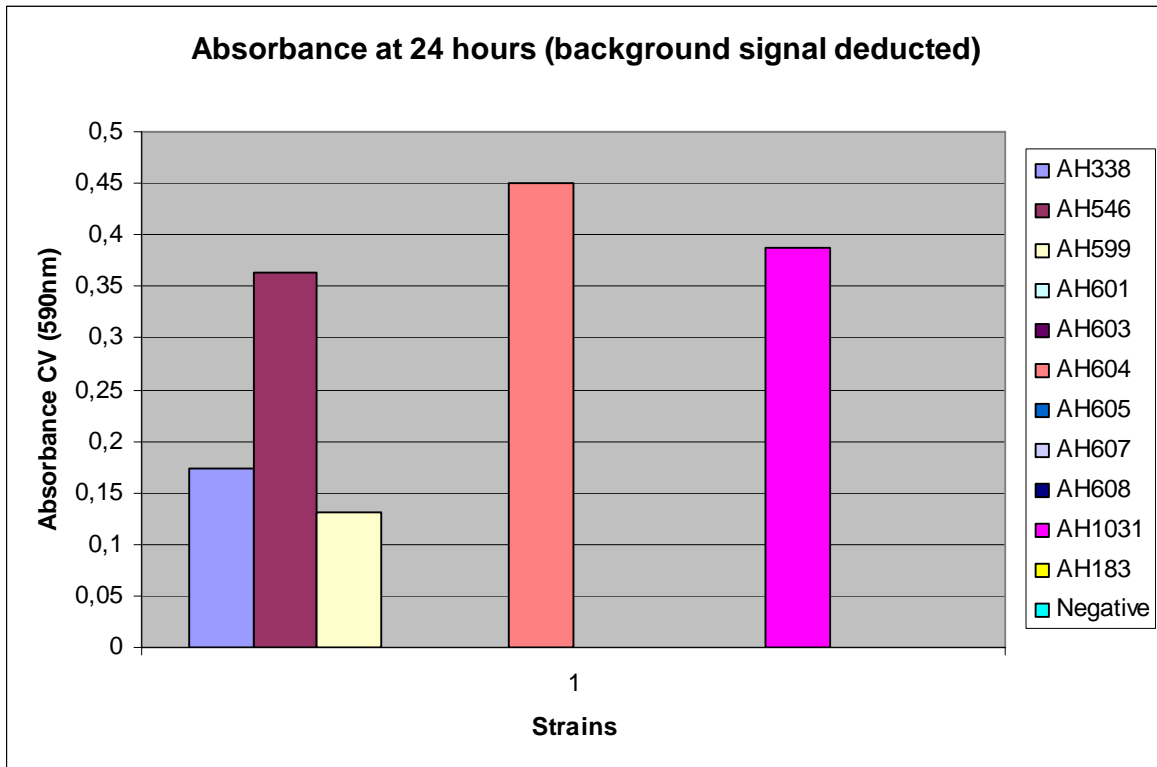


Figure 3.22: Biofilm formation as measured by crystal violet absorbance after 24 hours of incubation
(background signal from negative control deducted)

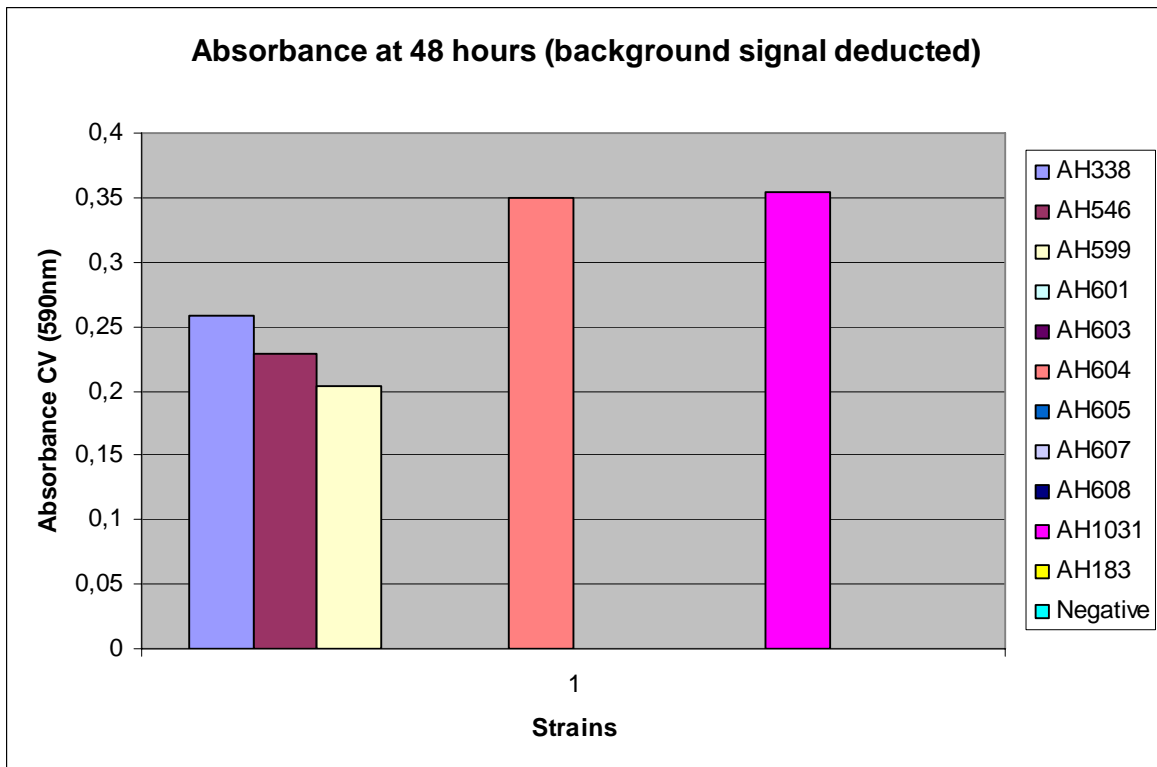


Figure 3.23: Biofilm formation as measured by crystal violet absorbance after 48 hours of incubation
(background signal from negative control deducted)

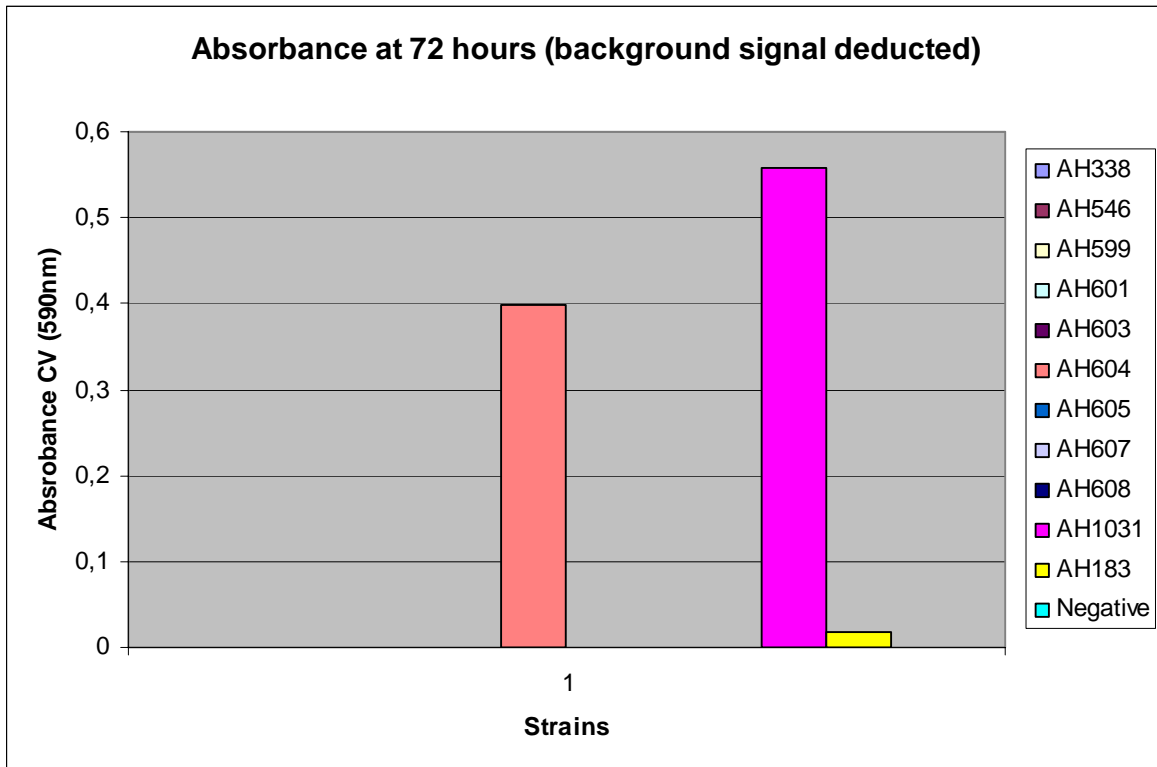


Figure 3.24: Biofilm formation as measured by crystal violet absorbance after 72 hours of incubation
(background signal from negative control deducted)

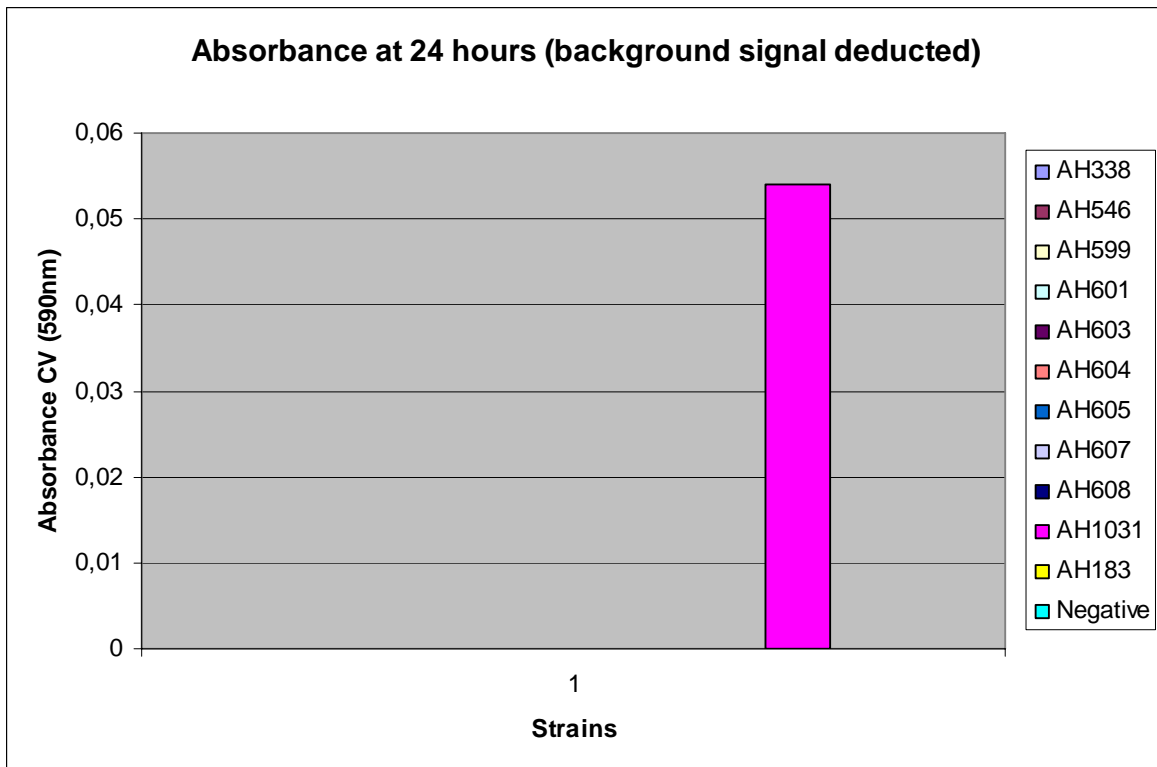


Figure 3.25: Biofilm formation as measured by crystal violet absorbance after 24 hours of incubation
(background signal from negative control deducted)

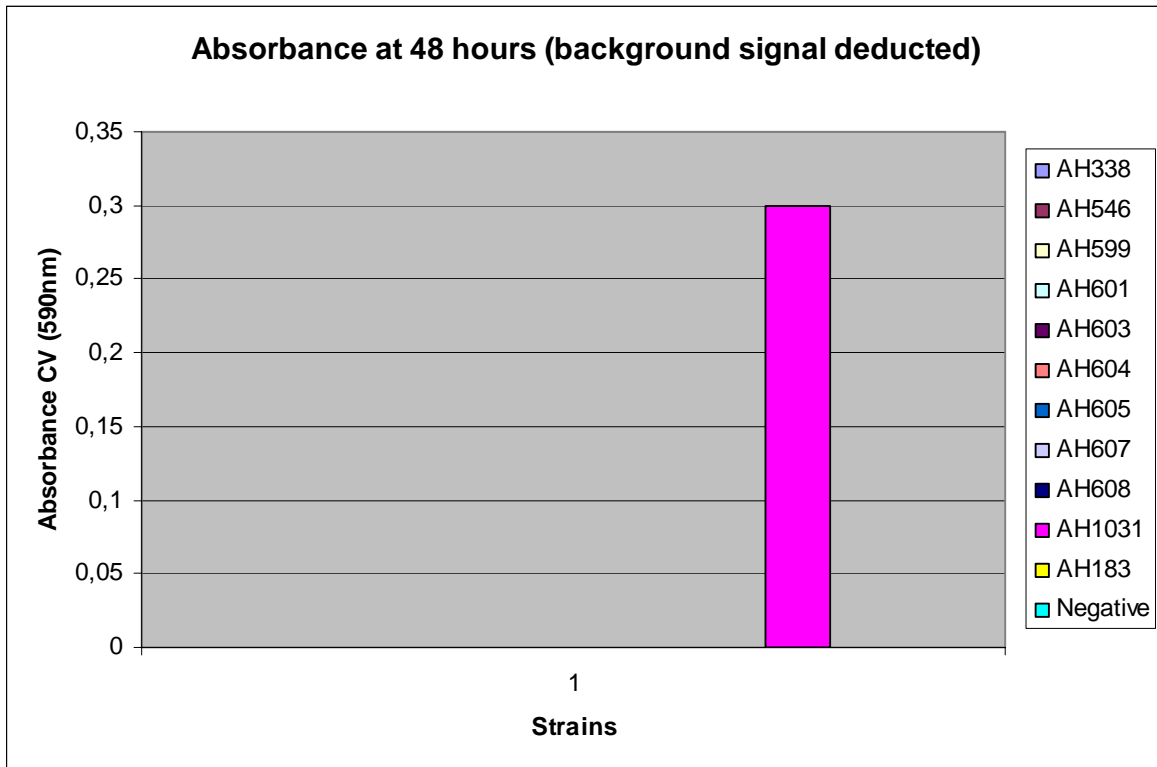


Figure 3.26: Biofilm formation as measured by crystal violet absorbance after 48 hours of incubation
(background signal from negative control deducted)

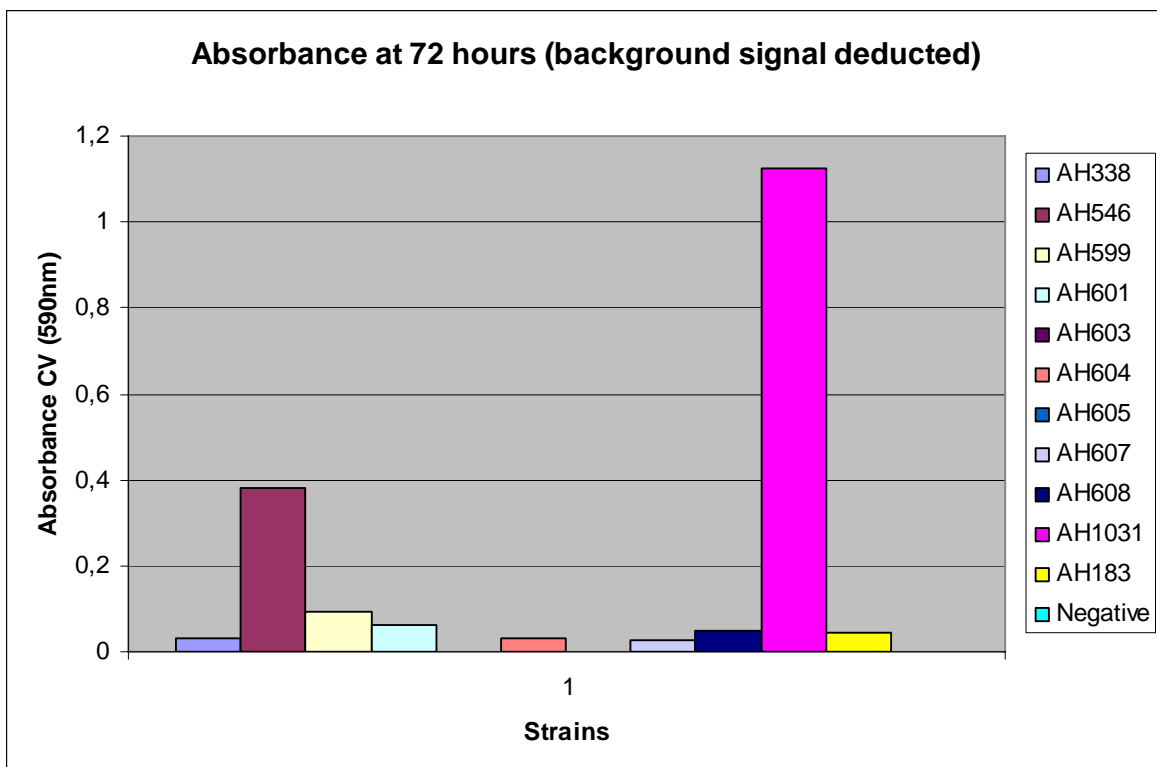


Figure 3.27: Biofilm formation as measured by crystal violet absorbance after 72 hours of incubation
(background signal from negative control deducted)

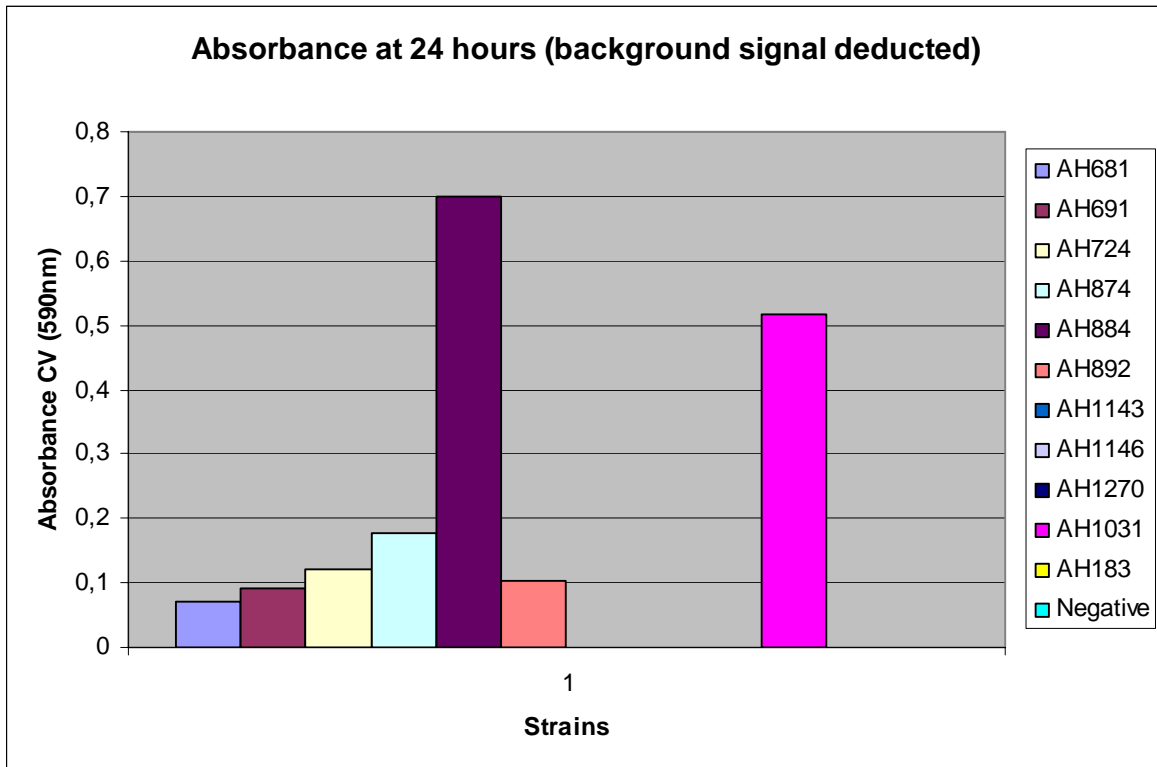


Figure 3.28: Biofilm formation as measured by crystal violet absorbance after 24 hours of incubation (background signal from negative control deducted)

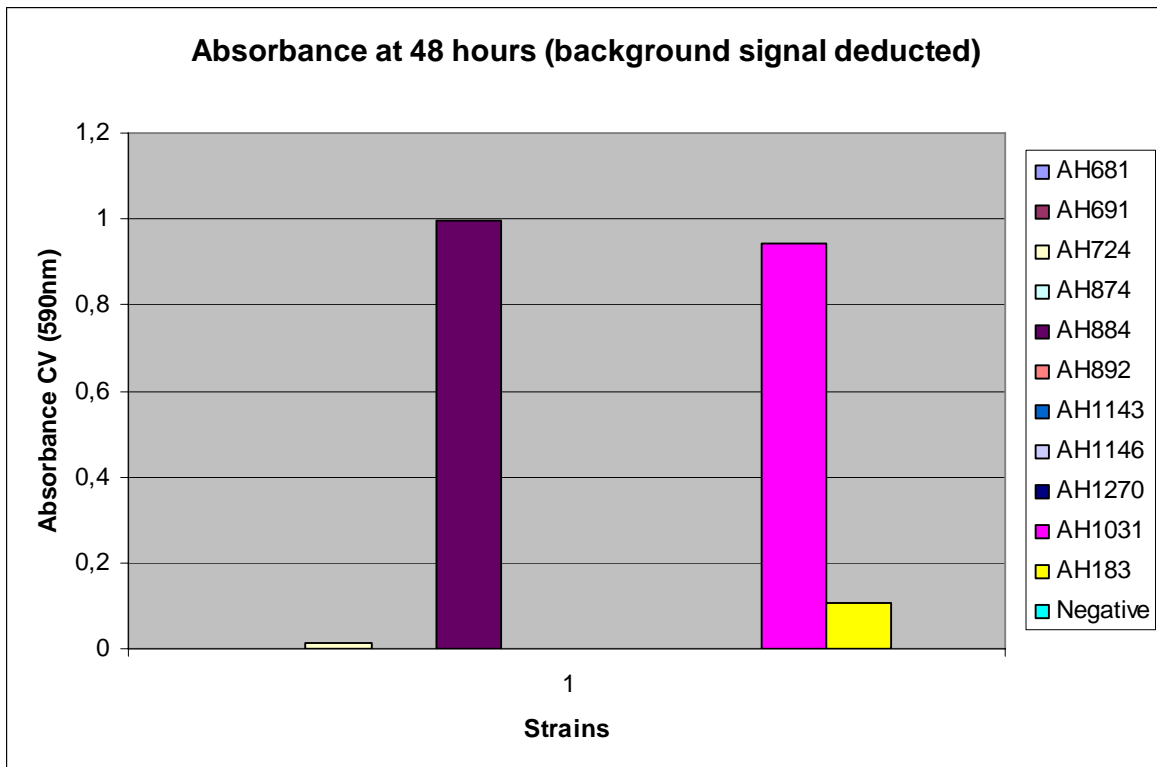


Figure 3.29: Biofilm formation as measured by crystal violet absorbance after 48 hours of incubation (background signal from negative control deducted)

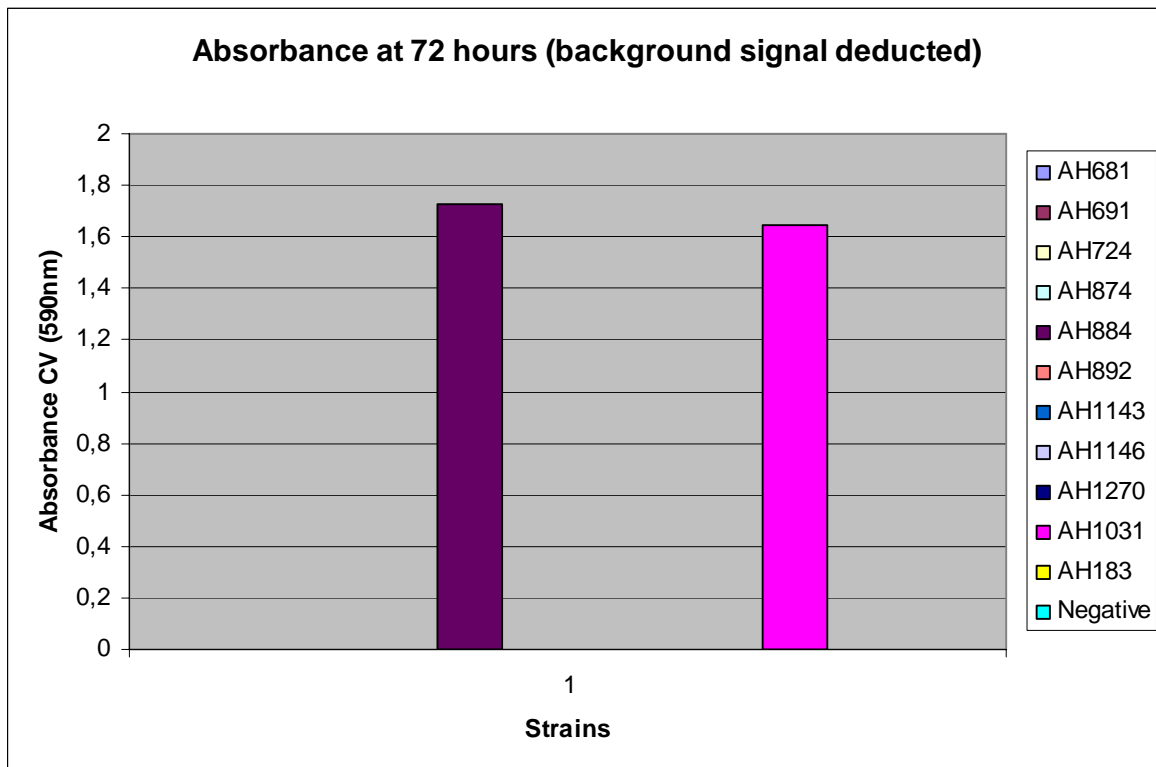


Figure 3.30: Biofilm formation as measured by crystal violet absorbance after 72 hours of incubation (background signal from negative control deducted)

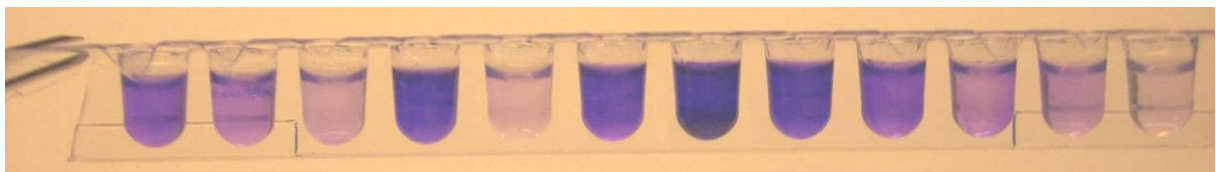
As mentioned, after screening 81 strains, were 7 strains observed to form biofilm and were determined biofilm-positive strains, while 74 strains were observed not to form biofilm and were determined biofilm-negative strains. The levels of absorbance seen for positive and negative control were relatively stable, but do vary in figures above due to somewhat different levels of background signal for each experiment. Differences seen at the different time points, 24, 48 and 72 hours, were taken into consideration when positive strains were picked for second round of screening (3.3.4). One could see some strains giving high levels of absorbance at 24 hours, but not at 48 or 72 hours, or visa versa, and this was only seen for strains, which did not form a ring after crystal violet staining. These strains were determined as biofilm-negative, because only observation of high levels of absorbance was not sufficient to determine a strain biofilm-positive.

3.3.4 Biofilm positive strain confirmation

The 7 strains, which were characterized as biofilm-positive, either by observing a consistently present biofilm ring in the wells (Picture 3.7 – 3.8) or by high levels of retained crystal violet measured (Figure 3.31 – 3.33), and 4 strains characterized as biofilm-negative, either by lack of observing a consistently present biofilm ring in the wells or by low levels of retained crystal violet measured, were screened separately to confirm the positive strains ability to form biofilm. The ability to form biofilm was visualised as a ring in the wells (Picture 3.7), after staining with crystal violet, and absorbance at 590nm measured after solubilisation (Picture 3.8; Figure 3.31 – 3.33). The presence of negative control, pure bactopectone, was added to show the levels of background signal seen in all experiments.



Picture 3.7: Biofilm ring formation for biofilm-positive (+) and biofilm-negative (-) strains, after 72 hours incubation. Left to right; AH75 (+), AH604 (+), AH226 (+), AH405 (+), AH183 (-), AH815 (+), AH884 (+), AH1031 (+), AH1248 (-), AH1271 (-), AH1353 (-) and negative control (pure bactopectone medium).



Picture 3.8: Solubilised crystal violet stained biofilm rings, after 72 hours incubation. Biofilm-positive strains (+), biofilm-negative (-) strains and negative control were screened. Left to right; AH75 (+), AH604 (+), AH226 (+), AH405 (+), AH183 (-), AH815 (+), AH884 (+), AH1031 (+), AH1248 (-), AH1271 (-), AH1353 (-) and negative control (pure bactopectone medium).

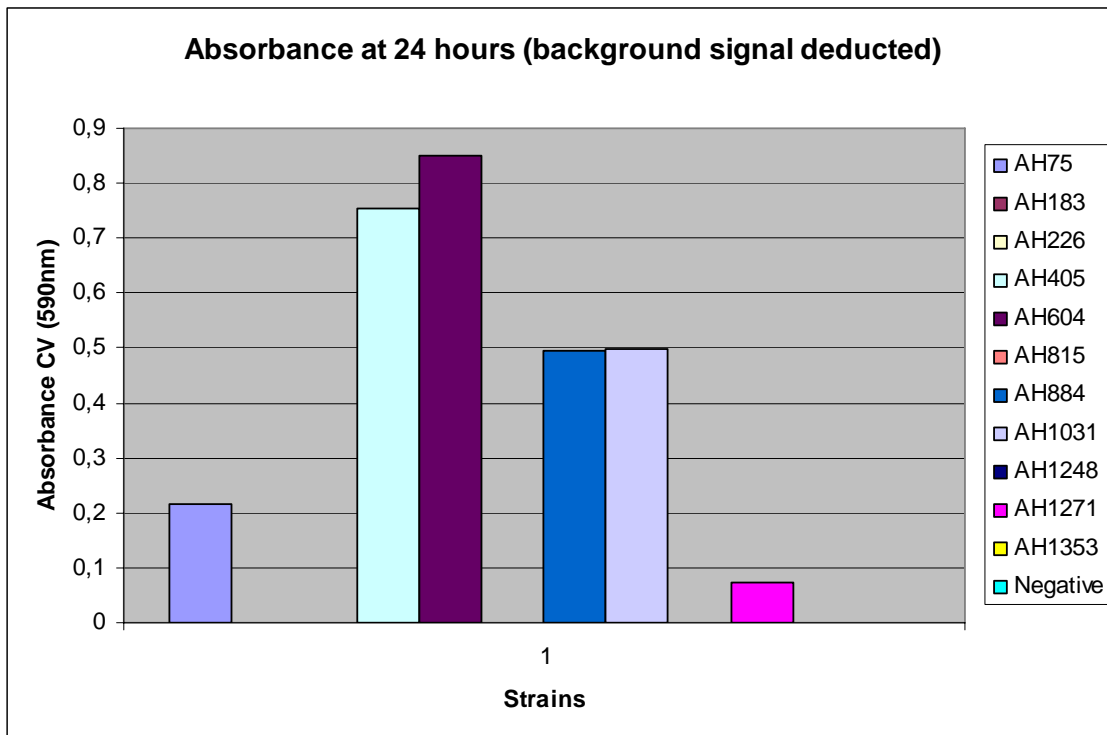


Figure 3.31: Biofilm formation as measured by crystal violet absorbance after 24 hours of incubation (background signal from negative control deducted)

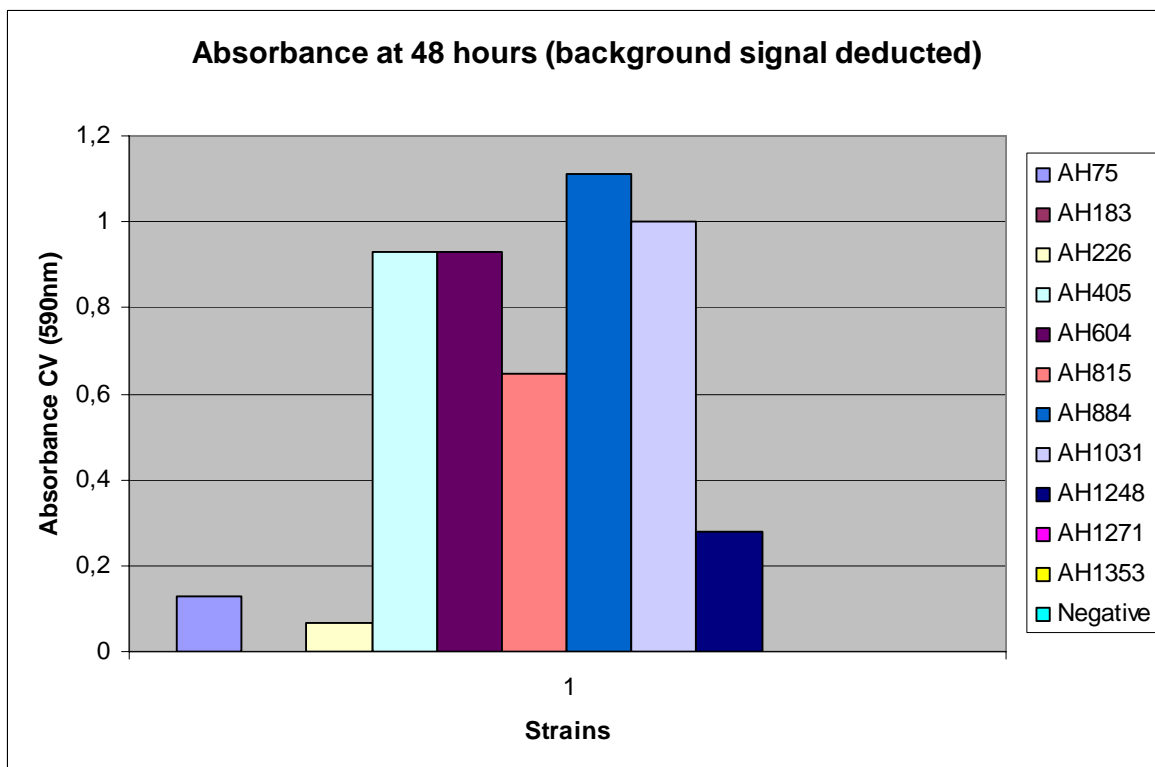


Figure 3.32: Biofilm formation as measured by crystal violet absorbance after 48 hours of incubation (background signal from negative control deducted)

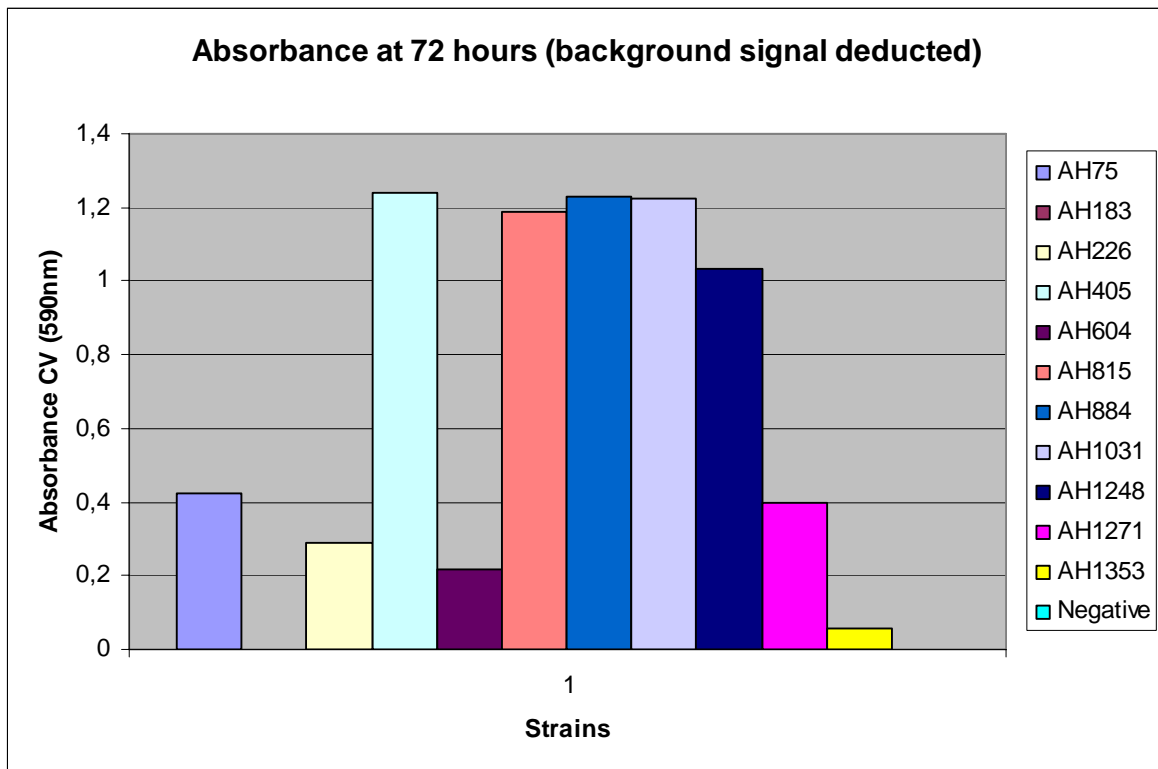


Figure 3.33: Biofilm formation as measured by crystal violet absorbance after 72 hours of incubation (background signal from negative control deducted)

These results clearly indicated that the 7 out of the 81 strains tested in this screening method were biofilm-positive (Table 3.1). However this also showed that for *B. cereus* AH 604, the presence of the ring and level of absorption was reduced after 72 hours, compared to after 24 and 48 hours. Also for *B. cereus* AH 1248, AH 1271 and AH 1353, which did show some level of absorbance after 72 hours, the presence of the biofilm ring was not seen and they were therefore determined biofilm-negative.

The frequency for biofilm formation was seen to be ~9% (7 biofilm-positive strains / 81 total strains screened).

Table 3.1: Biofilm formation according to strain origin. (-) indicates strains that do not form biofilm, while (+) indicates strain that do form biofilm.

Strain	Origin	Biofilm formation
AH 75	<i>Bacillus cereus</i> ATCC 10987 (dairy)	+
AH 181	<i>Bacillus cereus</i> ATCC 10876	-
AH 183	<i>Bacillus cereus</i> ATCC 14579 (dairy)	-
AH 186	<i>Bacillus cereus</i> F4433/73	-
AH 187	<i>Bacillus cereus</i> F4810/72 (vomit, patient)	-
AH 188	<i>Bacillus cereus</i> F837/76	-
AH 189	<i>Bacillus cereus</i> F2038/78	-
AH 226	<i>Bacillus cereus</i> ATCC 4342 (dairy)	+
AH 248	<i>Bacillus thuringensis</i> , subsp. <i>kurstaki</i> 4D1	-
AH 249	<i>Bacillus thuringensis</i> , subsp. <i>kurstaki</i> 4D4	-
AH 252	<i>Bacillus thuringensis</i> , subsp. <i>kurstaki</i> 4H2	-
AH 257	<i>Bacillus thuringensis</i> , subsp. <i>israelensis</i> 4Q1	-
AH 258	<i>Bacillus thuringensis</i> , subsp. <i>israelensis</i> 4Q5	-
AH 259	<i>Bacillus cereus</i> 6A1	-
AH 265	<i>Bacillus thuringensis</i> 4A4	-
AH 338	<i>Bacillus mycoides</i> (soil)	-
AH 401	<i>Bacillus cereus</i> 181 (dairy)	-
AH 404	<i>Bacillus cereus</i> 3048 (dairy)	-
AH 405	<i>Bacillus cereus</i> 1230 (dairy)	+
AH 407	<i>Bacillus cereus</i> 3122 (dairy)	-
AH 513	<i>Bacillus cereus</i> s1-2 (soil)	-
AH 535	<i>Bacillus cereus</i> s2-21 (soil)	-
AH 543	<i>Bacillus cereus</i> s3-1 (soil)	-
AH 546	<i>Bacillus cereus</i> s3-5 (soil)	-
AH 560	<i>Bacillus cereus</i> s4-3 (soil)	-
AH 580	<i>Bacillus cereus</i> s4-24 (soil)	-
AH 584	<i>Bacillus cereus</i> s4-28 (soil)	-
AH 588	<i>Bacillus cereus</i> s4-32 (soil)	-
AH 595	<i>Bacillus cereus</i> vet-1 (dairy)	-
AH 597	<i>Bacillus cereus</i> vet-3 (dairy)	-
AH 599	<i>Bacillus cereus</i> vet-5 (dairy)	-
AH 601	<i>Bacillus cereus</i> vet-8 (dairy)	-
AH 603	<i>Bacillus cereus</i> vet-10 (dairy)	-
AH 604	<i>Bacillus cereus</i> vet-11 (dairy)	+
AH 605	<i>Bacillus cereus</i> vet-17 (dairy)	-
AH 607	<i>Bacillus cereus</i> vet-59 (dairy)	-
AH 608	<i>Bacillus cereus</i> vet-61 (dairy)	-
AH 609	<i>Bacillus cereus</i> vet-68 (dairy)	-
AH 611	<i>Bacillus cereus</i> vet-87 (dairy)	-
AH 612	<i>Bacillus cereus</i> vet-131 (dairy)	-
AH 613	<i>Bacillus cereus</i> vet-132 (dairy)	-
AH 623	<i>Bacillus cereus</i> (soil)	-
AH 631	<i>Bacillus cereus</i> (soil)	-
AH 648	<i>Bacillus cereus</i> (soil)	-
AH 652	<i>Bacillus cereus</i> (soil)	-
AH 656	<i>Bacillus cereus</i> (soil)	-
AH 681	<i>Bacillus cereus</i> (soil)	-
AH 691	<i>Bacillus cereus</i> (soil)	-
AH 699	<i>Bacillus subtilis</i> 168	-
AH 724	<i>Bacillus cereus</i> (urine, patient)	-
AH 810	<i>Bacillus cereus</i> (periodontitis, patient)	-
AH 811	<i>Bacillus cereus</i> (periodontitis, patient)	-
AH 812	<i>Bacillus cereus</i> (periodontitis, patient)	-
AH 813	<i>Bacillus cereus</i> (periodontitis, patient)	-
AH 814	<i>Bacillus cereus</i> (periodontitis, patient)	-
AH 815	<i>Bacillus cereus</i> (periodontitis, patient)	+

Strain	Origin	Biofilm formation
AH 816	<i>Bacillus cereus</i> (periodontitis, patient)	-
AH 818	<i>Bacillus cereus</i> (periodontitis, patient)	-
AH 819	<i>Bacillus cereus</i> (periodontitis, patient)	-
AH 820	<i>Bacillus cereus</i> (periodontitis, patient)	-
AH 831	<i>Bacillus cereus</i> (periodontitis, patient)	-
AH 874	<i>Bacillus cereus</i> SIC (clinical, patient)	-
AH 884	<i>Bacillus cereus</i> (blood, patient)	+
AH 892	<i>Bacillus cereus</i> (wound after insect bite, patient)	-
AH 1031	<i>Bacillus thuringiensis</i> 407 (soil)	+
AH 1091	<i>Bacillus cereus</i> ATCC14579 (dairy, cured of linear 15kb-plasmid)	-
AH 1123	<i>Bacillus cereus</i> 9823 (clinical)	-
AH 1127	<i>Bacillus cereus</i> 9843 (clinical)	-
AH 1129	<i>Bacillus cereus</i> Bc004 (clinical, post-traumatic endophthalmitis)	-
AH 1134	<i>Bacillus cereus</i> Bc006 (clinical, post-traumatic endophthalmitis)	-
AH 1143	<i>Bacillus weihenstephanensis</i> WSBC 10201	-
AH 1146	<i>Bacillus weihenstephanensis</i> WSBC 10205	-
AH 1248	<i>Bacillus thuringiensis</i> subsp. <i>konkukian</i> str. 97-27 (leg wound infection)	-
AH 1270	<i>Bacillus cereus</i> 0001+31175 (cervix, patient)	-
AH 1271	<i>Bacillus cereus</i> 9903+02049 (secretary lamp)	-
AH 1273	<i>Bacillus cereus</i> 9708+03060 (blood, patient)	-
AH 1295	<i>Bacillus cereus</i> (veterinary)	-
AH 1297	<i>Bacillus cereus</i> (veterinary)	-
AH 1353	<i>Bacillus cereus</i> (food poisoning, diarrhoeal outbreak)	-
AH 1363	<i>Bacillus cereus</i> ATCC14579 (dairy, Δ plcR mutant)	-
AH 1369	<i>Bacillus cereus</i> 9901+17036 (amniotic fluid, patient)	-

3.3 Construction of a *plcR* knock-out of *Bacillus cereus* ATCC 10987

There are a wide variety of molecular pathways involved in the formation of biofilm amongst bacteria and therefore probably also in *Bacillus cereus* group bacteria. In this study, a candidate gene, *plcR*, found in the genome of *B. cereus* group bacteria, was investigated for involvement in biofilm formation. *plcR* was chosen as a candidate gene due to its observed role as a pleiotropic regulator of gene expression, and to the fact that PlcR has been observed to be expressed in biofilm (Michel Gohar, personal communication). *B. cereus* ATCC 10987 was chosen as the target strain for *plcR* gene disruption due to the fact that it is seen to form biofilm, its culture supernatant has the ability to induce biofilm formation in otherwise biofilm-negative strains, and is a strain which is fully sequenced (Rasko *et al.*, 2004), and therefore is possible to use in molecular studies.

3.3.1 Knock-out construct cloning and antibiotic resistance markers

For the construction of the knock-out clone, the use of cloning plasmids, expression plasmids, antibiotic resistance markers and restriction enzymes are essential tools. Figure 3.34 shows how the construction of the *plcR* locus knock-out clone in pUC19 was intended to be moved to pAT113 and used to disrupt the entire locus in *B. cereus* ATCC 10987.

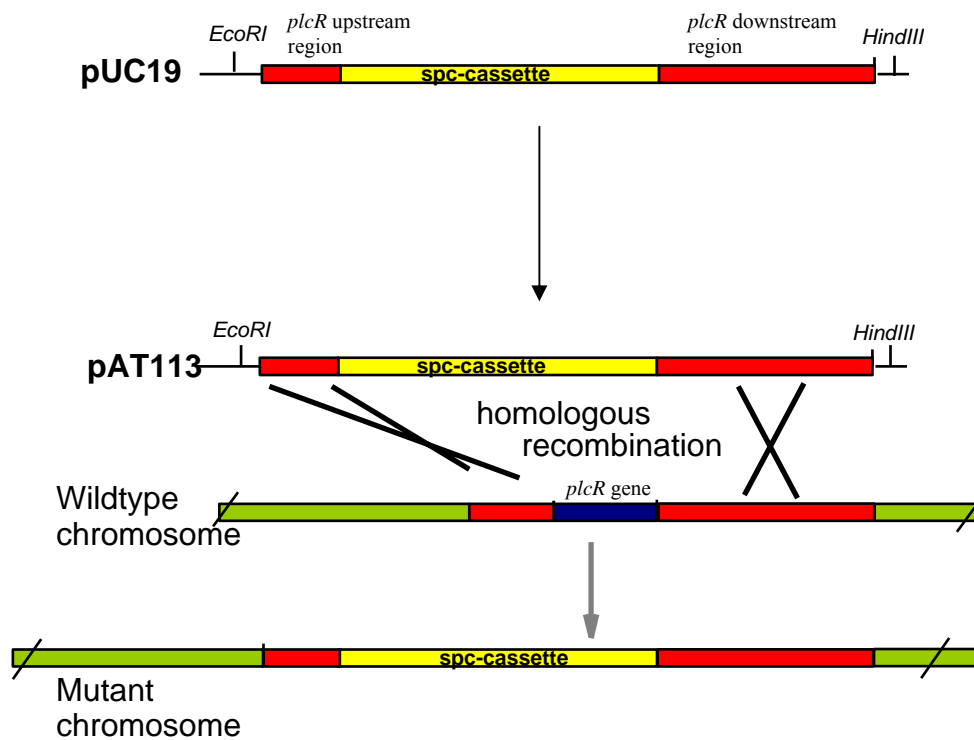


Figure 3.34: Method and way of cloning constructed *plcR* locus knock-out clone in pUC19 into pAT113 and using pAT113 as cloning vector for gene disruption of entire *plcR* locus in *B. cereus* ATCC 10987.

Resistance to antibiotics is an essential when screening clones for the presence of plasmid following transformations. The pUC19 plasmid contains an ampicillin resistance gene (Figure 6.28) conferring transformed bacterial cells resistance if grown on this antibiotic. However, there must also be present a second antibiotic resistance gene in the final knock-out clone (following integration into the host cell chromosome) to indicate that gene disruption

has occurred. For this procedure a spectinomycin- and an erythromycin-resistance gene cassette is cloned into to the knock-out construct. The spectinomycin resistance gene used here was originally from *Enterococcus faecalis* and works as a protein synthesis inhibitor by binding to the 30S subunit of bacterial ribosomes and inhibiting the translocation of peptides (LeBlanc, et al. 1991), while the erythromycin resistance gene was from *Staphylococcus aureus* and works as a protein synthesis inhibitor by binding to the 23S rRNA molecule in the 50S of the bacterial ribosome, an action, which blocks the exit of the growing peptide chain and thus inhibiting the translocation of peptides (Horinouchi, et al. 1980).

The multiple cloning site (MCS) present in pUC19 allows the linearization of the plasmid, the digestion of the plasmid by restriction enzymes (2.3.7) and the insertion of *plcR* upstream, *plcR* downstream, the antibiotic resistance cassette into the plasmid and movement of the entire construct from pUC19 into pAT113. *plcR* upstream was to be cloned into the *KpnI/SacI* site, *plcR* downstream was to be cloned into the *BamHI/SalI* site and the resistance cassettes were to be cloned into the *SmaI* site. *EcoRI* and *HindIII* were to be used to move entire construct from pUC19 into pAT113. See figure 3.35 for the sites present in the MCS, which were used for knock-out construction.

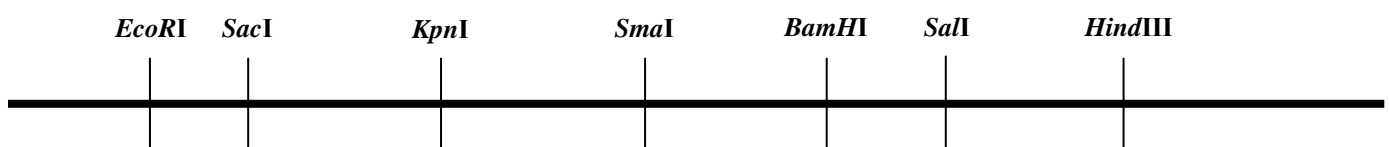


Figure 3.35: Multiple cloning site (MCS) of pUC19, showing selected restriction sites.

3.3.2 *plcR* locus sequence extraction and primer design

The construction of a *plcR* deletion mutant of *Bacillus cereus* ATCC 10987 was initiated with sequence analysis of the chromosomal region surrounding *plcR*. The genome region containing the *plcR* gene was extracted from EMBL entry AE017281 using *extractseq* from the EMBOSS sequence analysis suite (www.biotek.uio.no/EMBNET), including 1000 bp of flanking regions from each end of the *plcR* gene. One primer set for PCR was to be selected from genome region: 157256-156256 (-1000 bp) and another set was to be selected from genome region: 158113-159113 (+1000 bp). These sequences were tested for restriction sites *KpnI*, *SacI*, *Sall*, *BamHI*, *SmaI*, *EcoRI* and *HindIII* (*restrict*-program in EMBOSS) and no restriction sites were found. *primer3* (<http://frodo.wi.mit.edu>) was then used to design primers for the genome regions upstream and downstream of *plcR*, using default criteria. Primers were ordered from Invitrogen (U.S.A.). See table 3.2 for primer sequence.

Primer	Sequence	Size of PCR product
plcR_upstream_proximal (-1000 bp)	5'- <u>tttgg</u> tacactactactaccatcccactataacaa-3' <i>KpnI</i> site underlined	772 bp
plcR_upstream_distal (-1000 bp)	5'-ttttgagctcggggattgcgcatatagatt <i>SacI</i> site underlined	
plcR_downstream_distal (+1000 bp)	5'-ttttg <u>tcgactc</u> gccattaacccaaatcaa-3' <i>Sall</i> site underlined	891 bp
plcR_downstream_proximal (+1000 bp)	5'-ttttg <u>gatccg</u> caaatatgcataattgcataagatac-3' <i>BamHI</i> site underlined	

Table 3.2: Primers of the upstream and downstream regions of the *plcR*-locus from *B. cereus* ATCC 10987 used

in PCR to produce fragments for making the PlcR knock-out construct.

The primers were produced with terminal restriction sites to aid the cloning of the fragments in a plasmid vector (e.g. pUC19). This also allowed the cloning of the fragments in a correct orientation into the vector multiple cloning site (MCS/polylinker region). See Figure 6.28 for an overview of vector pUC19.

3.3.3 Isolation of template DNA for PCR amplification

DNA from *Bacillus cereus* ATCC 10987 was extracted (2.3.2), to be used as template to produce the *plcR* upstream- and the *plcR* downstream-fragments by PCR (2.3.3). Also, plasmids from clones AH 1337, containing the spectinomycin resistance cassette cloned in pUC19 (Figure 3.36), and AH 1363, containing the erythromycin resistance cassette cloned in pUC19 (Figure 3.36), were isolated by plasmid preparation (2.3.6). These plasmids were to be used as templates for PCR to amplify the spectinomycin- and the erythromycin-cassette fragments.

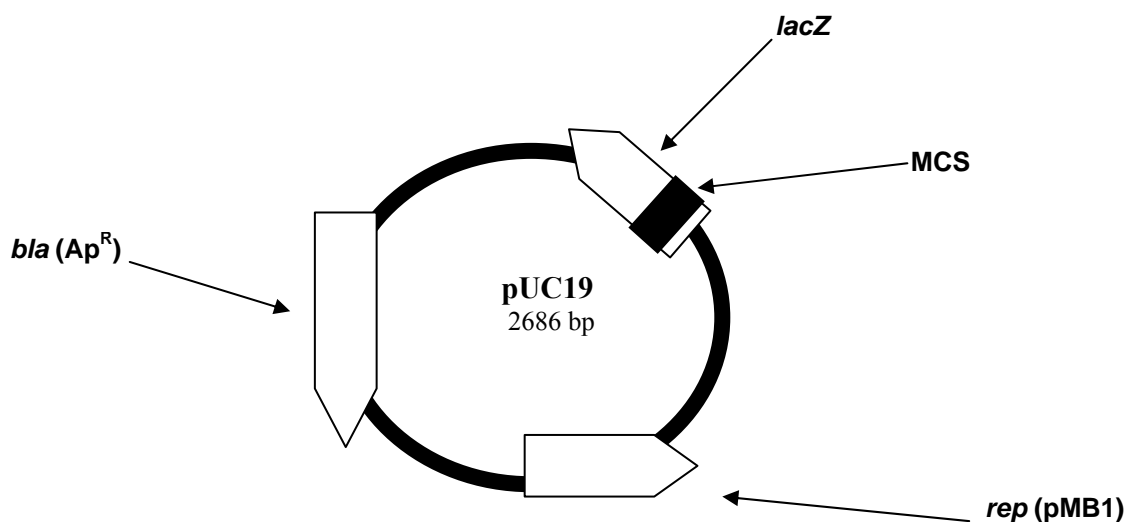
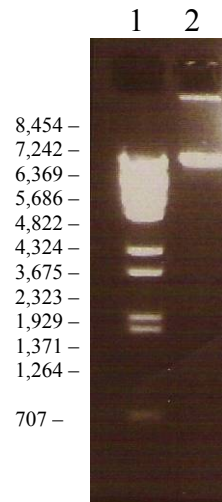


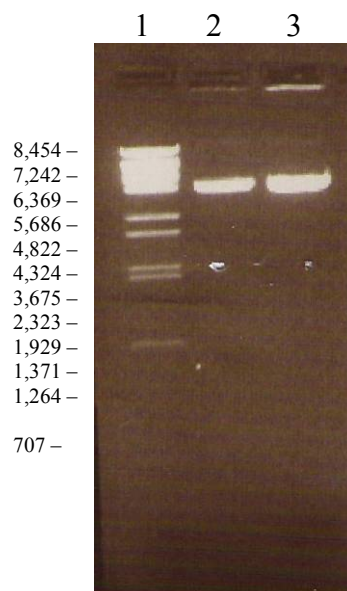
Figure 3.36: pUC19 vector, showing multiple cloning site (MCS), replication site (*rep* (pMB1)), ampicillin resistance cassette (*bla* (ApR)) and *lacZ* gene.

Agarose gel electrophoresis allowed observation of DNA extracted from *B. cereus* ATCC 10987 (Picture 3.9), plasmids extracted from AH 1337 and AH 1363 (Picture 3.10) and also allowed the quantification of DNA/plasmid amounts present in the sample.



Picture 3.9: Agarose gel electrophoresis of extracted DNA from *B. cereus* ATCC 10987 (lane 2) and size marker lambda/BstE II (lane 1).

Plasmids, pUC19_spectinomycin and pUC19_erythromycin, were digested with *EcoRI* I (2.3.7) for verification of size and concentration through agarose gel electrophoresis (2.3.4).



Picture 3.10: Agarose gel electrophoresis of linearized plasmids (*EcoRI* digested) isolated from AH 1337 (lane 2) and AH 1363 (lane 3). Size marker lambda/BstE II (lane 1).

B. cereus ATCC 10987 DNA sample was observed as clean and in large amounts, while plasmids containing the spectinomycin- and erythromycin-resistance cassettes were of expected sizes, clean and in large amounts.

3.3.4 PCR of *plcR* flanking regions and resistance cassettes

The 772 bp upstream region and the 891 bp downstream region of the *plcR* gene were amplified by PCR (2.3.3) using primers made for the specific sequences (Table 3.2; Figure 3.37) and *Bacillus cereus* ATCC 10987 DNA (3.3.3) was used as template. The spectinomycin-cassette and the erythromycin-cassette were also amplified by PCR (2.3.3), using purified plasmids from AH 1337 and AH 1338 respectively, as templates (3.3.3). Size and concentration of products were checked through agarose gel electrophoresis (2.3.4) (Picture 3.11 – 3.12).

plcR upstream and *plcR* downstream PCR products were observed and were of the expected size, ~772 bp and ~891 bp respectively, while spectinomycin- and erythromycin-resistance cassette PCR products were also observed and of the expected size, ~1200 bp. All PCR products were observed as clean and in large amounts.

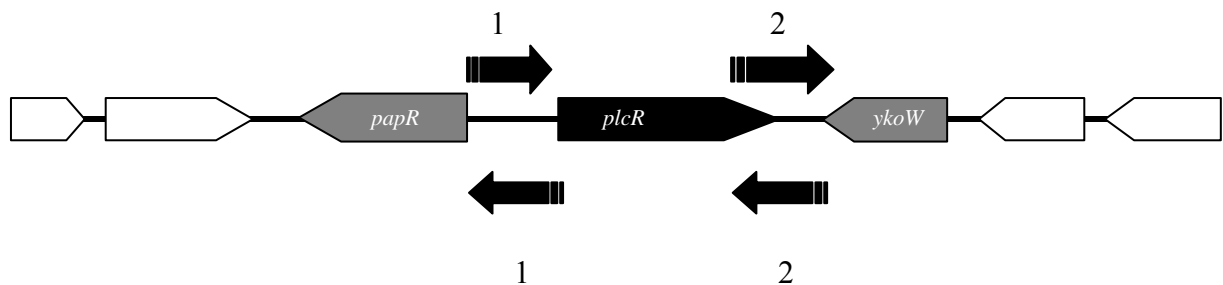
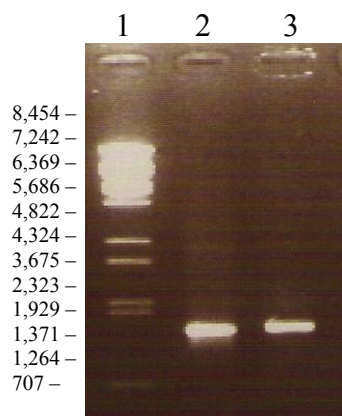


Figure 3.37: Placement of primers for upstream (1) and downstream (2) region of *plcR*.



Picture 3.11: Agarose gel electrophoresis of PCR products of spectinomycin- (lane 2) and erythromycin-resistance cassettes (lane 3). Size marker lambda/BstE II in lane 1.



Picture 3.12: Agarose gel electrophoresis of PCR products of upstream (lane 2-13) and downstream (lane 15-22) fragments of *plcR*. Size marker lambda/BstE II (lane 1 and 14).

3.3.5 Cloning of *plcR* upstream into pUC19

2 μ l (approx. 200 ng DNA) of purified *plcR*-upstream PCR product (3.3.4) and 10 μ l (approx. 1 μ g DNA) of pUC19 were digested, using *Kpn*I and *Sac*I (2.3.7). Both samples were purified (2.3.5) and ligated (2.3.9) at a 1:5 molar ratio (1 ng insert : 5 ng plasmid) over night at 16°C. 5 μ l of the ligation mixture was transformed using One Shot Top10 competent cells (Invitrogen) (2.3.9). Ampicillin (100 μ g/ml) was used as a selection marker when cells were grown on LB agar plates at 37°C, over night. Figure 3.38 shows a schematic of the cloning of the *plcR*-upstream fragment into pUC19 through PCR, restriction enzyme digestion, ligation

and transformation. Enzyme digestion was performed, as indicated, after PCR amplification and purification and allowed for the insertion of the fragment into the MCS of the pUC19 plasmid.

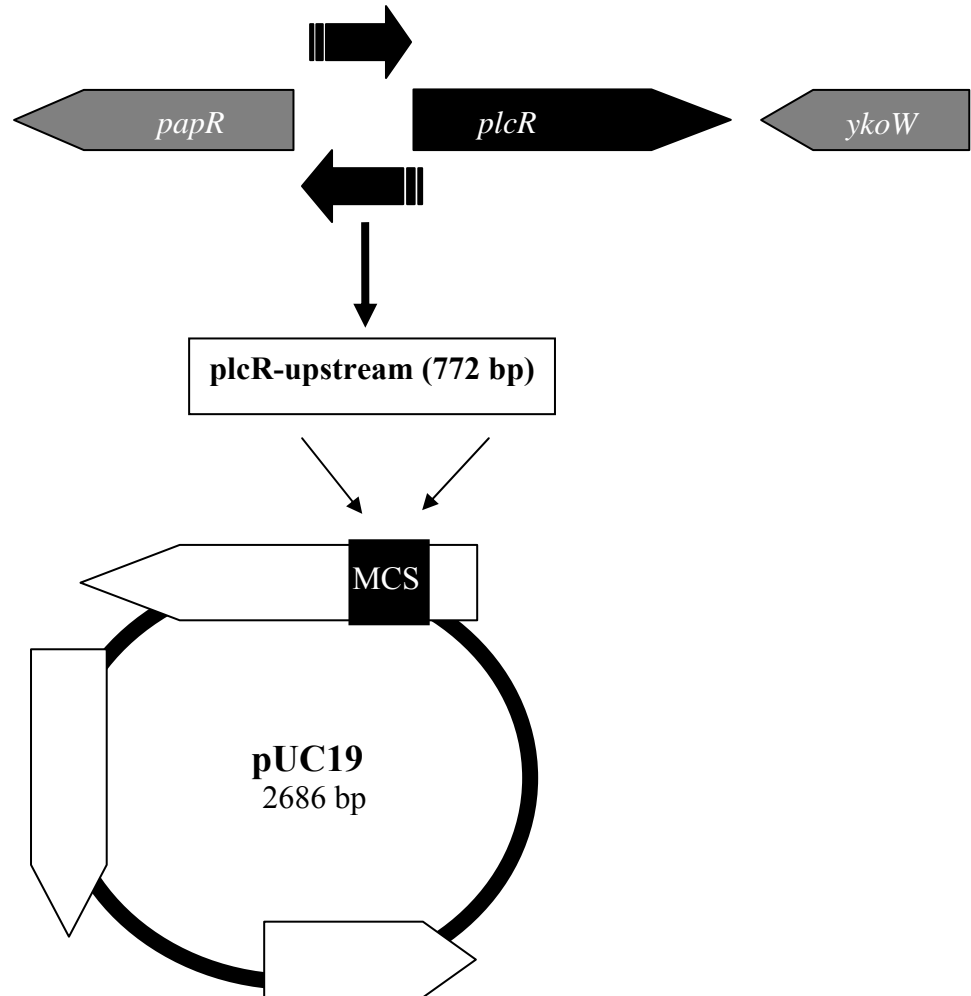
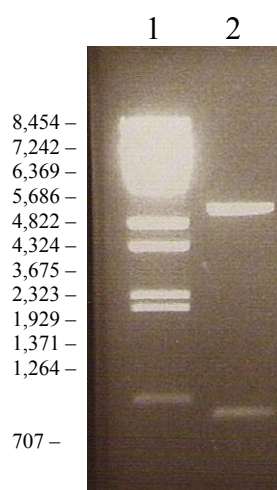


Figure 3.38: Cloning of the *plcR* upstream region into pUC19 vector.

After transformation, colonies were checked for presence of insert by plasmid purification (2.3.9), restriction enzyme digestion (2.3.7) with *KpnI* and *SacI*, and agarose gel electrophoresis (2.3.4). Picture 3.13 shows agarose gel electrophoresis analysis of the pUC19 plasmid containing the *plcR*-upstream fragment, after the recombinant plasmid has been digested with *KpnI* and *SacI*. Size of both plasmid and fragment bands were as expected, 2.6 kb and 772 bp respectively.



Picture 3.13: Agarose gel electrophoresis of pUC19_plcRupstream (lane 2) after cloning, purification and digestion with *KpnI* and *SacI*. Size marker lambda/BstE II in lane 1.

3.3.6 Cloning of *plcR* downstream into pUC19_plcRupstream

2 μ l (approx. 200 ng DNA) of purified *plcR*-downstream PCR product (3.3.4) and 10 μ l (approx. 1 μ g DNA) of recombinant plasmid pUC19_plcRupstream (3.3.5) were digested, using *Bam*HI and *Sal*II (2.3.7). Both samples were purified (2.3.5) and ligated (2.3.9) at a 1:5 molar ratio (1 ng insert : 5 ng plasmid) over night at 16°C. 5 μ l of the ligation mixture was transformed using One Shot Top10 competent cells (Invitrogen) (2.3.9). Ampicillin (100 μ g/ml) was used as a selection marker when cells were grown on LB agar plates at 37°C, over night. Figure 3.39 shows a schematic of the cloning of the *plcR*-downstream fragment into pUC19_plcRupstream through PCR, restriction enzyme digestion, ligation and transformation. Enzyme digestion was performed, as indicated, after PCR amplification and purification and allowed for the insertion of the fragment into the MCS of the pUC19 plasmid.

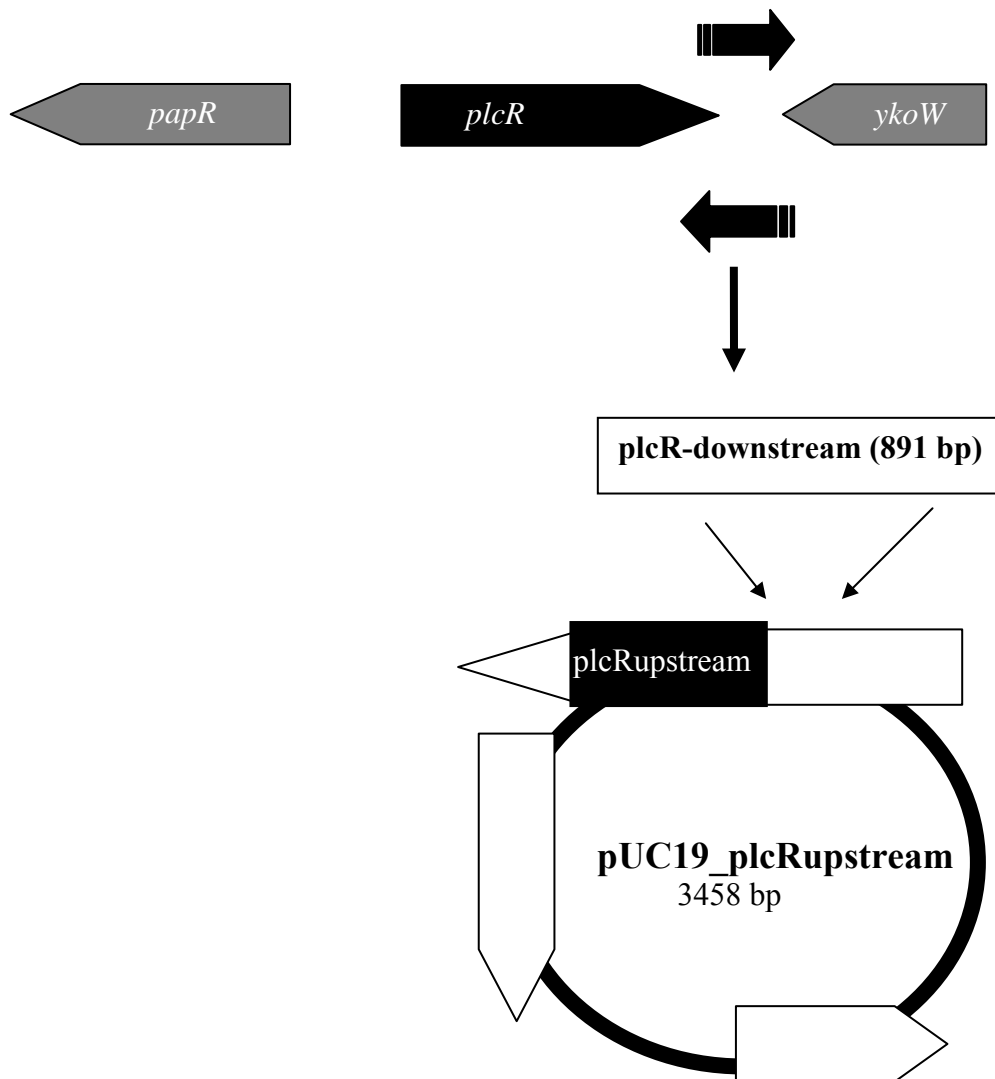
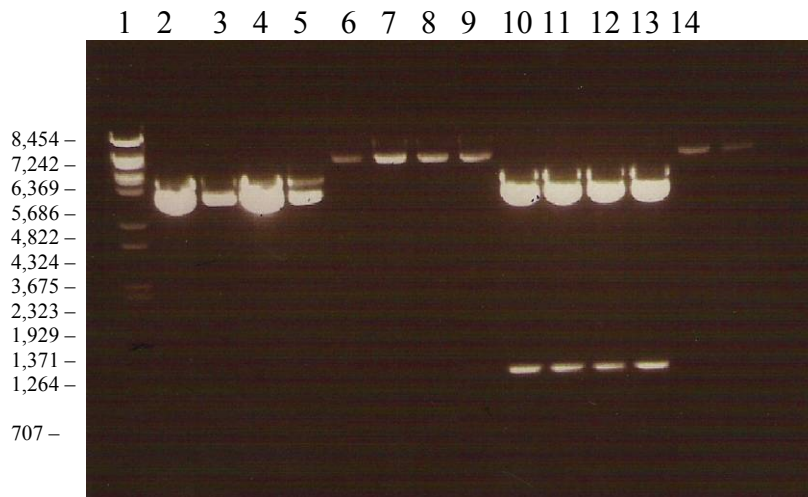


Figure 3.39: Cloning of the downstream region of *plcR* into the pUC19_plcRupstream plasmid.

After transformation, colonies were checked for presence of insert by plasmid purification (2.3.9), restriction enzyme digestion (2.3.7) with *Bam*HI and *Sal*I. Picture 3.14 shows agarose gel electrophoresis (2.3.4) analysis of the pUC19_plcRupstream plasmid containing the *plcR*-downstream fragment, after plasmid has been digested with *Bam*HI and *Sal*I. Size of both plasmid and fragment bands were as expected, ~3.4 kb and 891 bp respectively. Agarose gel electrophoresis also showed that some cloned did not contain the plcRdownstream fragment, indicating that this fragment had not been cloned into the pUC19_plcRupstream plasmid.



Picture 3.14: Agarose gel electrophoresis of restriction enzyme digestion by *Bam*HI and *Sal*II of pUC19_plcRupstream_plcRdownstream (lane 2-5 and 10-13). Size marker lambda/BstE II in lane 1.

3.3.7 Cloning antibiotic resistance cassette into pUC19_plcRupstream_plcRdownstream

2 µl (approx. 200 ng DNA) of either spectinomycin or erythromycin resistance cassette purified PCR product (3.3.4) and 10 µl (approx. 1 µg DNA) of the pUC19_plcRupstream_plcRdownstream construct were digested, using *Sma*I (2.3.7). Here dephosphorylation using alkaline phosphatase (2.3.8) was also necessary to prevent vector religation due to the use of only one restriction enzyme. Both samples were purified from gel (2.3.5; Picture 3.15) and ligated (2.3.9) at a 1:5 molar ratio (1 ng insert : 5 ng plasmid) over night at 16°C. 5 µl of the ligation mixture was transformed using One Shot Top10 competent cells (Invitrogen) (2.3.9). Ampicillin (100µg/ml) was used as a selection marker when cells were grown on LB agar plates at 37°C, over night. Figure 3.40 shows a schematic of the cloning of the spectinomycin resistance cassette into pUC19_plcRupstream_plcRdownstream construct through PCR, restriction enzyme digestion, ligation and transformation. Enzyme digestion was performed, as indicated, after PCR amplification and purification, and allowed for the insertion of the antibiotic resistance cassette into the MCS of the pUC19_plcRupstream_plcRdownstream plasmid.

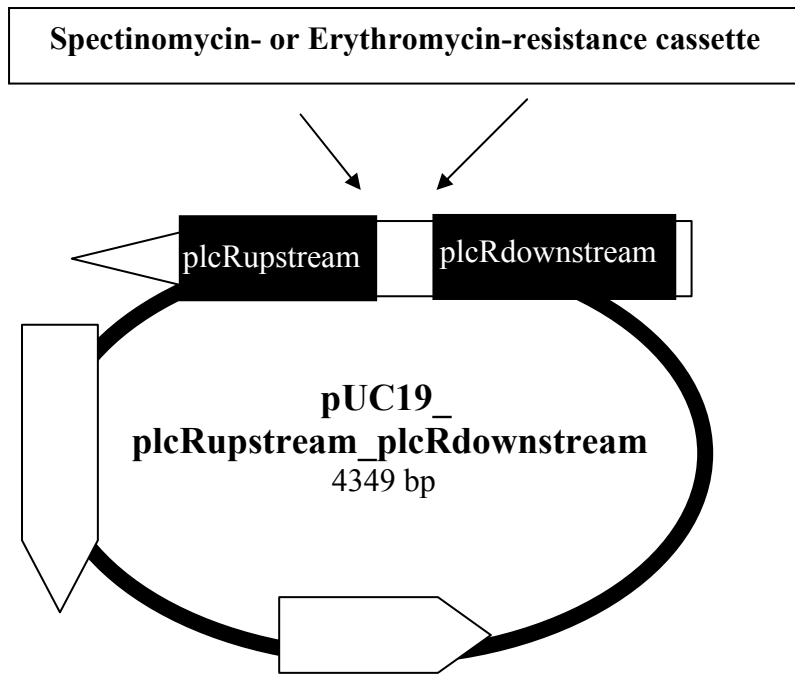
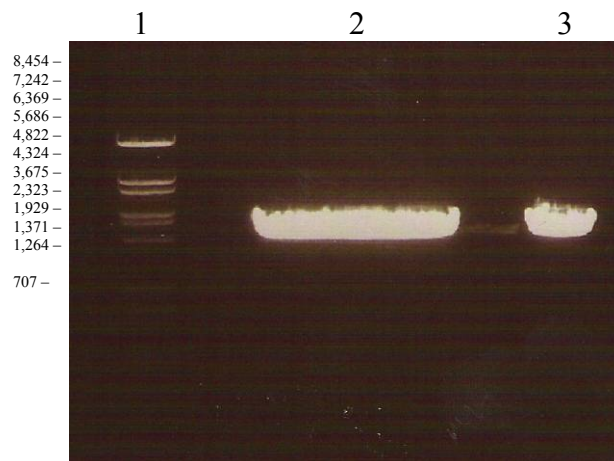
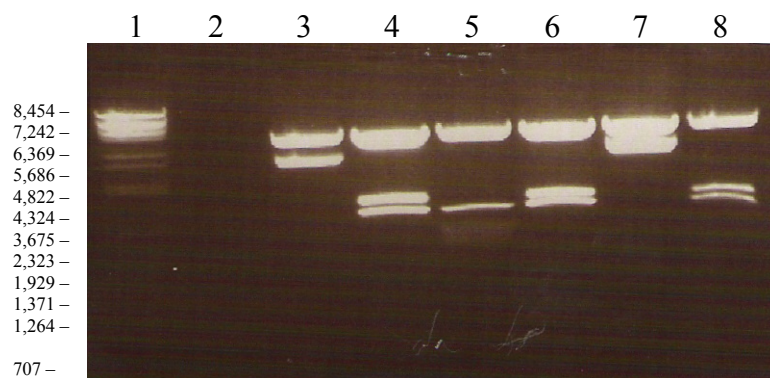


Figure 3.40: Cloning of resistance cassette (spectinomycin/erythromycin) into pUC19_plcRupstream_plcRdownstream.

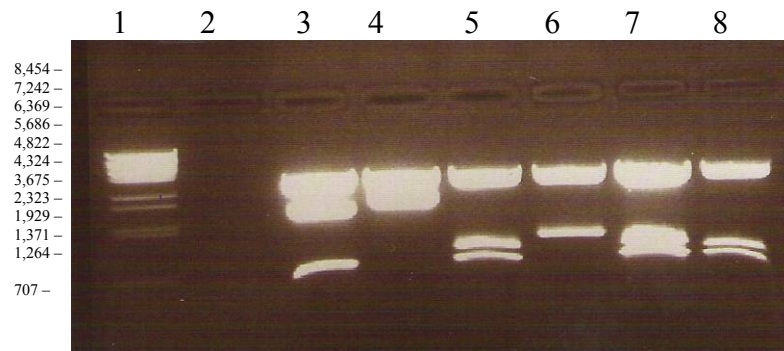


Picture 3.15: Agarose gel electrophoresis of restriction enzyme digestion of pUC19_plcRupstream_plcRdownstream_spectinomycin construct with *Sma* I (lane 2) and restriction enzyme digest of pUC19_plcRupstream_plcRdownstream_spectinomycin construct with *Sma* I (not dephosphorylated) (lane 3). Size marker lambda/BstE II in lane 1.

After transformation, colonies were checked for presence of insert by plasmid purification (2.3.9), restriction enzyme digestion (2.3.7) with *EcoRI* and *HindIII* and agarose gel electrophoresis (2.3.4). This restriction enzyme digestion was performed specifically to verify that the MCS contained the entire *plcR*upstream fragment, the entire *plcR*downstream fragment and the entire antibiotic resistance cassette. This would also be the same restriction enzyme digestion performed to clone the construct into pAT113. Picture 3.16 – 3.17 shows agarose gel electrophoresis analysis of the pUC19 *_plcR*upstream *_plcR*downstream-*_spectinomycin* construct, after the recombinant plasmid had been digested with *EcoRI* and *HindIII*. The size of the bands of both the plasmid and the fragment were not as expected in any of the clones analyzed (expected sizes were ~2.6 kb for the plasmid and ~2.8 bp for the fragment) (Picture 3.16 – 3.17). These agarose gels show through analysis of the band sizes that this step of cloning did not work and that the antibiotic resistance cassette was not cloned correctly into the plasmid.



Picture 3.16: Agarose gel electrophoresis of restriction enzyme digestion of pUC19 *_plcR*upstream *_plcR*downstream *_spectinomycin* (lane 3-8) with *EcoRI* and *HindIII*. Size marker *lambda/BstE II* in lane 1.



Picture 3.17: Agarose gel electrophoresis of restriction enzyme digestion of pUC19_plcRupstream_plcRdownstream_spectinomycin (lane 3-8) with *EcoRI* and *HindIII*. Size marker lambda/BstE II in lane 1.

A total of 24 colonies (only 12 colonies checked showed here) were checked for the presence of the inserted antibiotic resistance cassette, but none of the colonies gave expected band sizes through agarose gel electrophoresis analysis. Samples 7 (Picture 3.16) and 4 (Picture 3.17) were sent to sequencing for verification of agarose gel electrophoresis analysis.

3.4 Sequence analysis

3.4.1 Sequence analysis of resistance cassettes

Sequencing and sequence analysis of the antibiotic resistance cassettes, used in the construction of the *plcR* knock-out construct, was performed to confirm the sequence of the cassettes present in our clones (AH 1337 and AH 1363), to confirm that the sequence was correct and for comparison when sequencing the clones made in this thesis. Sequencing of pUC19_spectionmycin and pUC19_erythromycin (6.2.2) was performed by GATC (Germany), using M13F and M13R primers (Figure 6.29 – 6.30). Sequence analysis showed that both cassettes were correct and corresponded to sequence of reference (www.pubmed.org).

3.4.2 Sequence analysis of constructs made for *plcR* knock-out

Sequencing and sequence analysis of the constructs made for the *plcR* knock-out procedure was performed to confirm the sequences of the constructs. All constructs (3.3.5 – 3.3.7) were sequenced using M13forward and M13reverse primers (Figure 6.31 – 6.33).

During primer design and construct initiation the coordinates of the *plcR* locus in *B. cereus* ATCC 10987 (AE017197) were recorded as being from 5060487 to 5061344. When sequences inserted into pUC19 were compared to this sequence, the construct only containing the *plcR*upstream region gave a match to *B. cereus* ATCC 10987 at 5061978 to 5061344, indicating that the *PlcR* upstream region was correctly cloned. The pUC19_ *plcR*upstream_ *plcR*downstream construct gave a match to *B. cereus* ATCC 10987 at 5061978 to 5061344 and at 5060472 to 5060058, indicating that both the upstream and the downstream region was correctly cloned.

Further sequence analysis was done using Align (bl2seq) to compare the sequenced constructs against the known sequences of the upstream and downstream sequences of the *plcR* locus. These results gave an almost perfect match, indicating that the sequence inserted into the pUC19 vector is correct and matches the sequence present in *B. cereus* ATCC 10987 (Figure 3.41 – 3.42).



Figure 3.41: pUC19_ *plcR*upstream_ *plcR*downstream construct aligned with known *plcR* upstream sequence, using Align.



Figure 3.42: pUC19_plcRupstream_plcRdownstream construct aligned with known *plcR* downstream sequence, using Align.

However, when sequence analysis of the pUC19_plcRupstream_plcRdownstream_spectinomycin and pUC19_plcRupstream_plcRdownstream_erythromycin constructs were performed, the presence of the *plcR* upstream region and the *plcR* downstream region could not be detected in its entire size using blastn or bl2seq and only the presence of the entire resistance cassette was seen to be present in the construct (Figure 3.43). The construct containing the erythromycin cassette showed no sequence similarities with any *plcR* locus sequences and showed only the presence of the entire erythromycin resistance cassette, while the construct containing the spectinomycin cassette showed some similarities to the *plcR* locus, but sequences were very short (~38 bp) and not seen to be anywhere close to original length of upstream (772 bp) or downstream (891 bp) region inserted into the construct.



Figure 3.43: pUC19_plcRupstream_plcRdownstream_spectinomycin aligned with the known sequence of the spectinomycin cassette, using Align.

This indicated, through sequence analysis, that the constructs after cloning of the antibiotic resistance cassette, contained the antibiotic resistance cassette (in the case of the

erythromycin cassette construct), but unexpectedly, only small fragments of the *plcR* flanking sequences were retained (in the case of the spectinomycin cassette construct).

4 DISCUSSION AND CONCLUSIONS

4.1 The biofilm conundrum

The formation of biofilm by bacteria is often seen to happen, is thought to be an important part of some infections in humans (Gilbert *et al.*, 1997) and is also thought to be at least partly responsible for the ability of some bacteria to live in natural environments not suitable for normal growth (O'Toole *et al.*, 2000). Still very much is unknown of the processes involved, and the mechanisms behind will be discussed and studied by microbiologists for many years to come. The ability of certain bacterial strains to produce biofilm, the reason why they have this ability and the mechanism behind biofilm formation certainly extends beyond the scope of this thesis. However, this thesis does present an effective method for biofilm formation investigation that allows screening of a high number of strains with many parallels and does give indicative results of biofilm formation among the *Bacillus cereus* group of bacteria. This method for biofilm screening does of course not reflect the natural conditions of the source of origin of any of these strains, but the method gives a quick and reliable way to obtain results, which can initiate further studies into the ability of one particular strain to form biofilm. The setup for the biofilm screening procedure was done in collaboration with Dr. Michel Gohar at INRA, France. This has produced a method which is easily reproducible between laboratories and between groups studying the *Bacillus cereus* group bacteria and their ability to form biofilm.

4.2 Bacterial growth during biofilm screening

4.2.1 Colony morphology

We wished to investigate whether bacterial colony morphology could be indicative of the tendency for growth on surfaces. For the *B. cereus* group bacteria the morphology of the

colonies are somewhat variable, ranging from round, smooth colonies, to rough-edged colonies and from shiny to matte surfaced, but mostly differ in the size of the colony. As observed, some strains, e.g. AH 183 and AH 1031, form larger colonies with a somewhat jagged outline, while other strains, e.g. AH 75 and AH 1248, form small colonies with smooth outline. These differences did, however, not seem to have any effect of a strain's ability to form biofilm. While AH 183 is a biofilm-negative strain, AH 1031 is a strong biofilm former, and while AH 75 is a biofilm forming strain, AH 1248 is biofilm negative. Colony morphology could therefore be disregarded as a fundamental pathway for biofilm formation, clearly indicating that there are other more important factors involved in the formation of biofilm.

AH 884 was the only strain, which produced a colony morphology different from what generally observed. This strain gave “slimy” collection of colonies on the plate and single colonies were difficult to obtain. AH 884 was originally classified as *B. cereus* (by Rikshospitalet, Oslo, Norway), but due to the different colony morphology and the high level of biofilm formation ability, the strain was further investigated. Using universal 16S rRNA primers the species classification was determined (performed by Erlendur Helgason, National Veterinary Institute, Norway). The results showed that AH 884 actually is a *Bacillus licheniformis* strain, which can explain the unusual colony morphology and strong ability to form biofilm, as *B. licheniformis* strains have been observed to form biofilm (Ameur, et al., 2005).

4.2.2 Bacterial growth over time

The standard growth curve for the four reference strains and the standard growth for the selected strains (3.1.2 and 3.1.3) clearly indicate that the different strains grew with almost identical speed and reach exponential growth approximately at the same time (3 hours), under

the growth conditions used here. No difference between strains forming biofilm and those that do not could be observed. This time point (3 hours) was therefore used throughout the study, as the time point for extraction of samples for use during growth in microtiter plates.

4.3 Biofilm screening

4.3.1 Testing and optimisation of the biofilm screening system

Four strains were picked to establish the test system for biofilm screening. *Bacillus cereus* ATCC 10987 (AH75), *Bacillus cereus* ATCC 14579 (AH183), *Bacillus cereus* AH 812 and *Bacillus thuringensis* 407 (AH1031) were used as test strains, of which AH 75 and AH 1031 were known biofilm-positive strains and AH 183 and AH 812 were known biofilm-negative strains. This allowed the establishment of a screening system, based on a method used at INRA, France (Michel Gohar, personal communication). As indicated in section 3.2, neither the amount of culture in each well of the microtiter plate, nor the position of the cultures on the plate, were observed to affect the strains ability to form biofilm. However, the shape of the microtiter plate wells, the presence of moisture (H₂O soaked filter paper), and the type of medium in which the strains where grown had some effect. In the final protocol, biofilm screening was done in microtiter plates with round bottomed wells (not flat bottomed) and a lid, in the presence of a moist filter paper, Furthermore, strains were incubated in bactopectone medium when inoculated on the microtiter plates. Due to the fact that a somewhat high level of background signal was observed with “crude” crystal violet, sterile filtration of the crystal violet solution was included in the protocol to remove crystals not dissolved. This did help to remove some background signal, but, as indicated, the unspecific staining by crystal violet in some wells was not completely removed.

4.3.2 Crystal violet staining – technical consideration

This biofilm screening procedure is based on the crystal violet staining of cells attached to the well after washing with PBS. We therefore investigated whether the amount of crystal violet absorbed by cells at 590 nm was directly linked to the number of bacterial cells in the culture. To check this, three strains were picked, serially diluted and stained with the same amount of crystal violet (2.2.4; 3.1.4). The final result clearly indicated that a higher dilution of bacterial cells produced a lower absorbance of crystal violet, as expected, although not observing complete linearity for all strains.

The result of the serial dilution test confirmed the basis for the screening method, i.e. that the amount of crystal violet absorbed shows correlation with the amount of bacterial cells present. The number of bacterial cells present, after washing the wells with PBS, and forming the characteristic ring structure in the liquid-air interface were interpreted as cells that had formed a biofilm.

As mentioned above, the use of crystal violet also allows for direct visualisation of biofilm formation in the well (picture 3.5). This picture clearly shows that the crystal violet binds in a ring formation around the air-liquid phase of the wells and that this ring is actual bacterial cells bound to the PVC surface of the wells. This ring was clearly present for all positive strains, although in somewhat different thickness.

The use of crystal violet did however produce a somewhat high level of background signal and a relatively high standard deviation for samples. The level of background signal is clearly observed in the wells incubated with pure bactopectone medium only (no bacteria inoculated); a weak crystal violet ring may be observed and the crystal violet will give some level of colour when solubilised. The somewhat high standard deviation, i.e. the variability in absorbance between wells with the same strain incubated, was also a result of crystal violet binding unspecifically to the PVC in the well during staining, even when crystal violet was

sterile filtered. This could be observed by the presence of crystals of crystal violet spread around, not forming a ring, in the wells. Wells with crystal violet still present, i.e. unable to be washed away, for strains that were clearly biofilm-negative, i.e. did not form the ring structure, in some cases produced high level of absorbance, and large difference in absorbance between wells, and thus a high standard deviation. This was often observed in single wells of the 16 parallels wells that were inoculated for each strain, and since all wells were included in the analysis, contributed to the observed large standard deviations.

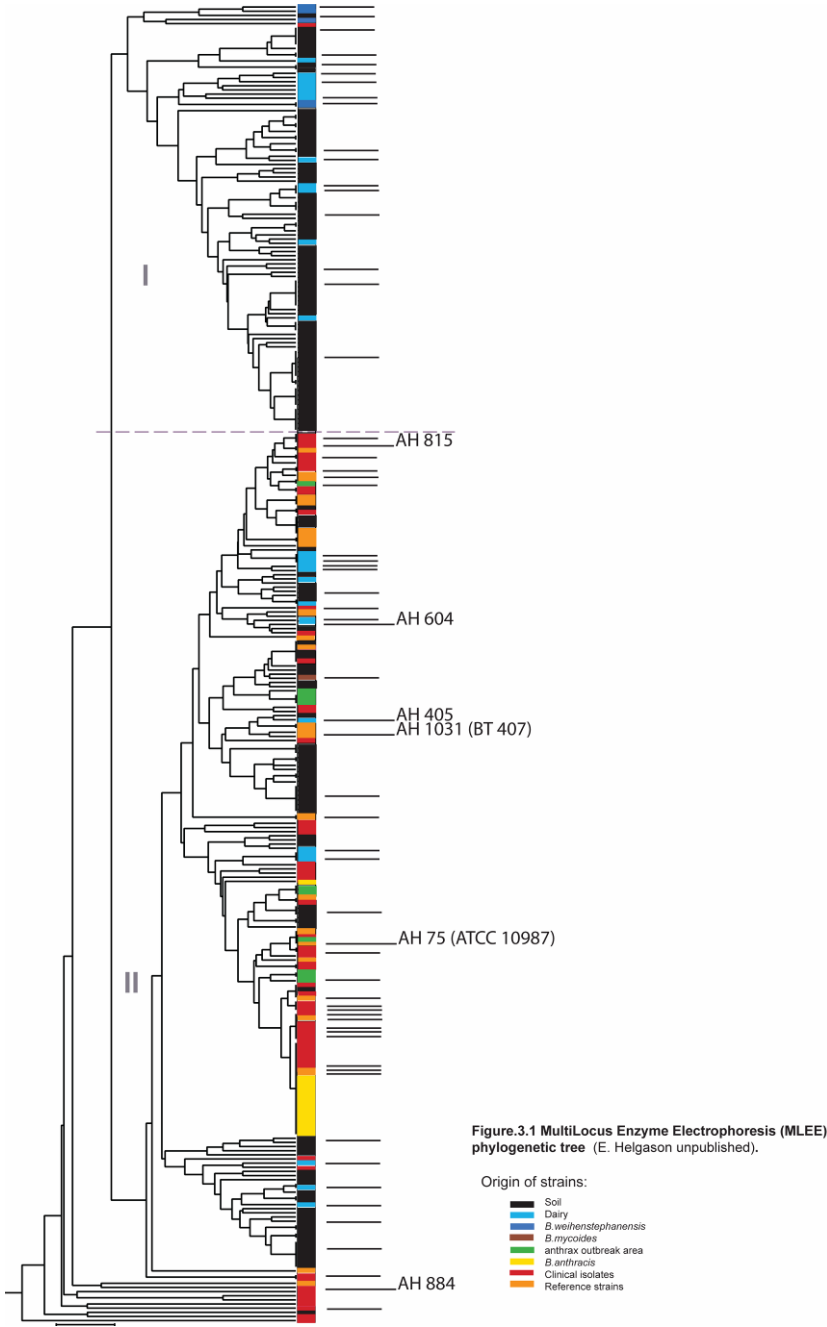
The numerical results following crystal violet staining were not used as the single criterium for biofilm formation. We decided on introducing a second criterium, the presence of a characteristic “ring” formation in the well (in the liquid/air interface), for comparison with the numerical results. High average absorbance values and the visualisation of the “ring” were in combination considered to give this method for biofilm screening the accuracy and specificity that is required.

4.3.3 Biofilm screening

An excellent model system for studying bacterial diversity is the formation of biofilm, a formation of surface-attached bacterial cells. Biofilm formation has been observed for a large collection of bacteria, e.g. *Pseudomonas aeruginosa*, *Escherichia coli*, *Vibrio cholerae*, *Staphylococcus epidermidis*, *Staphylococcus aureus*, *Bacillus subtilis* and *Bacillus cereus* and is observed to play a key role in the production and degradation of organic matter (Dahlberg *et al.*, 1997; Watnick *et al.*, 1999; Yildiz *et al.*, 1999). Bacterial cells are also thought to experience a certain degree of shelter and homeostasis when residing within a biofilm (Madigan *et al.*, 1997).

In this study the aim was to establish a method for screening *B. cereus* group of bacteria for their ability to form biofilm. Biofilm screening was performed on a total of 81

strains from the *Bacillus cereus* group of bacteria. The 81 strains screened were selected from a phylogenetic tree constructed by multilocus enzyme electrophoresis (MLEE) (Helgason *et al.*, unpublished) (Figure 4.1) and carefully chosen such that the 81 strains included strains from a variety of sources, and were spread throughout the tree. Strains screened for biofilm formation (indicated with horizontal line) and strains positive for biofilm formation (indicated with strain number) are marked on figure 4.1, when present in the tree.



In total, 7 strains were characterized as biofilm-positive and 74 strains as biofilm-negative, i.e. the frequency of positive strains was ~9%. This showed that only a limited number of strains from the *B. cereus* group bacteria screened in this thesis, had the ability to form biofilm. This percentage of biofilm positive strains was not far from expected, based on earlier results obtained by Michel Gohar, using a different set of strains (14% biofilm positive strains). The number of strains screened and the random selection of strains screened for this thesis could be the reason for the difference in frequency, but both results indicate that biofilm formation may not be a very frequent feature in the *B. cereus* group of bacteria.

The following strains were characterized as biofilm formers:

- *Bacillus cereus* ATCC 10987 (AH 75), isolated from spoiled cheese (dairy)
- *Bacillus cereus* ATCC 4342 (AH 226), isolated from milk
- *Bacillus cereus* 1230 (AH 405), dairy isolate
- *Bacillus cereus* vet-11 (AH 604), dairy isolate
- *Bacillus cereus* (AH 815), clinical isolate, periodontitis
- *Bacillus licheniformis* (AH 884), clinical isolate, blood culture
- *Bacillus thuringensis* Bt 407 (AH 1031), soil isolate

These 7 strains were isolated from dairy products, from human infections in blood and mouth (gum) and from soil, and indicate that the ability to form biofilm is not strictly linked to strain origin. These strains were also widely spread in phylogenetic trees (constructed by MLEE/MLST, Helgason, *et al.*, 2003), showing that biofilm formation is not a clonal property in the *B. cereus* group.

Some similarities are however seen, when looking at the origin of the strains and realising that six out of seven of the biofilm-positive strains were isolated outside of their natural environment, i.e. they are isolated from places not considered to be natural habitats of *B. cereus* group bacteria, which is soil and/or the insect gut (Jensen *et al.*, 2003). This can be indicative that the ability to form biofilm is a survival mechanism and not a direct virulence factor produced by the bacteria, such as allowing the bacteria to colonise the human gut, oral cavity or referring antibiotic resistance.

Vice versa, strains from the same source did not necessarily correlate with respect to biofilm formation. A total of 11 strains isolated from periodontal infections were screened and only 1 strain was seen to be biofilm-positive (AH 815). The same was seen with AH 75, AH 405 and AH 604, which are all dairy strains. A total of 18 dairy strains were screened and only 3 were seen to be biofilm-positive. For the clinical isolates, only 2 out of a total of 25 strains screened were biofilm-positive and only 1 out of 8 *B. thuringensis* strains showed biofilm formation, which again indicates that no specific correlation between isolation source and the ability for the strain to form biofilm was observed for *B. cereus* group bacteria.

There could not be found any large scale biofilm screening, performed on one group of bacterial species, for comparison with results from this study. Therefore could we not draw any conclusions whether biofilm formation by the *B. cereus* group bacteria is unique with reference to frequency of biofilm formation or correlation between source of isolation and ability to form biofilm.

4.4 Knock-out construction of *plcR*

4.4.1 Biofilm formation and genetics

Biofilm formation involves a large degree of gene regulation, which is evident from the fact that organisms have multiple genetic pathways that control biofilm behavior (O'Toole

et al., 2000). Up-regulation of genes has been seen to occur during biofilm formation, such as the up-regulation of adhesion molecule genes in *V. cholerae* (Yildiz *et al.*, 1999) and up-regulation of pili-mediated movement in *P. aeruginosa* (Wall *et al.*, 1999), and the number of genes thought to be involved in biofilm formation is high and has been observed to be constantly extended for each year of research. Within the scope of this thesis, the emphasis has been placed on the putative role of the *plcR* gene, a pleiotropic regulator of extracellular virulence factors in *B. cereus* ATCC 10987. PlcR was selected due to preliminary results indicating that PlcR could be involved in biofilm formation in *B. thuringensis* 407 and that supernatant of *B. cereus* ATCC 10987 could induce biofilm formation in strains otherwise not able to form biofilm (Michel Gohar, personal communication).

The construction of a knock-out construct of *plcR* was initiated to investigate a possible role of PlcR, a pleiotropic regulator of extracellular virulence factors in the *B. cereus* group bacteria, in the formation of biofilm. The knock-out construction was initiated to observe if the deletion of PlcR would influence the ability of *B. cereus* ATCC 10987 to form biofilm.

The strategy used to produce a *plcR* locus knock-out in *B. cereus* ATCC 10987, was to produce flanking fragments of the locus by PCR, and clone these fragments into a vector, with an antibiotic resistance cassette cloned between the PlcR flanking fragments, as a selection marker. The upstream- and downstream-fragments of the *plcR* locus and the antibiotic resistance cassette was to be first cloned into pUC19 (smaller and easier vector to work with than pAT113). The entire insert was then to be cloned into pAT113 using *E. coli* as host, before transfer of the construct into *B. cereus* ATCC 10987 via conjugation (Figure 3.34).

4.4.2 Cloning of *plcR* flanking regions

From agarose gel electrophoresis analysis and the sequence analysis of the clones, the *plcR* upstream and downstream regions were successfully cloned into pUC19, and correctly inserted (oriented) into the plasmid.

4.4.3 Cloning of resistance cassettes

Agarose gel electrophoresis analysis did not show a band of the expected size (~2.9 kb) and this was confirmed by sequence analysis, showing that the last step of the knock-out construct was unsuccessful. Sequence analysis showed that the upstream and downstream regions of *plcR* were absent in the constructs containing the resistance cassettes. During the insertion of the resistance cassettes, the initial insertions of the construct have seemingly been disturbed, digested away or degraded, leaving only partial or no remaining elements of the upstream and downstream fragments. Only present is the complete resistance cassette, which produced false positive results during the cloning procedure. As seen when digestion with *SmaI* (Picture 3.15) only one band was produced, ~4.2 kb in size. This may indicate that the difficulties arise during the ligation or the transformation of the antibiotic resistance cassette into the clone. Unfortunately this left the final construct useless for knock-out procedure of the *plcR* locus in *B. cereus* ATCC 10987 and for future work, the final cloning step must be repeated, using preliminary construct in which *plcR* upstream and downstream regions are correctly inserted.

4.5 Further studies

A method for biofilm screening of *Bacillus cereus* group bacteria was through this work established in the laboratory and the limits are only the number of strains available to screen. Further screening, of the more than 200 strains left in our collection, could give

additional knowledge of any correlation between strains and their source of origin. The screening is cheap, effective and gives results that are reliable, although perhaps somewhat crude. Efforts could be made to establish an alternative method for second-round screening of strains positive in the microtiter assay, such as a glass wool based approach (Oosthuizen *et al.*, 2001). This would allow a high number of strains to be screened in round one and a lower number of strains needed to screen by more elaborate assays.

Future work on the knock-out construct will include finalizing the cloning of the spectinomycin cassette and moving the whole construct into pAT113, to be used to knock-out the *plcR* locus in *B. cereus* ATCC 10987. This will entail going back to the construct containing the upstream and downstream regions of the *plcR* locus and proceed with the insertion of the spectinomycin or the erythromycin resistance cassette once more. Due to the obvious difficulties during the construction, additional control steps will also need to be implemented, such as ligation controls (positive and negative), and the counting of the colonies after transformation and transformation efficiency calculation. This would allow the construction of the Δ *plcR* construct and the investigation of the speculated role of PlcR in biofilm formation, following biofilm screening of wild type *B. cereus* ATCC 10987 and the Δ *plcR* strain. This work will also be linked with the molecular studies of a unique exopolysaccharide (EX-1) locus from *B. cereus* ATCC 10987 (Rasko *et al.*, 2004) performed in our laboratory (Christine Jensen, master thesis) and by Michel Gohar, INRA, France. Mutational deletion of EX-1 in *B. thuringensis* 407 has shown that the locus is involved in motility and in biofilm formation (Michel Gohar, unpublished).

In combination, biofilm screening and genetic studies, will allow for a deeper insight into the genetics involved in biofilm formation in *B. cereus* group bacteria and could result in further discovery of new genes and proteins involved in this process.

5 REFERENCES

- Adal, K.A., Farr, B.M.**, Central venous catheter-related infections: a review. *Nutrition*. 1996, 12, 208-213.
- Agaisse, H., Gominet, M., Okstad, O.A., Kolsto, A.-B., Lereclus, D.**, PlcR is a pleiotropic regulator of extracellular virulence factor gene expression in *Bacillus thuringensis*. *Mol. Microbiol.* 1999, 32, 1043-1053.
- Agaisse, H. and Lerecluse, D.**, How does *Bacillus thuringensis* produce so much insecticidal crystal protein? *J. Bacteriol.*, 1995, 177, 6027-6032.
- Ameur, M.A., Dubrous, P., Koeck, J.L.** *Bacillus licheniformis*: an unusual cause of erysipelosis. *Medici. Maladies Infectieuses*. 2005, 35, 417-418.
- Archibald, L.K., Gaynes, R.P.**, Hospital acquired infection in the United States: the importance of interhospital comparisons. *Nosocom. Infect.*, 1997, 11, 245-255.
- Arnaout, M.K., Tamburro, R.F., Bodner, S.M., Sandlund, J.T., et al.**, *Bacillus cereus* causing fulminant sepsis and haemolysis in two patients with acute leukaemia. *J. Pediatr. Hematol. Oncol.* 1999, 21, 431-435.
- Aronson, A.**, Sporulation and δ -endotoxin synthesis by *Bacillus thuringensis*. *CMLS*, 2002, 59, 417-425.
- Atrih, A. and Foster, S.J.**, The role of peptidoglycan structure and structural dynamics during endospore dormancy and germination. *Antoine Van Leeuwenhoek*, 1999, 75, 299-307.
- Auger, S., Krin, E., Aymerich, S., Gohar, M.**, Autoinducer 2 affects biofilm formation by *B. cereus*. *Appl. Envi. Microbiol.*, 2006, 72, 937-941.

Baumann, L., Okamoto, K., Unterman, B.M., Lynch, M.J., Baumann, P., Phenotypic characterization of *Bacillus cereus* and *Bacillus thuringensis*. *J. Invertebr. Pathol.*, 1984, 44, 329-341.

Beecker, D.J., Olsen, T.W., Somers, E.B., Wong, A.C.L., Evidence for contribution of tripartite haemolysin BL, phosphatidylcholine-preferring phospholipase C, and collagenase to virulence of *Bacillus cereus* endophthalmitis. *Infect. Immun.* 2000, 68, 5269-5276.

Bhatnagar, R. and Batra, S., Antrax toxin. *Crit. Rev. Microbiol.*, 2001, 27, 167-200.

Branda, S.S., Gonzales-Pastor, J.E., Ben-Yehuda, S., Losick, R., Kolter, R., Fruiting body formation by *Bacillus subtilis*. *Proc. Natl. Acad. Sci. USA*, 2001, 98, 11621-11626.

Branda, S.S., Gonzales-Pastor, J.E., Dervyn, E., Ehrlich, D., Losick, R., Kolter, R., Genes involved in formation of structured communities by *Bacillus subtilis*. *J. Bacteriol.*, 2004, 186, 3970-3979.

Busch, W., Saier, M.H., The transporter classification (TC) system. *CRC Crit. Rev. Biochem. Mol. Biol.*, 2002, 37, 287-337.

Costerton, J.W., Cheng, K.-J., Geesey, G.G., Ladd, T.I., Nickel, J.G., Dasgupta, M., Marrie, T.J., Microbial biofilms. *Annu. Rev. Microbiol.*, 1995, 49, 711-745.

Daffonchio, D., Cherif, A., Borin, S., Homoduplex and heteroduplex polymorphisms of the amplified ribosomal 16S-23S internal transcribed spacers describe genetic relationships in the “*Bacillus cereus* group”. *Appl. Environ. Microbiol.* 2000, 66, 5460-5468.

Dahlberg, C.C., Lindberg, V.L., Torsvik and Hermansson M. Conjugative plasmids isolated from bacteria in marine environments show various degrees of homology to each other and are not closely related to well-characterized plasmids. *Appl. Environ. Microbiol.* 1997, 63, 4692-4697.

Damgaard, P.H., Natural occurrence and dispersal of *Bacillus thuringensis* in the environment. In *Entomopathogenic Bacteria: from Laboratory to Field Application*. Charles,

J.-F., Delecluse, A., Nilesen-LeRoux, C. (Eds.). Dordrecht: Kluwer Academic Publishers, 2000, pp. 23-40.

Davaine, C., Recherches sur les infuaires du sang dans la maladie de la pustule maligne, *C. R. Acad. Sci.*, 1863, 60, 1296-1299.

Dickinson, M., Bisno, A.L., Infections associated with prosthetic devices: clinical considerations. *Int. J. Artif. Organs.*, 1993, 16, 749-754.

Driks, A., *Bacillus subtilis* spore coat. *Microbiol. Mol. Biol. Rev.* 1999, 63, 1-20.

Driks, A., Overview: development in bacteria; spore formation in *Bacillus subtilis*. *CMLS*, 2002, 59, 389-391.

Drobniewski, F.A., *Bacillus cereus* and related species. *Clin. Microbiol. Rev.* 1993, 6, 324-338.

Du, H., Fuh, R.A., Li, J., Corkan, A. and Lindsey, J.S. PhotochemCAD: a computer-aided design and research tool in photochemistry. *Photochem. Photobiol.* 1998, 68, 141-142.

Dubnau, D., DNA uptake in bacteria. *Annu. Rev. Microbiol.*, 1999, 53, 217-244.

Ehling-Schulz, M., Fricker, M., Scherer, S., *Bacillus cereus*, the causative agent of an emetic type of food-borne illness. *Mol. Nutr. Food Res.* 2004, 48, 479-487.

Errington, J., *Bacillus subtilis* sporulation: regulation of gene expression and control of morphogenesis. *Microbiol. Rev.* 1993, 57, 1-33.

Feinber, L., Jorgensen, J., Haselton, A., Pitt, A., Rudner, R., Margulis, L., Arthomitus (*Bacillus cereus*) symbionts in the cockroach *Blaberus giganteus*: dietary influence on bacterial development and population density. *Symbiosis.* 1999, 27, 104-123.

Fleischmann, R.D., Adams, M.D., White, O., Clayton, R.A., Kirkness, E.F., Kerlavage, A.R., Bult, C.J., Tomb, J.F., Dougherty, B.A., Merrick, J.M., Whole-genome random sequencing and assembly of *Haemophilus influenzae*. *Rd. Science*, 1995, 269, 496-512.

- Flemming, H.-C.**, Biofilms and environmental protection. *Water. Sci. Technol.*, 1993, 27, 1-10.
- Francis, C.A. and Tebo, B.M.**, Marine *Bacillus* spore as catalyists for oxidative precipitation and sorption of metals. *J. Mol. Microbiol. Biotechnol.* 1999, 1, 71-78.
- Geesey, G.G., Richardson, W.T., Yeomans, H.G., Irvin, R.T., Costerton, J.W.**, Microscopic examination of natural sessile bacterial populations from an alpine stream. *Can. J. Microbiol.*, 1977, 23, 7401-7404.
- Genevaux, P., Muller, S., Bauda, P.**, A rapid screening procedure to identify mini-Tn10 insertion mutants of *Escherichia coli* K-12 with altered adhesion properties. *FEMS Microbiol. Lett.*, 1996, 142, 27-30.
- Gohar, M., Økstad, O.A., Gilois, N., Sanchis, V., Kolstø, A-B., Lereclus, D.** Two-dimensional electrophoresis analysis of the Extracellular proteome of *Bacillus cereus* reveals the importance of the PlcR regulon. *Proteomics.* 2002, 2, 784-791.
- Gilbert, P., Das, J., Foley, I.**, Biofilms susceptibility to antimicrobials. *Adv. Dent. Res.*, 1997, 11, 160-167.
- Glare, T.R., O'Callaghan, M.**, *Bacillus thuringiensis*: Biology, Ecology and Safety. Chichester, U.K.: John Wiley & Sons, 2000.
- González, J.M., Jr., Carlton, B.C.**, A large transmissible plasmid is required for crystal toxin production in *Bacillus thuringiensis* variety *israelensis*. *Plasmid.* 1984, 11, 28-38.
- Gordon, R.E., Haynes, W.C., Pang, C.H.-N.**, The genus *Bacillus*. US Department of Agriculture, Washington. DC, 1973.
- Granum, P.E.**, *Bacillus cereus*. In: Doyle, M.P., et al. (Eds.), *Food microbiology: Fundamentals and Frontiers*, ASM Press, Washington, DC, 2001, pp. 373-381.
- Hamon, M.A., Lazazzera, B.A.**, The sporulation transcription factor Spo0A is required for biofilm development in *Bacillus Subtilis*. *Mol. Microbiol.* 2001, 42, 1199-1209.

- Hamon, M.A., Stanley, N.R., Britton, R.A., Grossman, A.D., Lazazzera, B.A.,** Identification of AbrB-regulated genes involved in biofilm formation by *Bacillus subtilis*. *Mol. Microbiol.*, 2004, 52, 847-860.
- Hansen, B.M., Salamitou, S.** Virulence of *Bacillus thuringiensis*. In *Entomopathogenic Bacteria: from Laboratory to field Application*. Cahrls, J.-F., Delecluse, A., Nielsen-LaRoux, C. (Eds.) Dordrecht: Kluwer Academic Publishers, 2000, pp. 41-46.
- Haug, S.,** Food poisoning caused by aerobic spore forming bacilli. *J. Appl. Bacteriol.* 1955, 18, 591-595.
- Heilmann, C., Gerke, C., Perdreau-Remington, F., Gotz, F.,** Characterization of Tn917 insertion mutants of *Staphylococcus epidermidis* affected in biofilm formation. *Infect. Immune.*, 1996, 64, 277-282.
- Heilmann, C., Gotz, F.,** Furter characterization of *Staphylococcus epidermidis* transposon mutants deficient in primary attachment or intercellular adhesion. *Zentralbl. Bakteriol.*, 1998, 287, 69-83.
- Heilmann, C., Hussain, M., Peters, G., Gotz, F.,** Evidence for autolysin mediated primary attachment of *Staphylococcus epidermidis* to a polystyrene surface. *Mol. Microbiol.*, 1997, 24, 1013-1024.
- Heilmann, C., Schweitzer, O., Gerke, C., Vanittanakom, N., Mack, D., Gotz, F.,** Molecular basis of intercellular adhesion in the biofilm-forming *Staphylococcus epidermidis*. *Mol. Microbiol.*, 1996, 20, 1083-1091.
- Helgason, E., Caugant, D.A., Olsen, I., Kolstø, A.-B.,** Genetic structure of population of *Bacillus cereus* and *Bacillus thuringiensis* associated with periodontitis and other human infections. *J. Clin. Microbiol.* 2000, 38, 1615-1622.

- Helgason, E., Okstad, O.A., Caugant, D.A., Johansen, H.A., et al.,** *Bacillus anthracis*, *Bacillus cereus* and *Bacillus thuringiensis* – One species on the basis of genetic evidence. *Appl. Environ. Microbiol.* 2000, 66, 2627-2630.
- Henrichsen, J.,** Bacterial surface translocation: a survey and a classification. *Microbiol. Rev.*, 1972, 36, 478-503.
- Hendriksen, N.B. Hansen, B.M.** Long-term survival and germination of *Bacillus thuringiensis* var. *kurstaki*; a field trial. *Can. J. Microbiol.* 2002, 48, 256-261.
- Herron, W.M.** Rancidity in cheddar cheese. Master's thesis, Queen's University, Kingston, Ontario, Canada. 1930.
- Hillard, N. J., Schelonka, R.L., Waites, K.B.** *Bacillus cereus* bacteremia in preterm neonates. *J. Clin. Microbiol.* 2003, 41, 3441-3444.
- Holbrook, R., Anderson, J.M.,** An improved selective and diagnostic medium for the isolation and enumeration of *Bacillus cereus* in food. *Can. J. Microbiol.* 1980, 26, 753-759.
- Horinouchi, S. and Weisblum, B.** Posttranscriptional modification of mRNA conformation: mechanism that regulates erythromycin-induced resistance. *Proc. Natl. Acad. Sci.* 1980, 12, 7079-7083.
- Hussain, M., Herrmann, M., von Eiff, C., Perdreau-Remington, F., Peters, G.,** A 140-kilodalton Extracellular protein is essential for the accumulation of *Staphylococcus epidermidis* strains on surfaces. *Infect. Immun.* 1997, 65, 519-524.
- Ivanova, N., Sorokin, A., Anderson, I., Galleron, N., Cadelon, B., et al.,** Genome sequence of *Bacillus cereus* and comparative analysis with *Bacillus anthracis*. *Nature*, 2003, 423, 87-91.
- Jensen, G.B., Hansen, B.M., Eilenberg, J., Mahillon, J.,** The hidden lifestyles of *Bacillus cereus* and relatives. *Environmental Microbiology*, 2003, 5, 631-640.

Jukowska, D., Obuchowski, M., Holland, I.B., Seror, S.J., Branched swarming patterns in a synthetic medium formed by wild-type *Bacillus subtilis* strain 3610: Detection of different cellular morphologies and constellations of cells as the complex architecture develops.

Microbiology. 2004, 150, 1839-1849.

Jukowska, D., Obuchowski, M., Holland, I.B., Seror, S.J., Comparative analysis of the development of swarming communities of *Bacillus subtilis* 168 and a natural wild-type: critical effects of surfactin and the composition of the medium. *J. Bacteriol.* 2005, 187, 65-76.

Kenney, L.J. Structure/function relationships in OmpR and other winged-helix transcription factors. *Curr. Opin. Microbiol.* 2002, 5, 135-141.

Kornberg, A., Spudich, J.A., Nelson, D.L. and Deuthcer, M., Origin of proteins in sporulation. *Ann. Rev. Bioch.,* 1968, 37, 51-78.

Kotiranta, A., Lounatmaa, K., Haapasalo, M., Epidemiology and pathogenesis of *Bacillus cereus* infections. *Microbes. Infect.,* 2000, 2, 189-198.

Kramer, J.M., Gilbert, R.J., *Bacillus cereus* and other *Bacillus* species. In: Doyle, M.P. (Ed.), *Food borne bacterial pathogens*, Marcel Dekker, New York 1989, pp. 21-70.

Kronstad, J.W., Schnepf, H.E., Whiteley, H.R. Diversity of location for *Bacillus thuringensis* crystal proteins genes. *J. Bacteriol.* 1983, 154, 419-428.

Leblanc, D.J., Lee, L.N., Inamine, J.M. Cloning and nucleotide base sequence analysis of a spectinomycin adenylyltransferase AAD determinant from *Enterococcus faecalis*. *Antimicrob. Agents. Chemother.* 1991, 35, 1804-1810.

Lecadet, M.M., Frachon, E., Dumanoir, V.C., Ripouteau, H., Hamon, S., Laurent, P.,

Thiery, I., Updating the H-antigen classification of *Bacillus thuringensis*, *J. Appl. Microbiol.* 1999, 86, 660-672.

- Lechner, S., Mayr, R., Francis, K.P., Prüß, B.M., et al.,** *Bacillus weihenstephanensis* sp. Nov. is a new psychrotolerant species of the *Bacillus cereus* group. *Int. J. Sys. Bacteriol.* 1998, 48, 1373-1382.
- Lindbäck, T., Økstad, O.A., Rishovd, A.L., Kolstø, A.B.** Insertional inactivation of *hblC* encoding the L2 component of *Bacillus cereus* ATCC 14579 haemolysin BL strongly reduces enterotoxigenic activity, but not the haemolytic activity against human erythrocytes. *Microbiology.* 1999, 145, 3139-3146.
- Lindsay, D., Brözel, V.S., Mostert, J.F., von Holy, A.** Physiology of dairy-associated *Bacillus* spp. over a wide pH range. *Int. J. Food Microbiol.* 2000, 54, 49-62.
- Lund, T., De Buyser, M.L., Granum, P.E.,** A new cytotoxin from *Bacillus cereus* that may cause necrotic enteritis. *Mol. Microbiol.* 2000, 38, 254-261.
- Luxananil, P., Atomi, H., Panyim, S., Imanaka, T.** Isolation of bacterial strains colonisable in mosquito larval guts as novel host cells for mosquito control. *J. Biosci. Bioeng.* 2001, 92, 342-345.
- Mack, D., Nedelmann, M., Krokotsch, A., Schwarzkopf, A., Heeseman, J., Laufs, R.,** Characterization of transposon mutants of biofilm-producing *Staphylococcus epidermidis* impaired in the accumulative phase of biofilm production: genetic identification of a hexosamine-containing polysaccharide intracellular adhesin. *Infect. Immun.*, 1994, 62, 3244-3253.
- Madigan, M.T., Martinko, J.M., Parker, J.,** Microbial ecology. In Brock biology of microorganisms, 8th edition, 1997, 532-605.
- Mahler, H., Pasi, A., Kramer, J.M., Schulte, P., et al.,** Fulminant liver failure in association with the emetic toxin of *Bacillus cereus*. *N. Engl. J. Med.* 1997, 336, 1142-1148.
- Martin, P.A.W., Travers, R.S.** Worldwide abundance and distribution of *Bacillus thuringiensis* isolates. *Appl. Environ. Microbiol.* 1989, 55, 2437-2442.

- McGregor, C.H., Wolff, J.A., Arora, S.K., Phibbs, P.V. Jr.,** Cloning of the catabolite repression control (*crc*) gene from *Pseudomonas aeruginosa*, expression of the gene in *Escherichia coli*, and identification of the gene product in *Pseudomonas aeruginosa*. *J. Bacteriol.*, 1991, 173, 7204-7212.
- McKenney, D., Hubner, J., Muller, E., Wang, Y., Godlmann, D.A., Pier, G.B.,** The *ica* locus of *Staphylococcus epidermidis* encodes production of the capsular polysaccharide/adhesion. *Infect. Immun.*, 1998, 66, 4711-4720.
- McLean, R.J., Whitely, M., Stickler, D.J., Fuqua, W.C.,** Evidence of autoinducer activity in naturally occurring biofilms. *FEMS. Microbiol. Lett.*, 1997, 154, 259-263.
- Mizuno, T.** Compilation of all genes encoding two-component phosphotransfer signal transducers in the genome of *Escherichia coli*. *J. Bacteriol.* 1997, 4, 161-168.
- Mock, M., Fouet, A.** Anthrax. *Annu. Rev. Microbiol.* 2001, 55, 647-671.
- Murell, W.G.,** The biochemistry of the bacterial endospore. *Adv. Microbiol. Phys.*, 1967, 1, 133-251.
- Murell, W.G.,** Chemical composition of spores and spore structures. *The Bacterial Spore.*, 1969, 215-273.
- Nakamura, L.** *Bacillus pseudomycolides* sp. nov. *Int. J. Syst. Bacteriol.* 1998, 48, 1031-1035.
- Okinaka, R., Cloud, K., Hampton, O., Hoffmaster, A., Hill, K., Keim, P., et al.** Sequence, assembly and analysis of pXO1 and pXO2. *J. Appl. Microbiol.* 1999a, 87, 261-262.
- Okinaka, R., Cloud, K., Hampton, O., Hoffmaster, A., Hill, K., Keim, P., et al.** Sequence, assembly and organization of pXO1, the large *Bacillus anthracis* plasmid harbouring the anthrax toxin genes. *J. Bacteriol.* 1999b, 181, 6509-6515.
- Okstad, O.A., Gominet, M., Purnelle, B., Rose, M., et al.,** Sequence analysis of three *Bacillus cereus* loci carrying PlcR-regulated genes encoding degradative enzymes and enterotoxin. *Microbiology* 1999, 145, 3129-3138.

Oosthuizen, M.C., Steyn, B., Lindsay, D., Brözel, V.S., von Holy, A. Novel method for the proteomic investigation of a dairy-associated *Bacillus cereus* biofilm. *FEMS Microbiol. Let.* 2001, 194, 47-51.

Oosthuizen, M.C., Steyn, B., Theron, J., Cosette, P., Lindsay, D., von Holy, A., Brözel, V.S. Proteomic analysis reveals differential protein expression by *Bacillus cereus* during biofilm formation. *Appl. Environ. Microbiol.* 2002, 68, 2770-2780.

Orduz, S., Restrepo, W., Patino, M.M., Rojas, W., Transfer of toxin genes alternate bacterial hosts for mosquito control. *Memorias Do Inst. Oswaldo Cruz,* 1995, 90, 97-107.

O'Toole, G.A., Kaplan, H.B., Kolter, R. Biofilm formation as microbial development. *Ann. Rev. Microbiol.* 2000, 54, 49-79.

O'Toole, G.A., Gibbs, K.A., Hager, P.W., Phibbs, P.V. Jr., Kolter, R., The global carbon metabolism regulator Crc is a component of signal transduction pathway required for biofilm development by *Pseudomonas aeruginosa*. *J. Bacteriol.* 2000, in press.

O'Toole, G.A., Kolter, R., The initiation of biofilm formation in *Pseudomonas fluorescens* WCS365 proceeds via multiple convergent signalling pathways: a genetic analysis. *Mol. Microbiol.,* 1998, 28, 449-461.

Patra, G., Fouet, A., Vaissaire, J., Guesdon, L.L., Mock, M., Variation in rRNA operon number as revealed by ribotyping of *B. anthracis* strains. *Res. Microbiol.* 2002, 153, 139-148.

Pearson, T., Busch, J.D., Ravel, J., Read, T.D., Rhoton, S.D., U'Ren, J.M., Simonson, T.S., Kachur, S.M., Leadem, R.R., Cardon, M.L., Van Ert, M.N., Huynh, L.Y., Fraser, C.M., Keim, P., Phylogenetic discovery bias in *Bacillus anthracis* using single-nucleotide polymorphisms from whole-genome sequencing. *Proce. Nat. Acd. Scie. U.S.A.,* 2004, 101, 13536-13541.

Peng, J.S., Tsai, W.C., Chou, C.C., Inactivation and removal of *Bacillus cereus* by sanitizer and detergent. *Int. J. Food. Microbiol.,* 2002, 77, 11-18.

- Piggot, P.J. and Hilbert, D.W.**, Sporulation of *Bacillus subtilis*. *Curr. Opin. Microbiol.* 1994, 7, 579-586.
- Porcar, M., Caballero, P.** Molecular and insecticidal characterization of a *Bacillus thuringiensis* strain isolated during natural epizootic. *J. Appl. Microbiol.* 2000, 89, 309-316.
- Pratt, L.A., Kolter, R.**, Genetic analysis of *Escherichia coli* biofilm formation: defining the roles of flagella, motility, chemotaxis and type I pili. *Mol. Microbiol.*, 1998, 30, 285-294.
- Priest, L.A.**, Systematics and ecology of *Bacillus*. *Bacillus subtilis and other Gram-positive bacteria: biochemistry, physiology and molecular genetics*. 1993, 3-16.
- Priest, F.G., Goodfellow, M., Todd, C.**, A frequency matrix for probabilistical identification of some bacilli. *J. Gen. Microbiol.* 1998, 134, 1847-1882.
- Rasko, D.A., Altherr, M.R., Han, C.S., Ravel, J.**, Genomics of the *Bacillus cereus* group of organisms. *FEMS. Microbiol. Rev.* 2005, 29, 303-329.
- Rasko, D.A., Ravel, J., Økstad, O.A., Helgason, E., Cer, R.Z., et al.**, The genome sequence of *Bacillus cereus* ATCC 10987 reveals metabolic adaptations and a large plasmid related to *Bacillus anthracis* pXO1. *Nucl. Aci. Resea.* 2004, 32, 977-988.
- Rayer, P.** Inoculation du sang de rate. *C. R. Soc. Biol. Paris.* 1850, 2, 141-144.
- van Rie, J., McGaughey, W.H., Johnson, D.E., Barnet, B.D., van Mellaert, H.** Mechanism of insect resistance to the microbial insecticide *Bacillus thuringiensis*. *Science.* 1990, 247, 72-74.
- Read, T.D., Peterson, S.N., Tourasse, N., Bailie, L.W., Paulsen, I.T., Nelson, K.E., Tettelin, H., Fouts, D.E., Eisen, J.A., Gill, S.R., et al.** The genome sequence of *Bacillus anthracis* Ames and comparison to closely related bacteria. *Nature.* 2003, 423, 81-86.
- Saier M.H. Jr.** A functional-phylogenetic classification system for transmembrane solute transporters. *Microbiol. Mol. Biol. Rev.*, 2000, 64, 354-411.

Saleh, S.M., Harris, R.F., Allen, O.N. Fate of *Bacillus thuringiensis*. soil: effect of soil pH and organic amendment. *Can. J. Microbiol.* 1970, 16, 677-680.

Sauer, K., Cullen, M.C., Rickard, A.H., Zeef, L.A.H., Davies, D.G., Gilbert, P., Characterization of nutrient-induced dispersion in *Pseudomonas aeruginosa* PAO1 biofilm. *J. Bacteriol.*, 2004, 186, 7312-7326.

Schumacher-Perdreau, F., Heilmann, C., Peters, G., Gotz, F., Pulverer, G., Comparative analysis of a biofilm-forming *Staphylococcus epidermidis* strain and its adhesion-positive, accumulation-negative mutant M7. *FEMS. Microbiol.*, 1994, 117, 71-78.

Shinagawa, K., Analytical methods for *Bacillus cereus* and other *Bacillus* species. *Int. J. Food Microbiol.* 1990, 10, 125-141.

Slamti, L., Perchat, S., Gominet, M., Vilas-Boas, G., et al., Distinct mutations in PlcR explain why some strains of the *Bacillus cereus* group are nonhemolytic. *J. Bacteriol.* 2004, 186, 3531-3538.

Smith, N. Aerobic spore forming bacteria. *US. Dep. Agric. Monogr.* 1952, 16, 1-148.

Sneath, P.H.A., Endospore-forming Gram-positive rods and cocci. *Bergey's Manual of Systematic Bacteriology*, 1986, 2, 1131.

Solomon, J.M., Grossman, A.D., Who's competent and when: Regulation of natural genetic competence in bacteria. *Trends. Genet.*, 1996, 12, 150-155.

Stanley, P., Losick, R., Molecular genetics of sporulation in *Bacillus subtilis*. *Annu. Rev. Genet.* 1996, 30, 297-341.

Stenfors, L.P., Mayr, R., Scherer, S., Granum, P.E. Pathogenic potential of fifty *Bacillus weihenstephanensis* strains. *Fems. Microbiol. Let.* 2002, 215, 47-51.

Stickler, D.J., Morris, N.S., McClean, R.J.C., Fuqua, C., Biofilms on indwelling urethral catheters produce quorum-sensing signal molecules *in situ* and *in vitro*. *Appl. Environ. Microbiol.*, 1998, 64, 3486-3490.

Straiger, P., Losick, R., Molecular genetics of sporulation in *Bacillus subtilis*. *Annu. Rev. Genet.*, 1996, 30, 297-341.

Turnbull, P.C.B., Kramer, J.M., *Bacillus*. In: Balows, A., Hausler, W.J., Hermann, K.L., Isenberg, H.D., Shadomy, H.J. (Eds.), *Manual of Clinical Microbiology*, American Society for Microbiology, Washington. DC 1991, pp. 296-303.

Turnbull, P.C.B., Kramer, J., Melling, J., *Bacillus*, In: Topley and Wilson's principles of bacteriology, virology and immunity, 1990, 2, 188-210.

Vankova, J., Purrini, K. Natural epizooties caused by bacilli of the species *Bacillus thuringensis* and *Bacillus cereus*. *Z. Gen. Microbiol.* 1979, 88, 216-221.

Vidal, O.L., Prigent-Combaret, R.C., Dorel, C., Hooreman, M., Lejune, P., Isolation of an *Escherichia coli* K-12 strain able to form biofilm on inert surfaces: involvement of a new *ompR* allele that increases curli expression. *J. Bacteriol.*, 1998, 180, 2442-2449.

Wall, D., Kaiser, D., Type IV pili and cell motility. *Mol. Microbiol.* 1999, 32, 1-10.

Warth, A.D., Ohye, D.F. and Murell, W.G., The composition and structure of bacterial spores. *J. Cell. Biol.* 1963, 16, 579-592.

Watnick, P.I. and Kolter, R. Steps in the development of a *Vibrio cholerae* El Tor biofilm. *Mol. Microbiol.* 1999, 34, 586-595.

Wenzel, M., Schonig, I., Berchtold, M., Kampfer, P., Konig, H. Aerobic and facultative anaerobic cellulolytic bacteria from the gut of the termite *Zootermopsis angusticollis*. *J. Appl. Microbiol.* 2002, 92, 32-40.

Wolff, J.A., MacGregor, C.H., Eisenberg, R.C., Phibbs, P.V. Jr., Isolation and characterization of catabolic repression control mutants of *Pseudomonas aeruginosa* PAO. *J. Bacteriol.*, 1991, 173, 4700-4706.

Yildiz, F.H. and Schoolnik, G.K. *Vibrio cholerae* O1 El Tor: identification of a gene cluster required for the rugose colony type, exopolysaccharide production, chlorine resistance, and biofilm formation. *Proc. Natl. Acad. Sci.* 1999, 96, 4028-4033.

Økstad, O.A., Hegna, I., Lindbäck, T., Rishovd, A.L., Kolstø, A.B. Genome organization is not conserved between *Bacillus cereus* and *Bacillus subtilis*. *Microbiology.* 1999, 145, 621-631.

6 APPENDIX

6.1 Biofilm formation

Biofilm screening graphs with raw data for, which background signal has not been deducted and with standard deviation included:

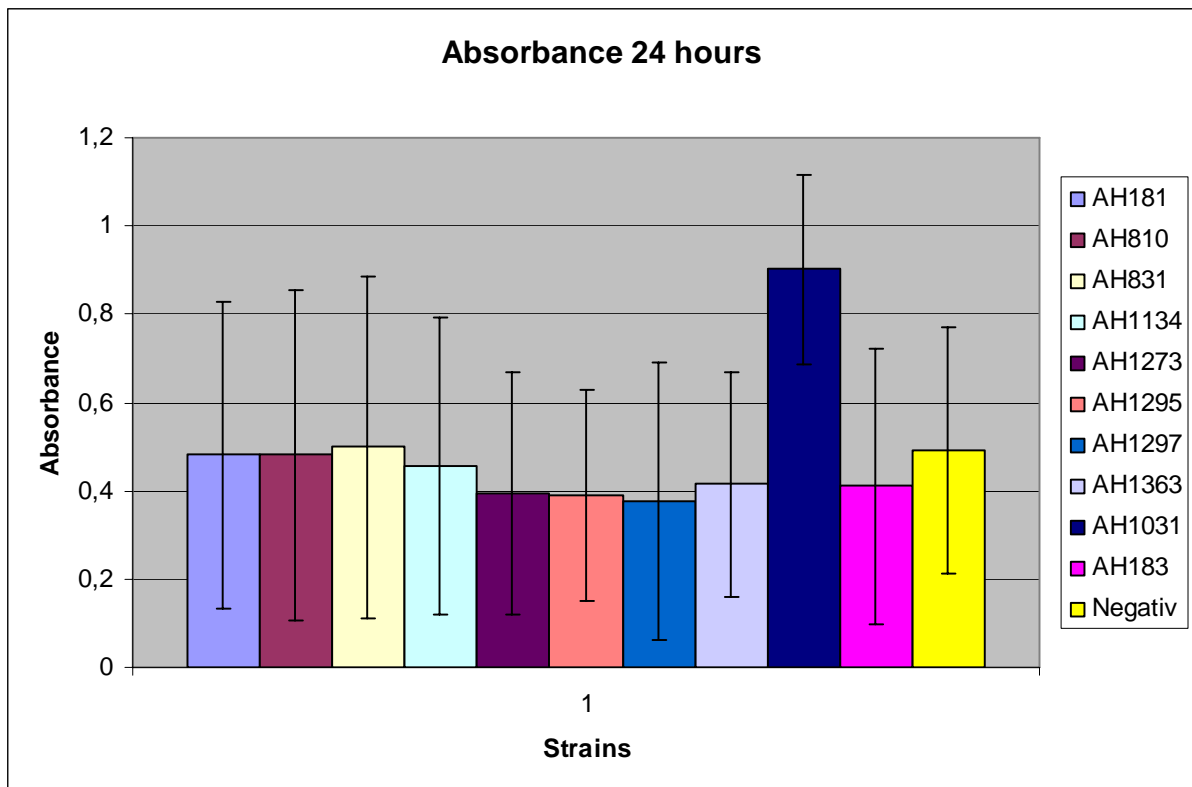


Figure 6.1: Biofilm formation as measured by crystal violet absorbance after 24 hours of incubation (background signal from negative control not deducted), with standard deviation from 16 parallels included.

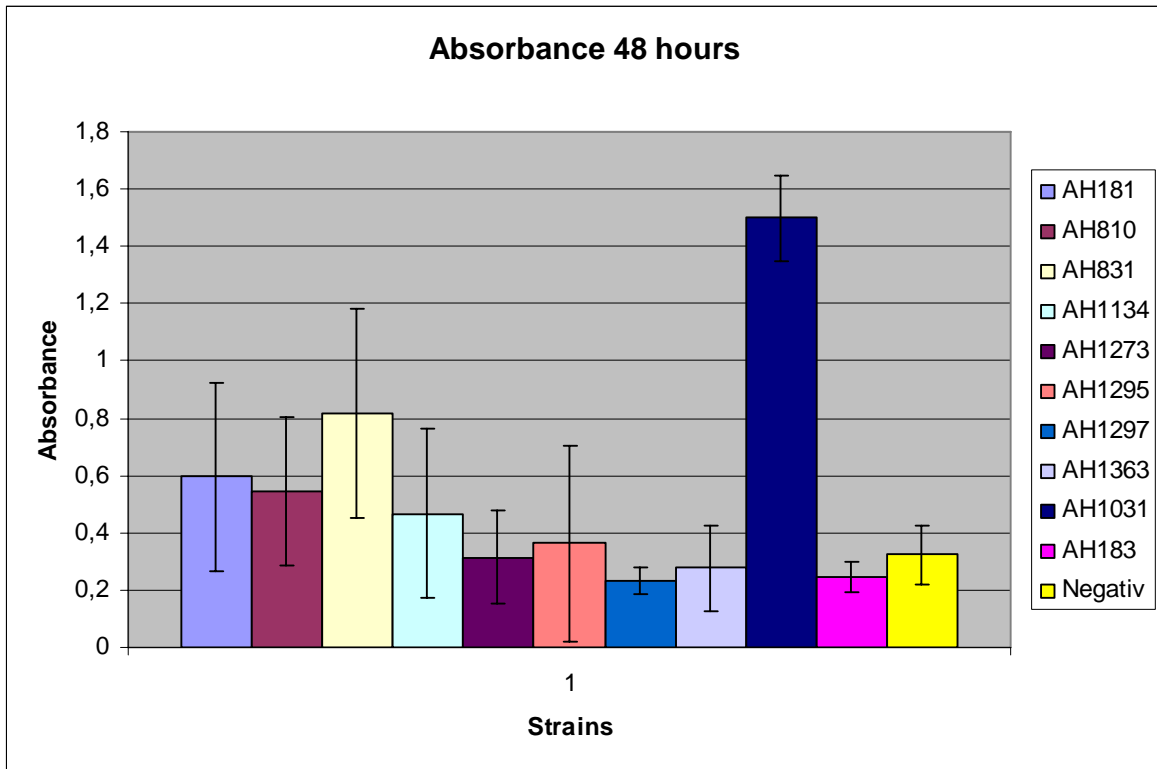


Figure 6.2: Biofilm formation as measured by crystal violet absorbance after 48 hours of incubation (background signal from negative control not deducted), with standard deviation from 16 parallels included.

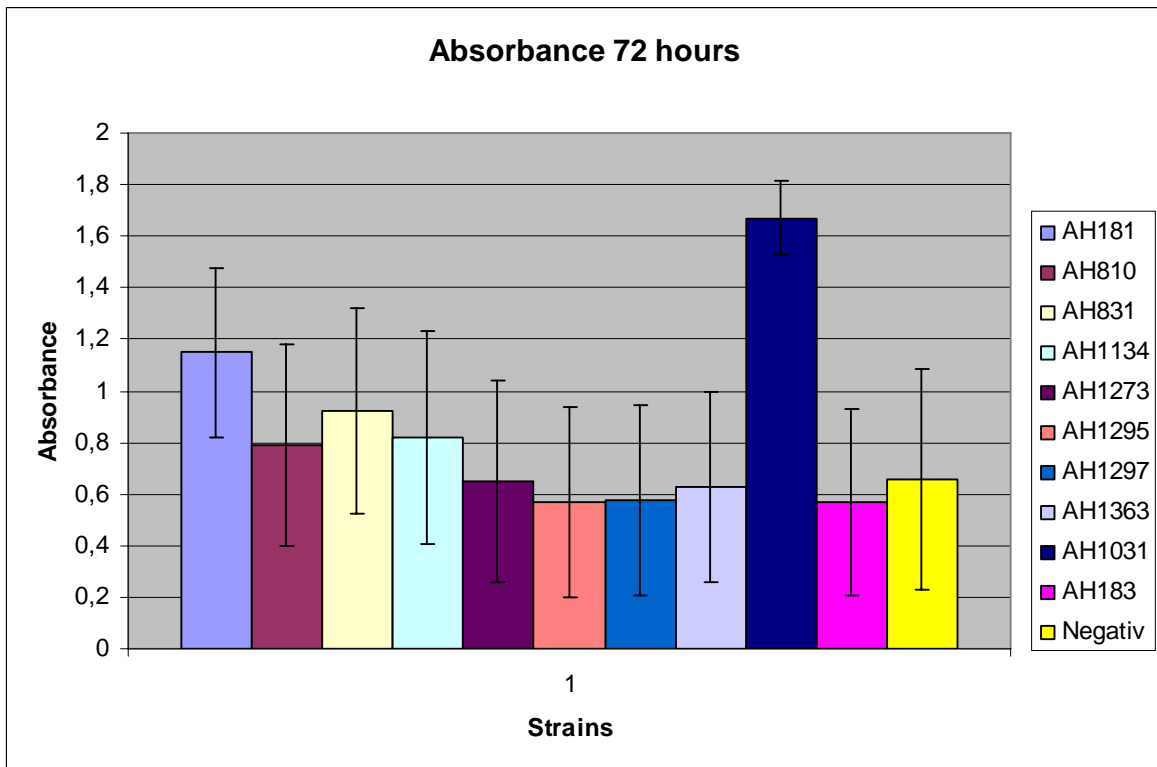


Figure 6.3: Biofilm formation as measured by crystal violet absorbance after 72 hours of incubation (background signal from negative control not deducted), with standard deviation from 16 parallels included.

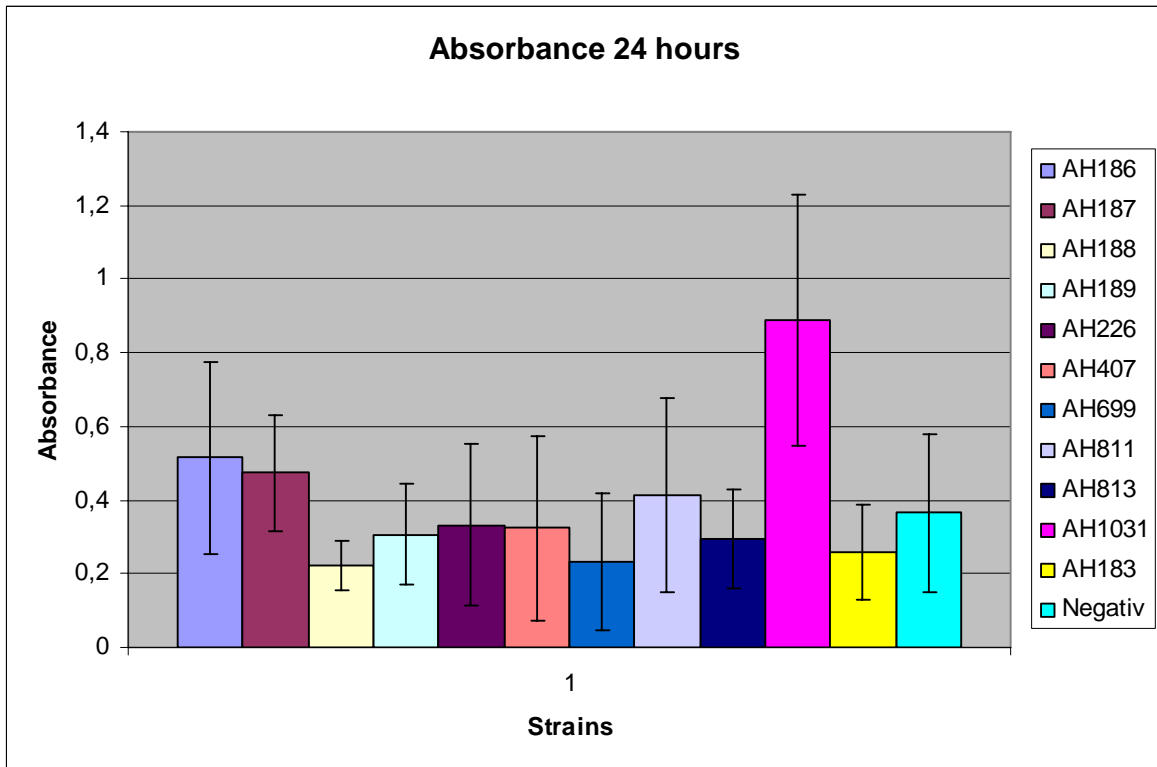


Figure 6.4: Biofilm formation as measured by crystal violet absorbance after 24 hours of incubation (background signal from negative control not deducted), with standard deviation from 16 parallels included.

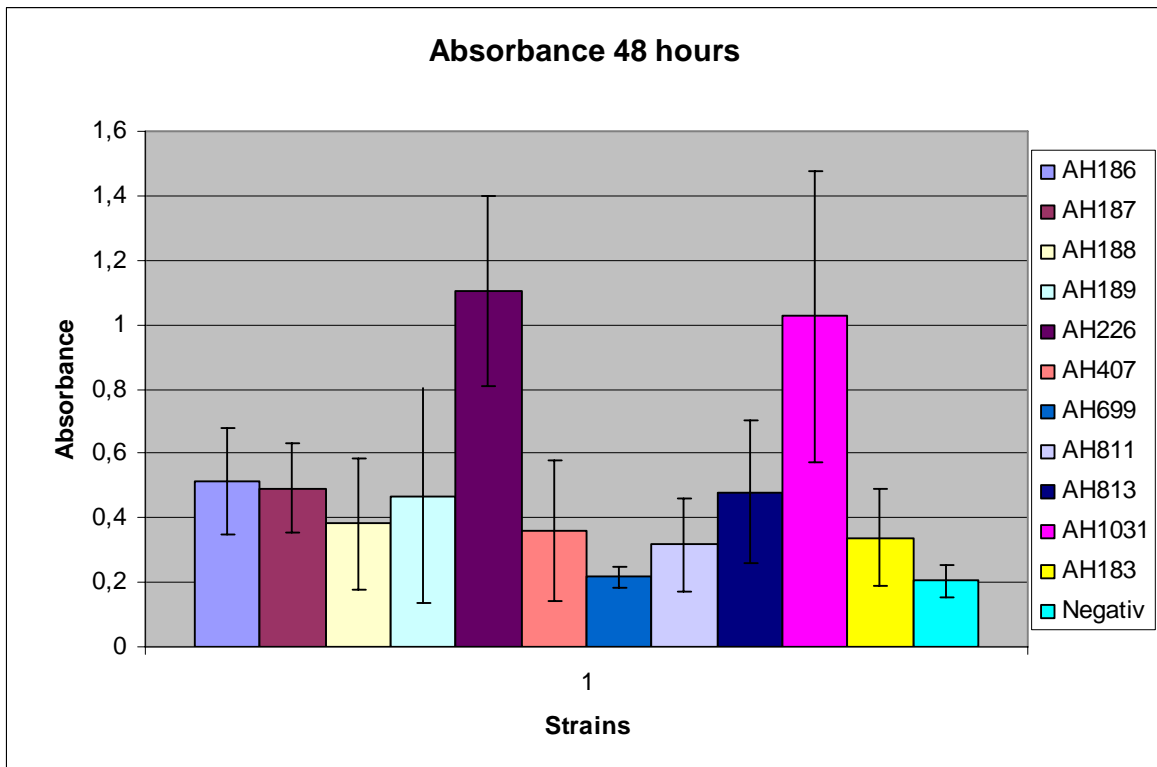


Figure 6.5: Biofilm formation as measured by crystal violet absorbance after 48 hours of incubation (background signal from negative control not deducted), with standard deviation from 16 parallels included.

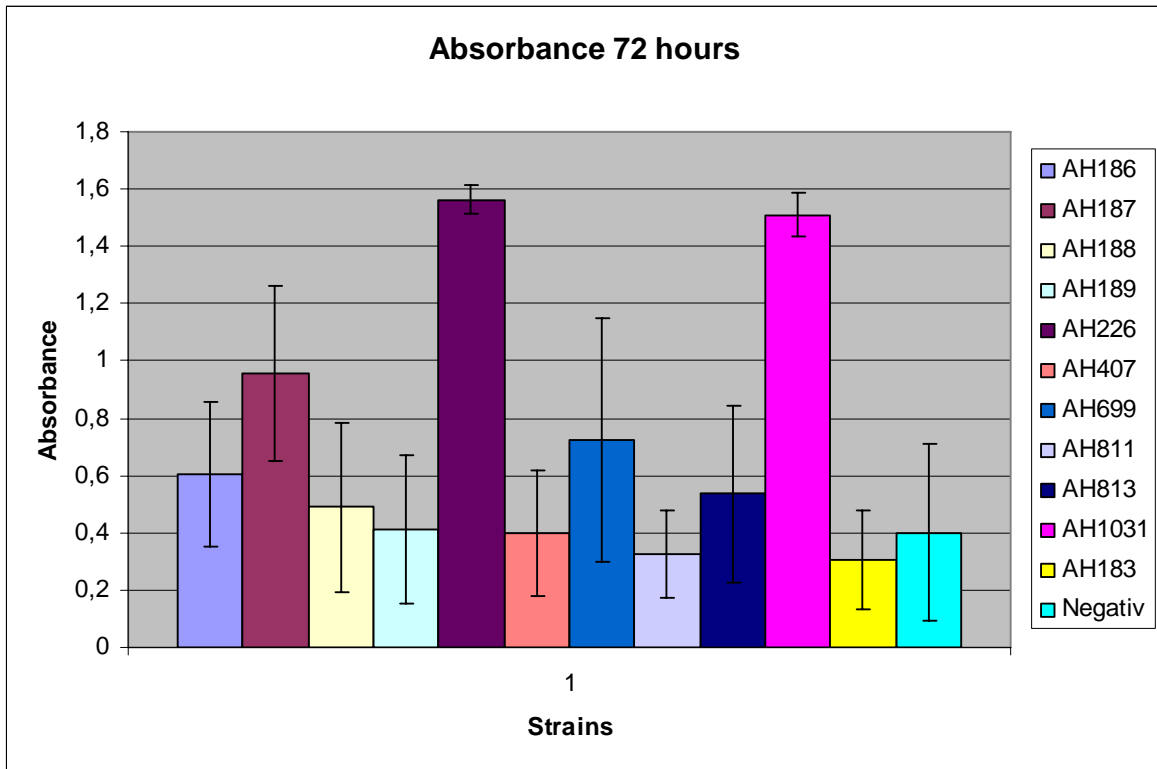


Figure 6.6: Biofilm formation as measured by crystal violet absorbance after 72 hours of incubation (background signal from negative control not deducted), with standard deviation from 16 parallels included.

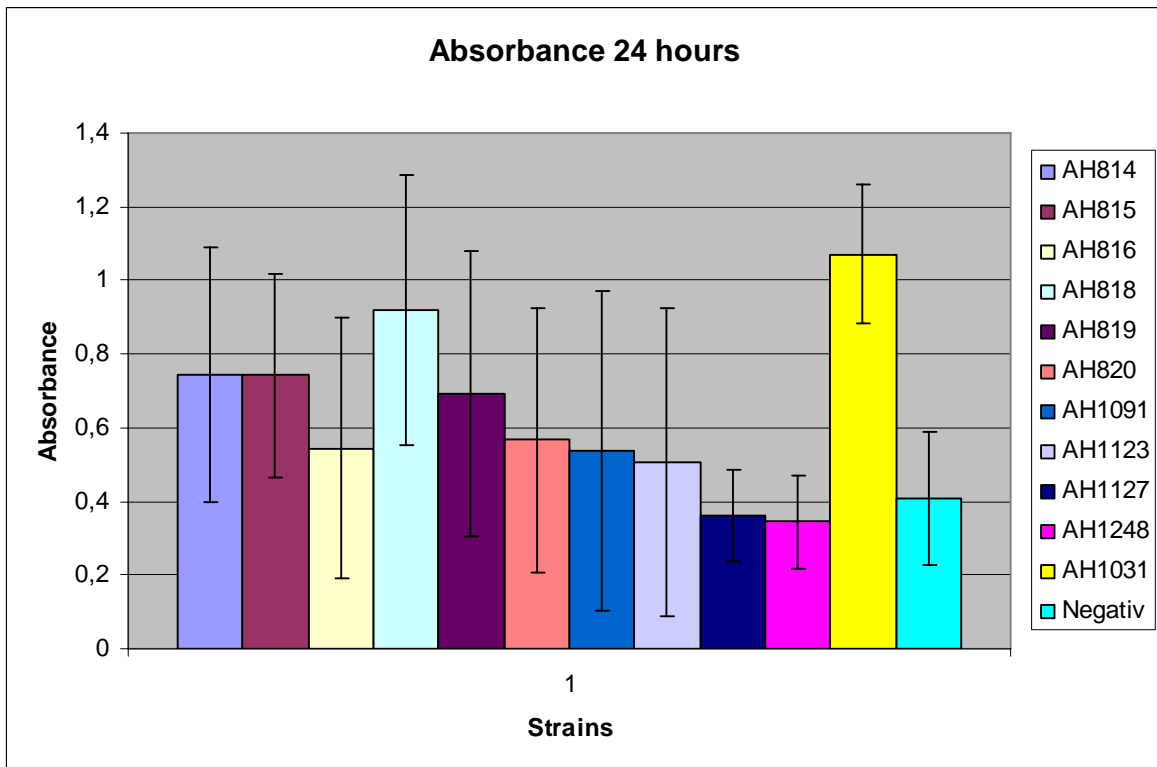


Figure 6.7: Biofilm formation as measured by crystal violet absorbance after 24 hours of incubation (background signal from negative control not deducted), with standard deviation from 16 parallels included.

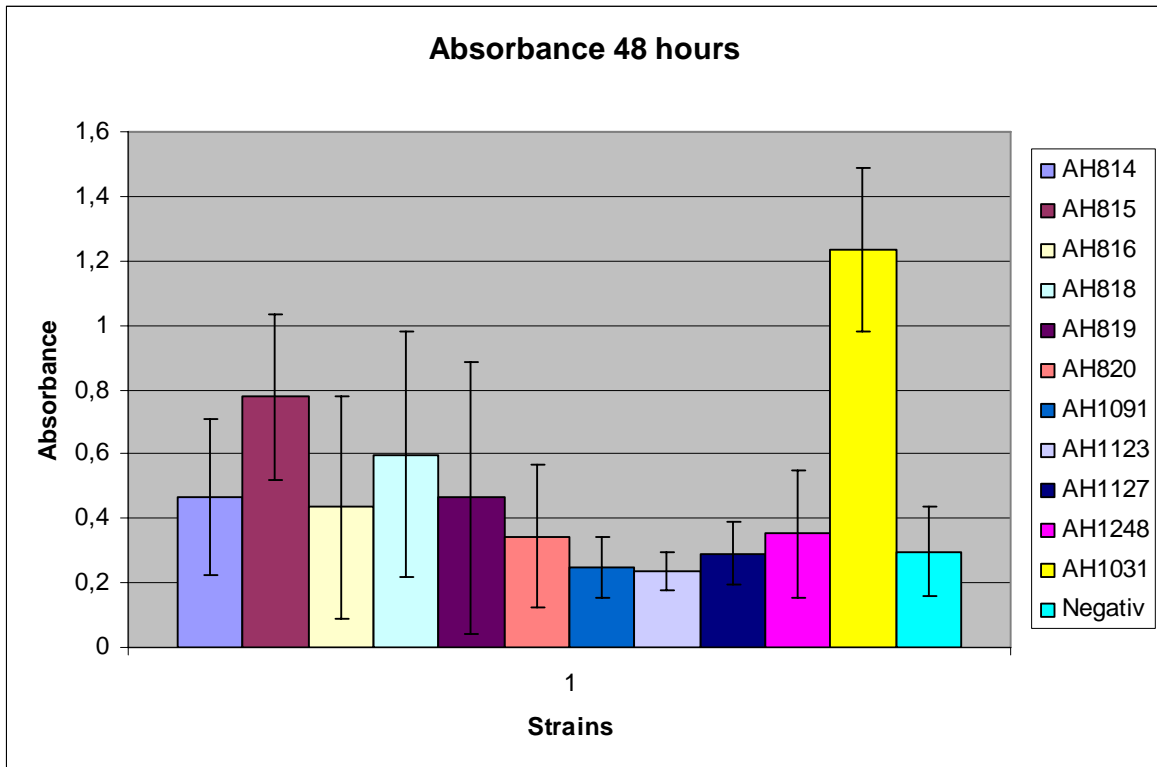


Figure 6.8: Biofilm formation as measured by crystal violet absorbance after 48 hours of incubation (background signal from negative control not deducted), with standard deviation from 16 parallels included.

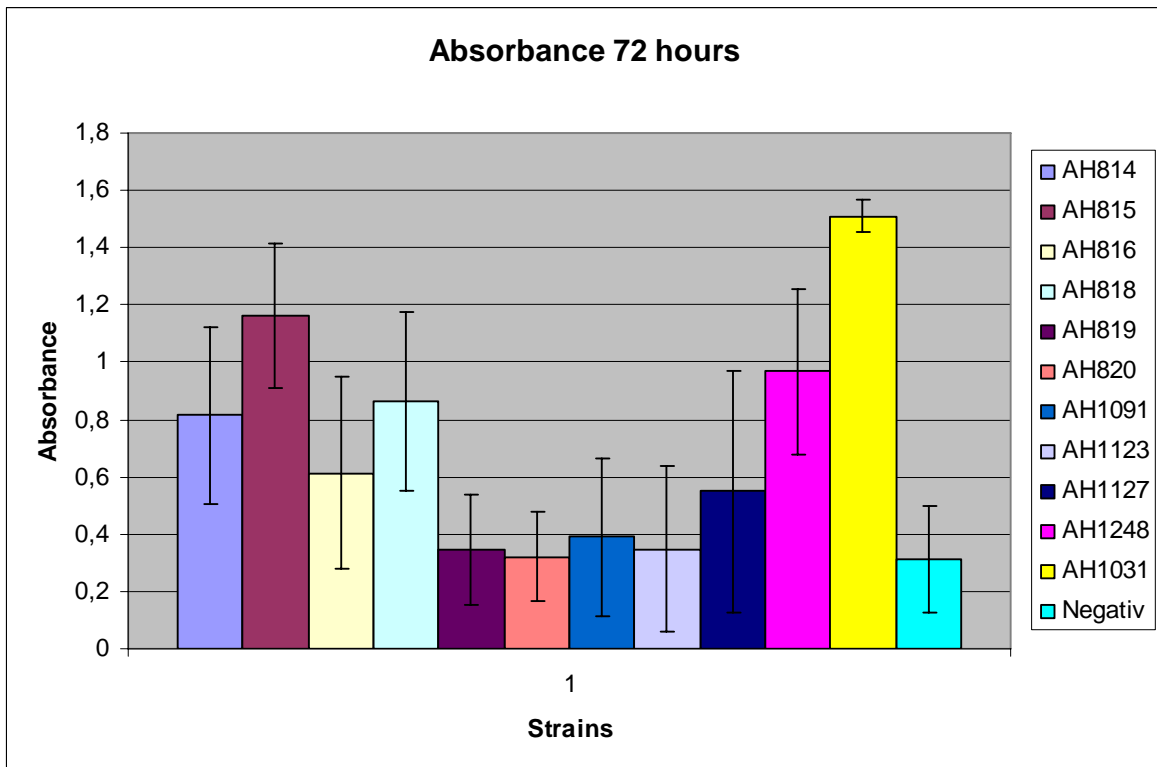


Figure 6.9: Biofilm formation as measured by crystal violet absorbance after 72 hours of incubation (background signal from negative control not deducted), with standard deviation from 16 parallels included.

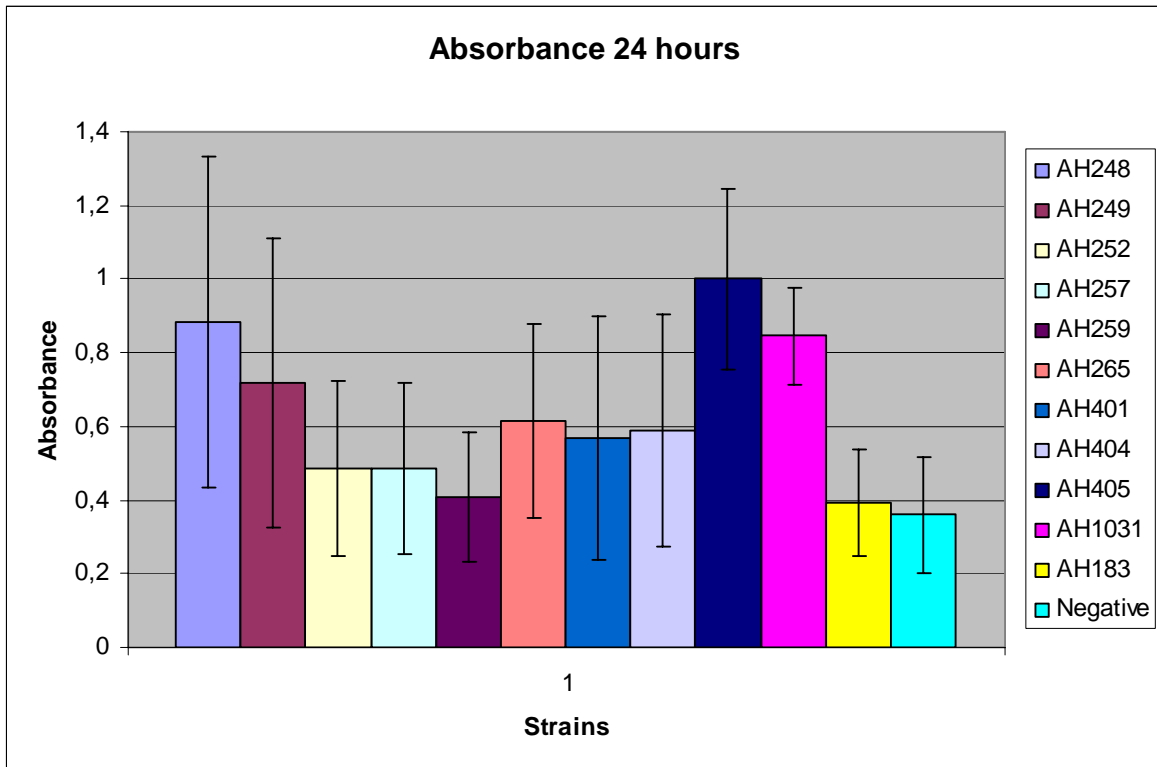


Figure 6.10: Biofilm formation as measured by crystal violet absorbance after 24 hours of incubation (background signal from negative control not deducted), with standard deviation from 16 parallels included.

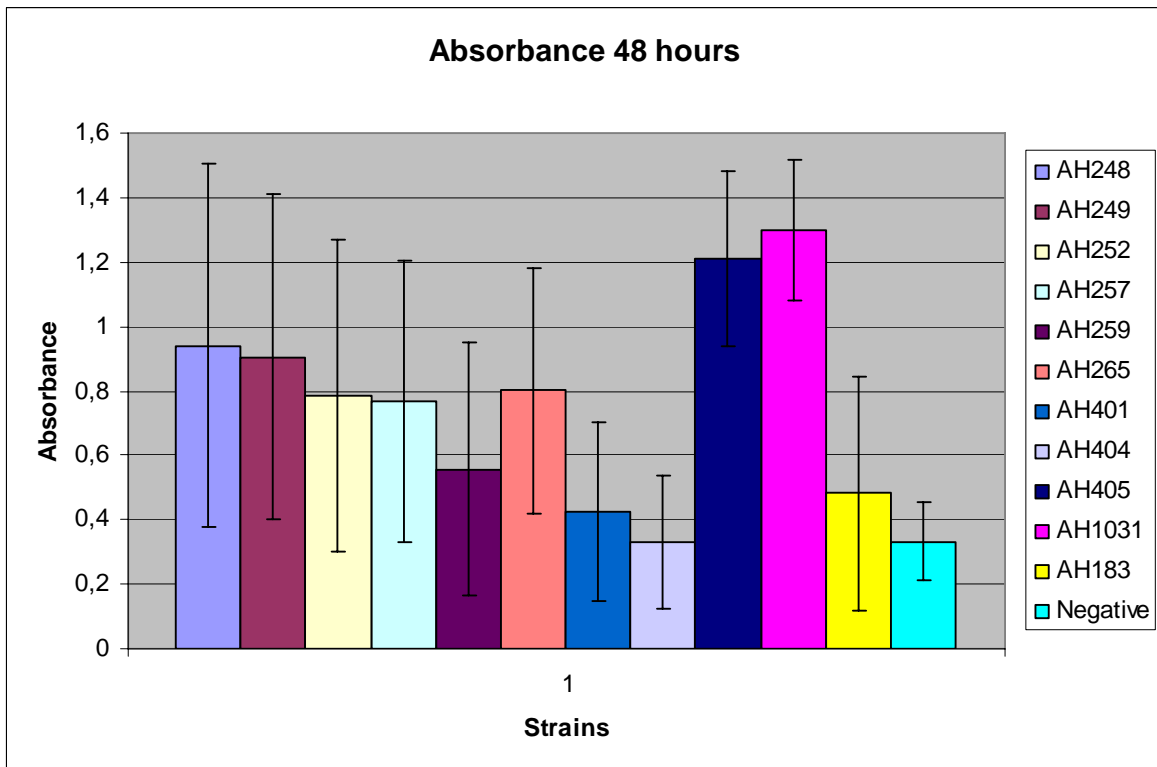


Figure 6.11: Biofilm formation as measured by crystal violet absorbance after 48 hours of incubation (background signal from negative control not deducted), with standard deviation from 16 parallels included.

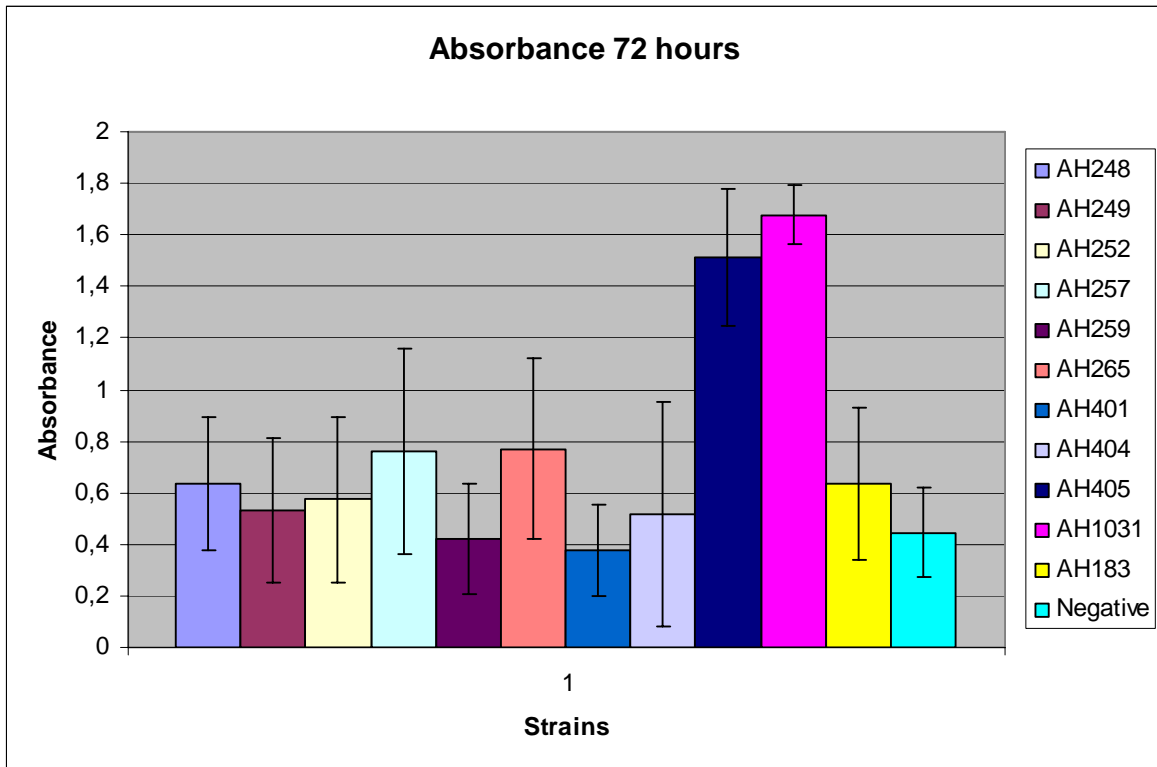


Figure 6.12: Biofilm formation as measured by crystal violet absorbance after 72 hours of incubation (background signal from negative control not deducted), with standard deviation from 16 parallels included.

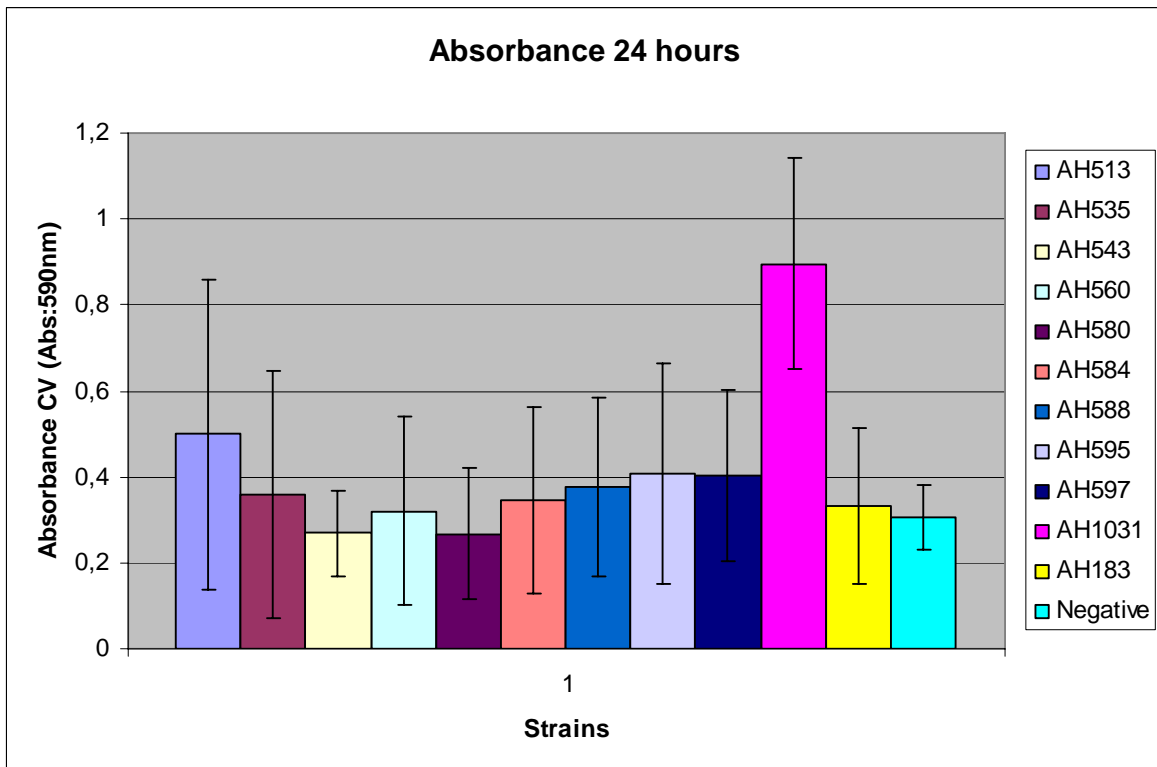


Figure 6.13: Biofilm formation as measured by crystal violet absorbance after 24 hours of incubation (background signal from negative control not deducted), with standard deviation from 16 parallels included.

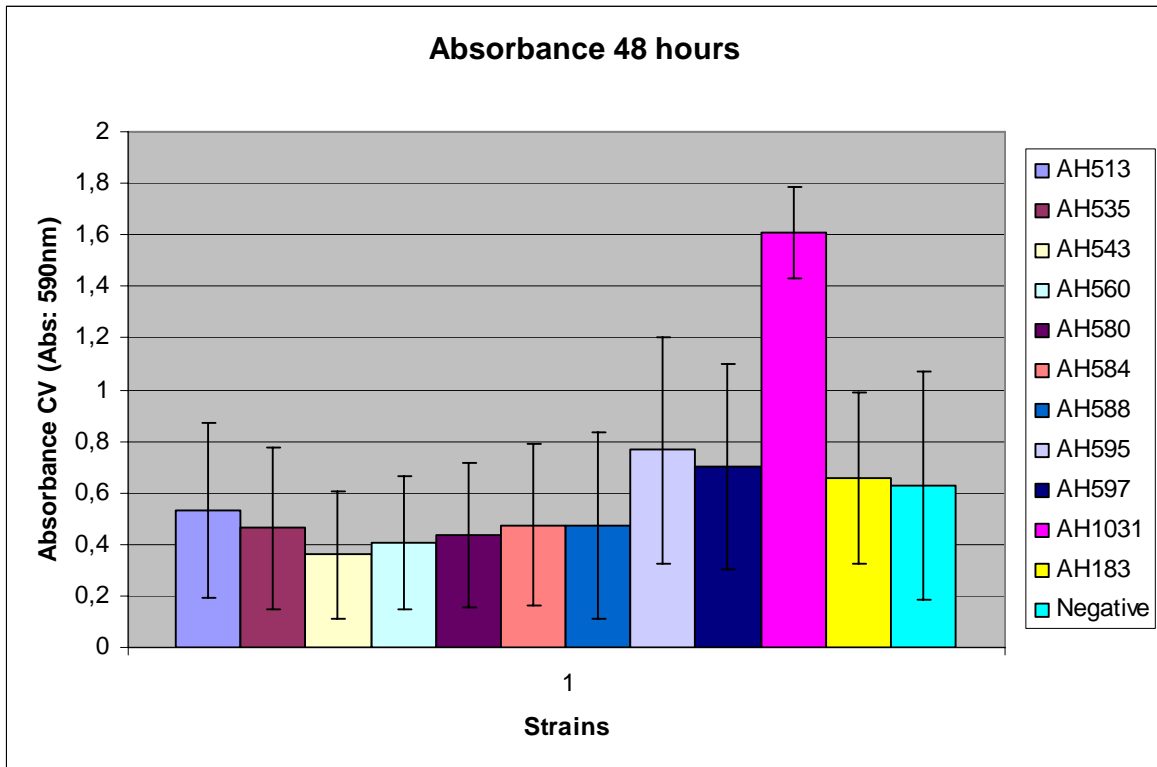


Figure 6.14: Biofilm formation as measured by crystal violet absorbance after 48 hours of incubation (background signal from negative control not deducted), with standard deviation from 16 parallels included.

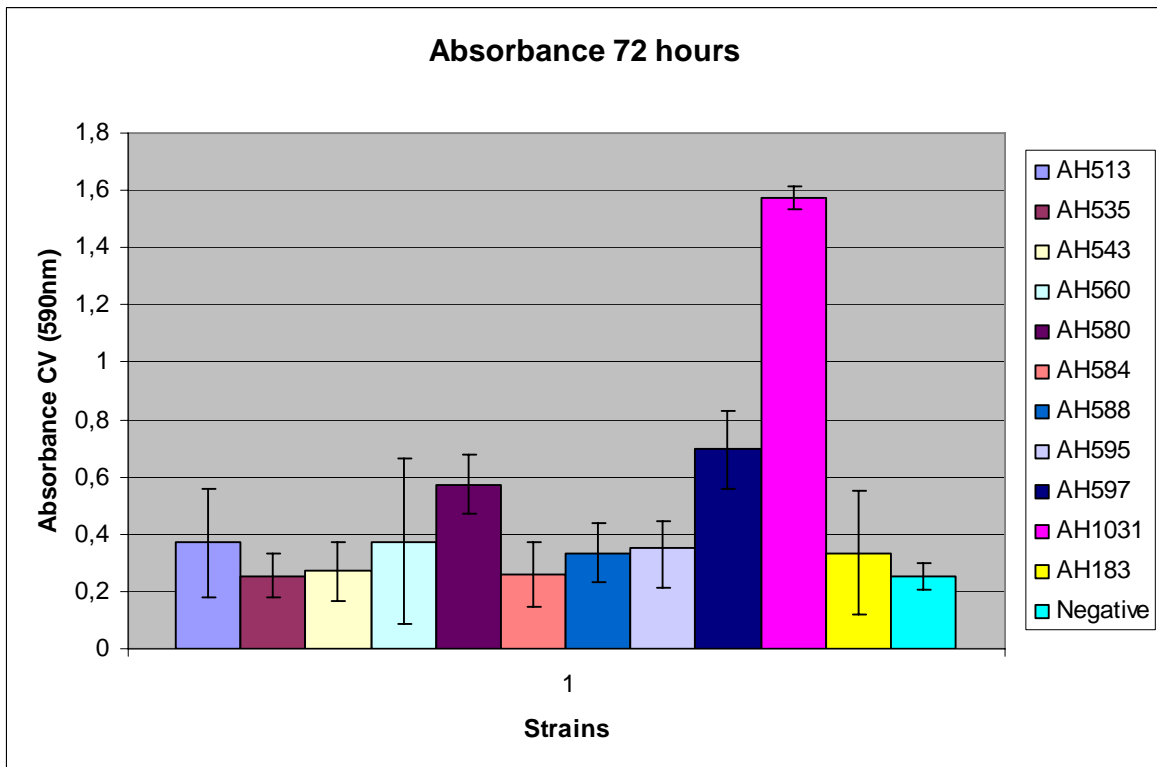


Figure 6.15: Biofilm formation as measured by crystal violet absorbance after 72 hours of incubation (background signal from negative control not deducted), with standard deviation from 16 parallels included.

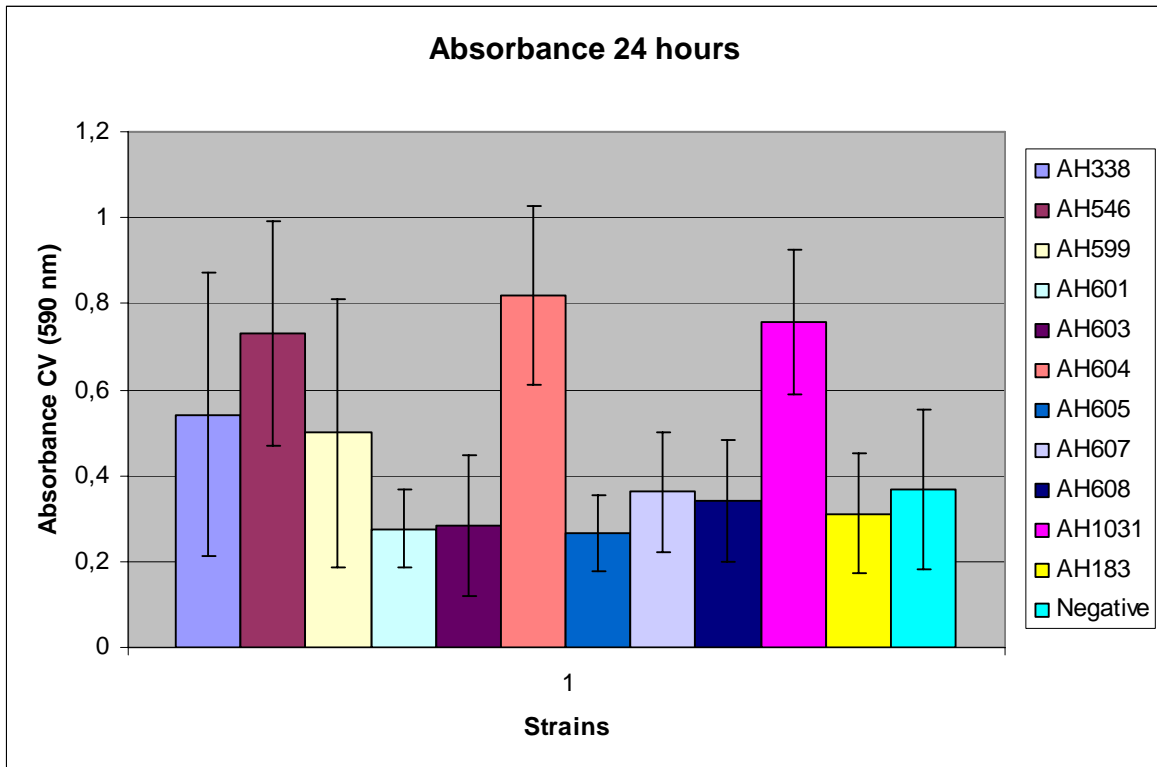


Figure 6.16: Biofilm formation as measured by crystal violet absorbance after 24 hours of incubation (background signal from negative control not deducted), with standard deviation from 16 parallels included.

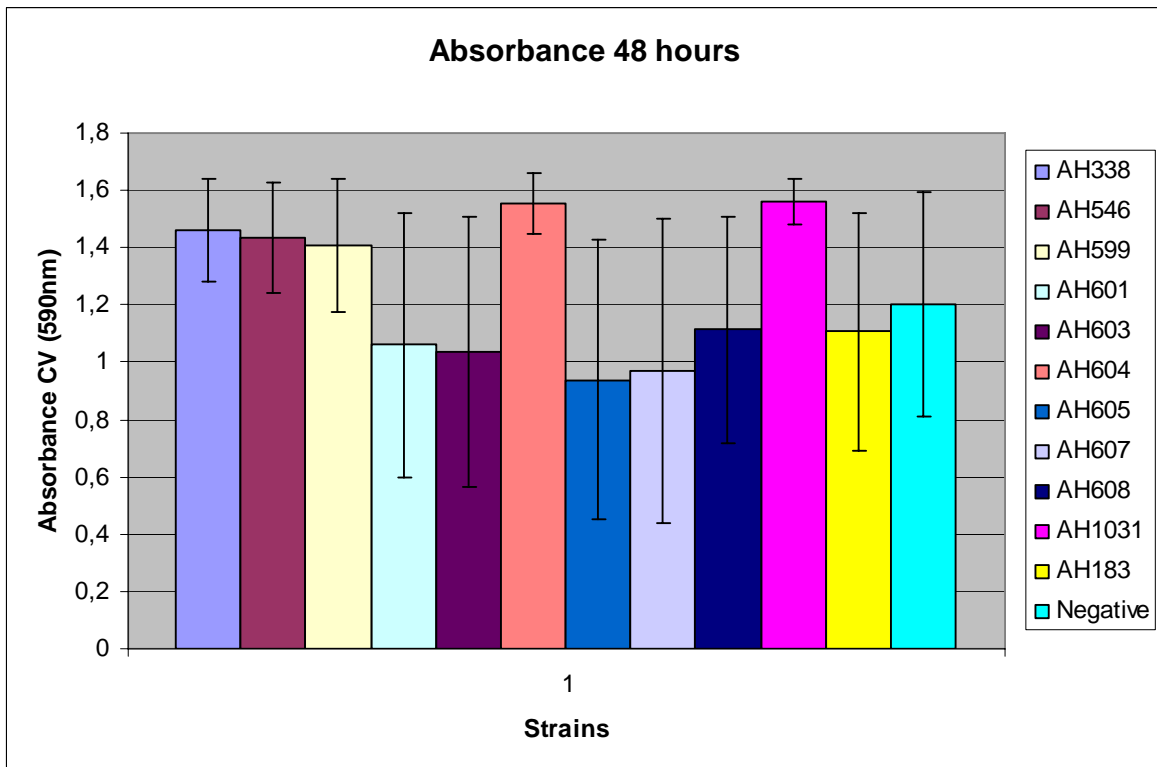


Figure 6.17: Biofilm formation as measured by crystal violet absorbance after 48 hours of incubation (background signal from negative control not deducted), with standard deviation from 16 parallels included.

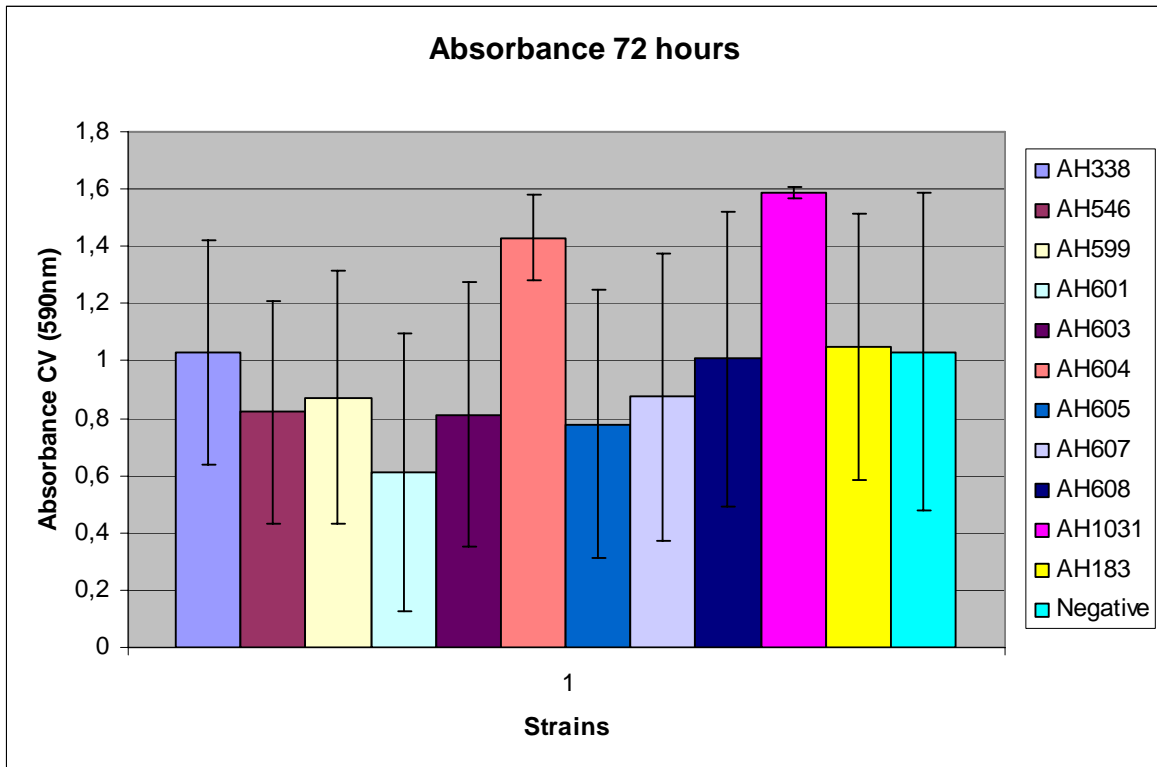


Figure 6.18: Biofilm formation as measured by crystal violet absorbance after 72 hours of incubation (background signal from negative control not deducted), with standard deviation from 16 parallels included.

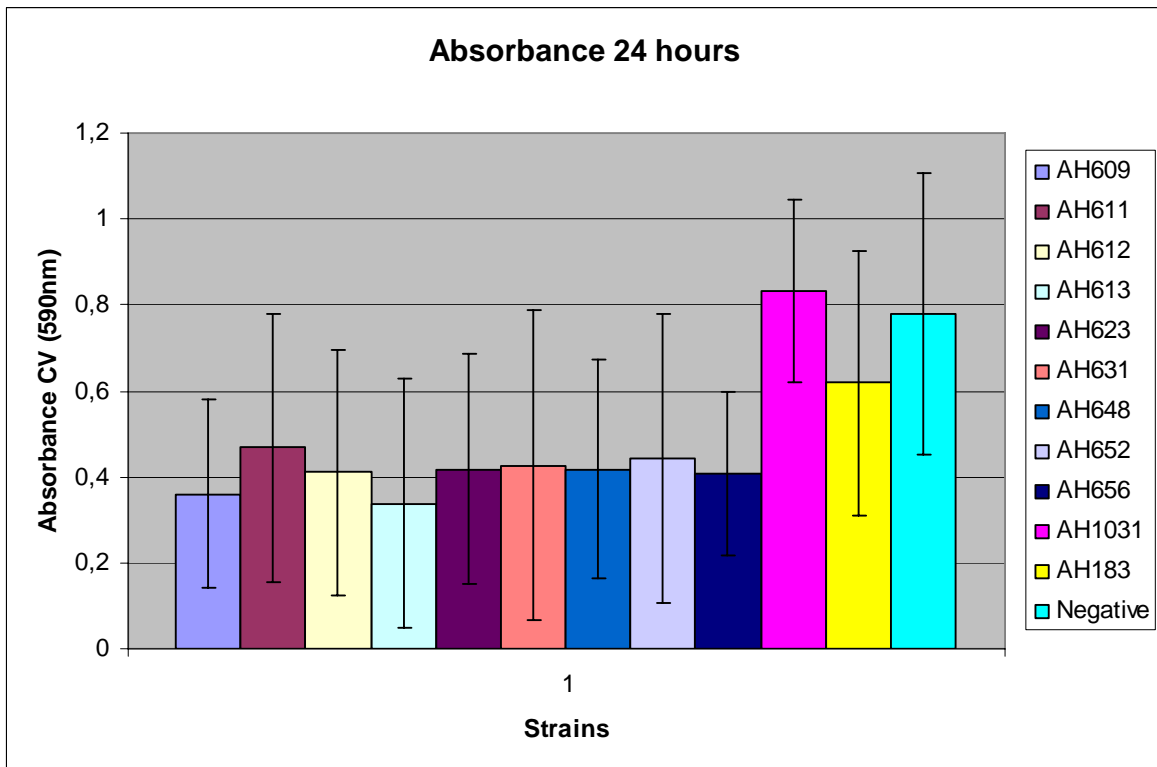


Figure 6.19: Biofilm formation as measured by crystal violet absorbance after 24 hours of incubation (background signal from negative control not deducted), with standard deviation from 16 parallels included.

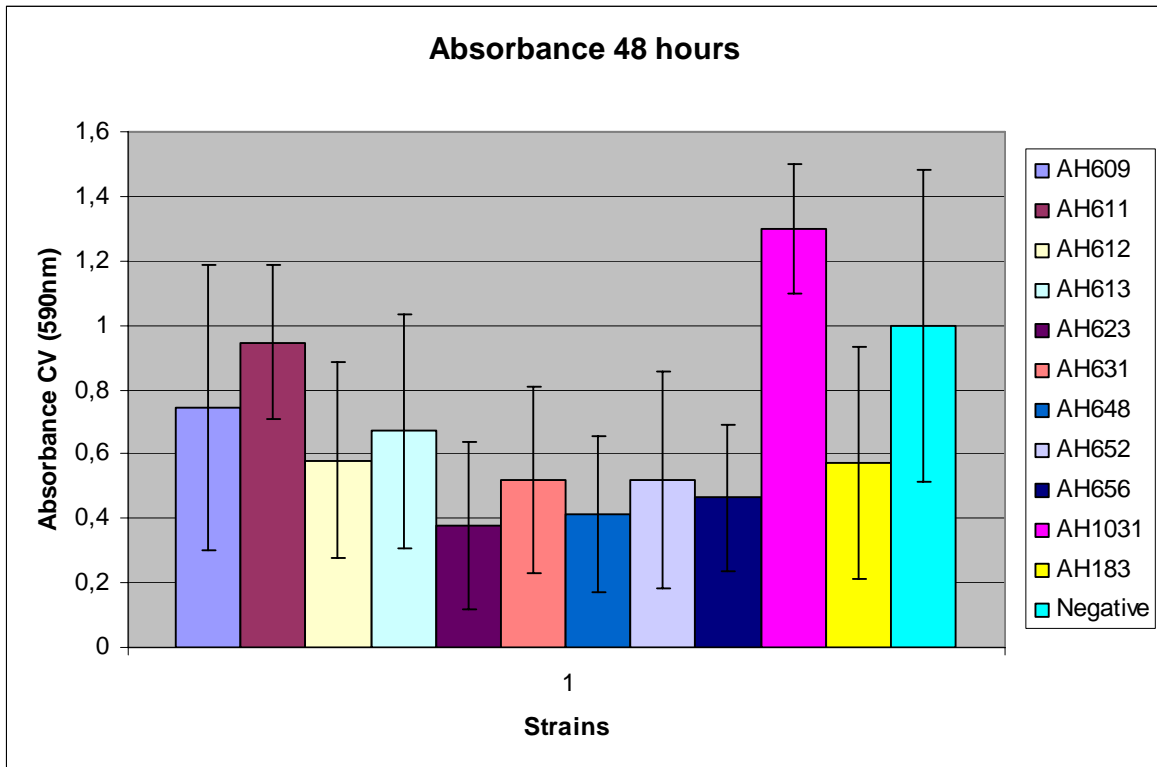


Figure 6.20: Biofilm formation as measured by crystal violet absorbance after 48 hours of incubation (background signal from negative control not deducted), with standard deviation from 16 parallels included.

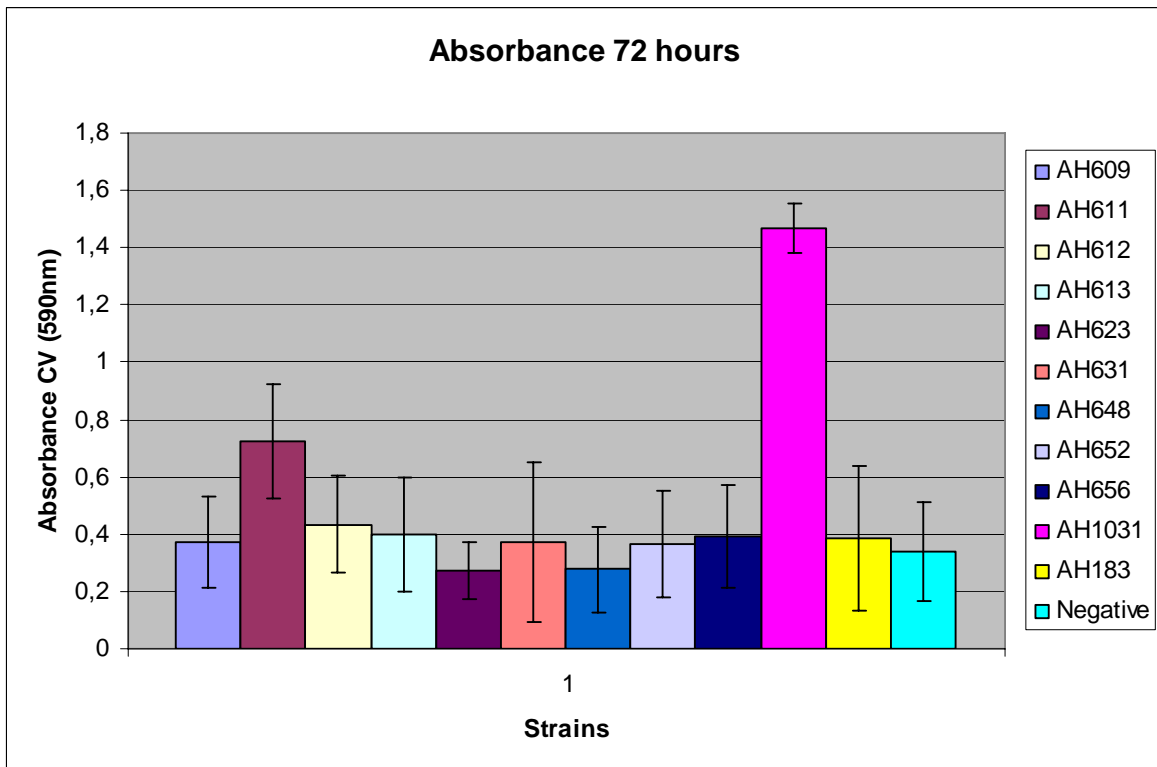


Figure 6.21: Biofilm formation as measured by crystal violet absorbance after 72 hours of incubation (background signal from negative control not deducted), with standard deviation from 16 parallels included.

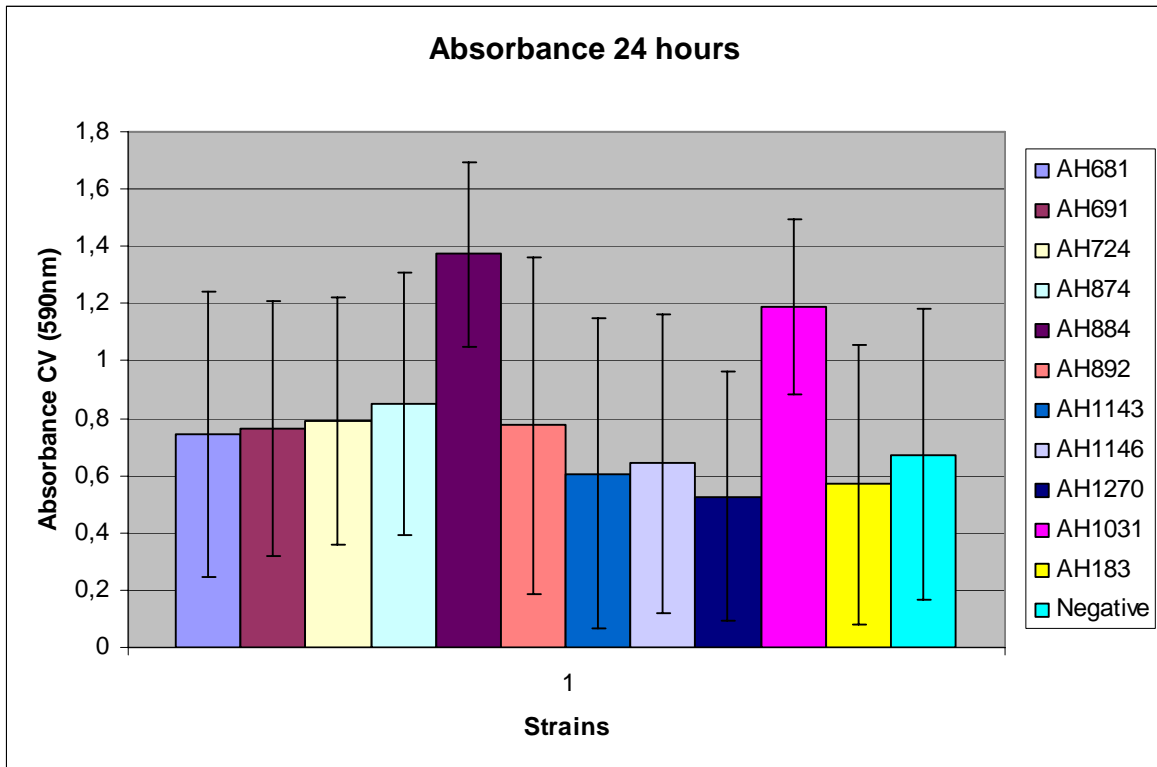


Figure 6.22: Biofilm formation as measured by crystal violet absorbance after 24 hours of incubation (background signal from negative control not deducted), with standard deviation from 16 parallels included.

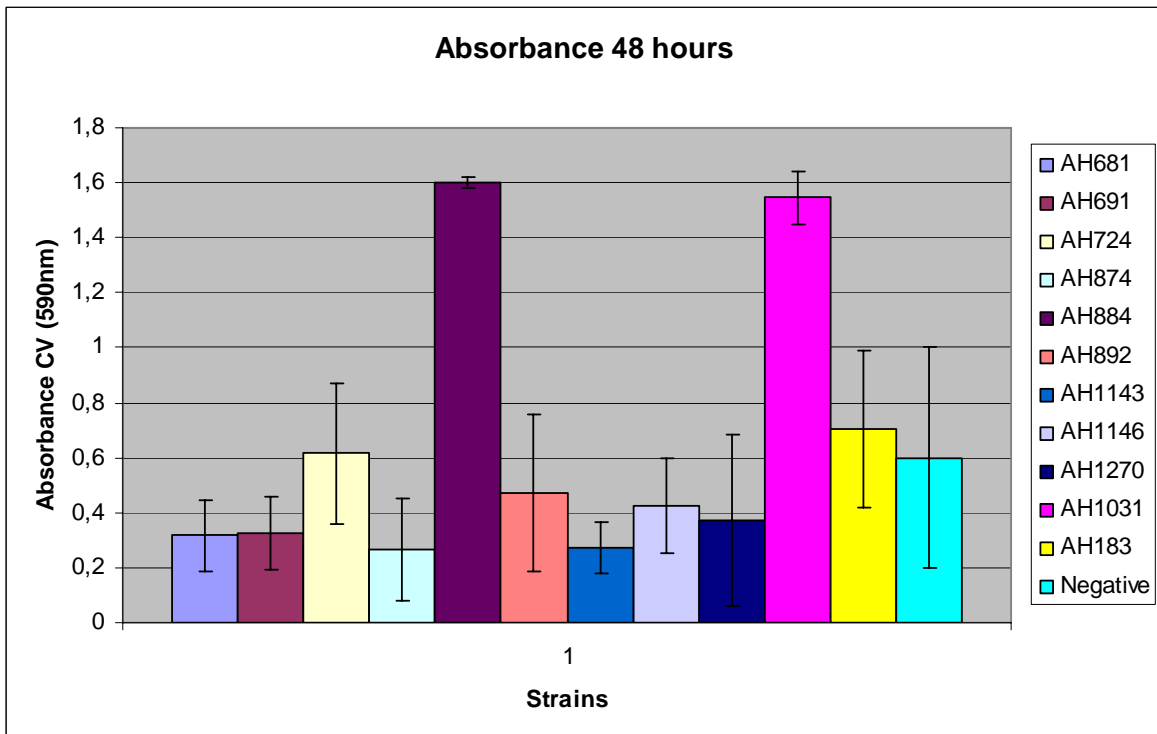


Figure 6.23: Biofilm formation as measured by crystal violet absorbance after 48 hours of incubation (background signal from negative control not deducted), with standard deviation from 16 parallels included.

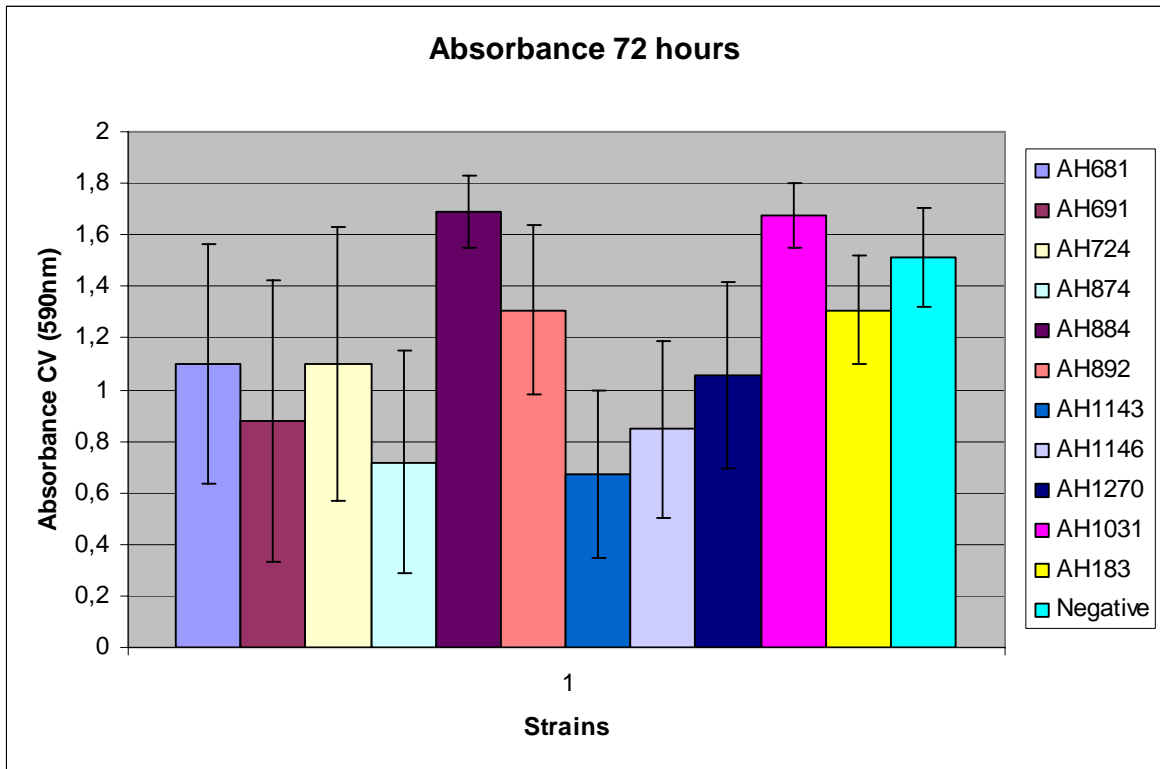


Figure 6.24: Biofilm formation as measured by crystal violet absorbance after 72 hours of incubation (background signal from negative control not deducted), with standard deviation from 16 parallels included.

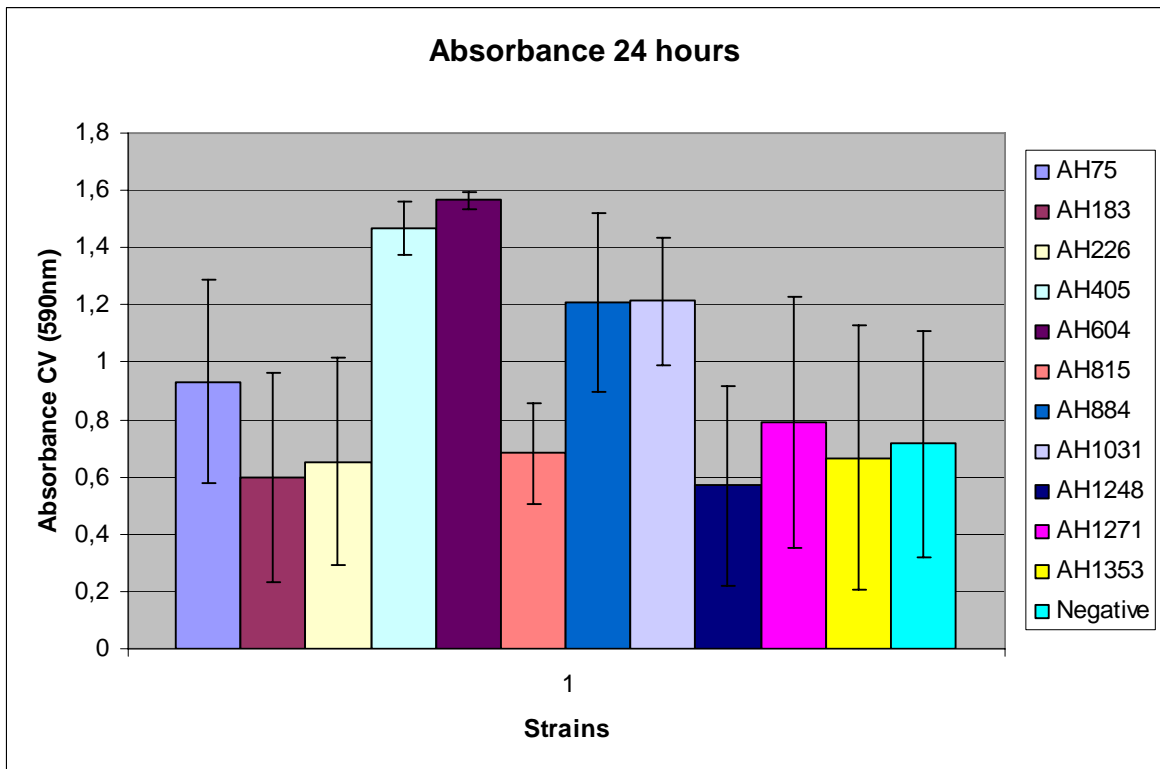


Figure 6.25: Biofilm formation as measured by crystal violet absorbance after 24 hours of incubation (background signal from negative control not deducted), with standard deviation from 16 parallels included.

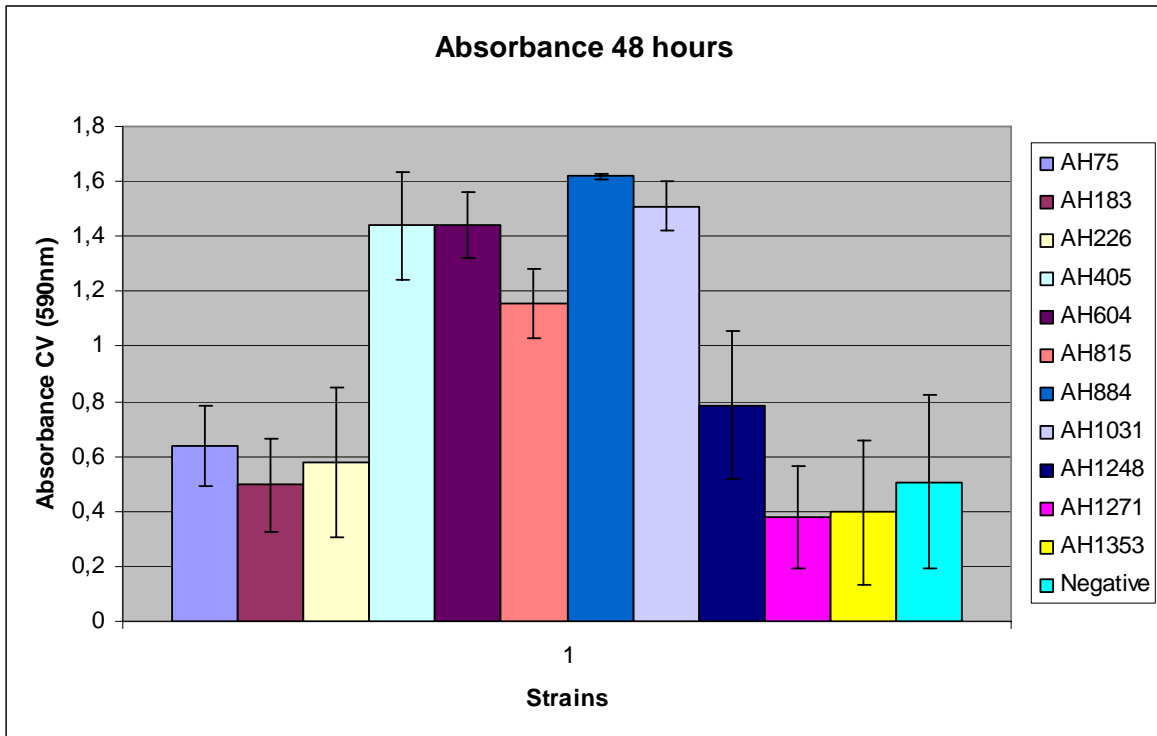


Figure 6.26: Biofilm formation as measured by crystal violet absorbance after 48 hours of incubation (background signal from negative control not deducted), with standard deviation from 16 parallels included.

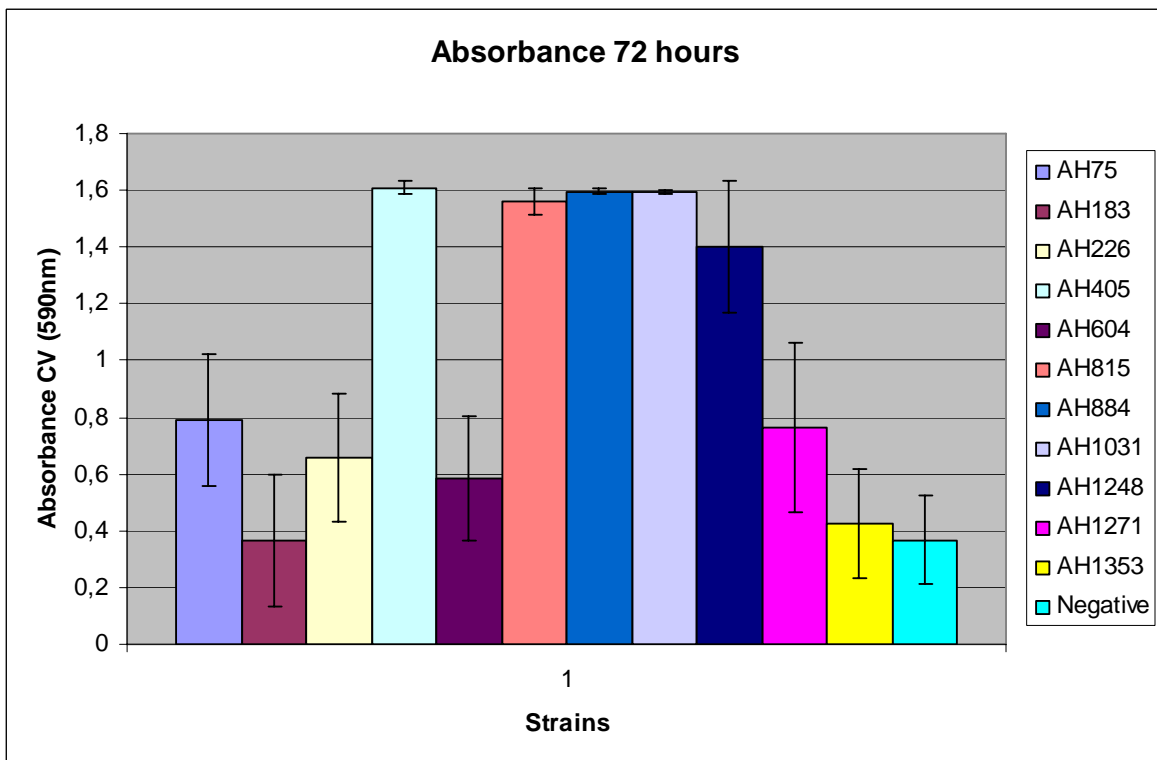


Figure 6.27: Biofilm formation as measured by crystal violet absorbance after 72 hours of incubation (background signal from negative control not deducted), with standard deviation from 16 parallels included.

6.2 Construction of a *plcR* knock-out of *Bacillus cereus* ATCC 10987

6.2.1 pUC19 cloning vector

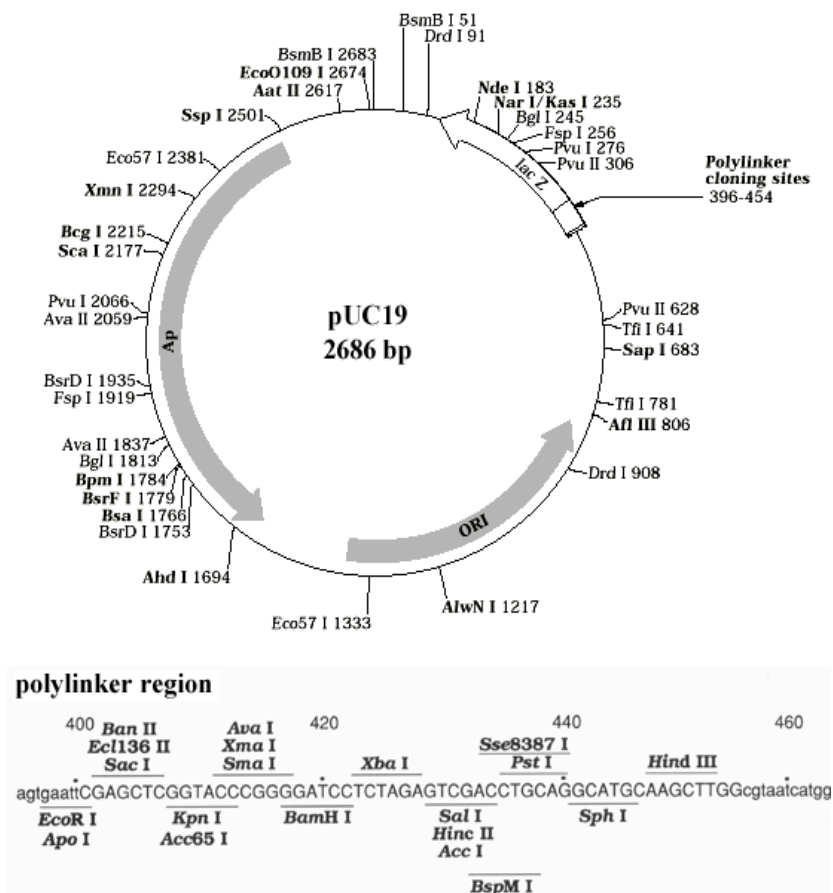


Figure 6.28: pUC19 cloning vector. See also polylinker region depicted underneath, from

www.bio.classes.ucsc.edu.

6.2.2 Sequence of resistance cassettes

GAATAATTATTAATCTGTAGNCAATTGTGAAAGGATGTACTTAAACGCTAACGGTCAGCT
TTATTGAACAGTAATTTAAGTATATGTCCAATCTAGGGTAAGTAAATTGAGTATCAATAT
AAACTTTATATGAACATAATCAACGAGGTGAAATCATGAGCAATTTGATTAACGGAAAAA
TACCAAATCAAGCGATTCAAACATTAATAAATCGTAAAAGATTTATTTGGAAGTTCAATAG
TTGGAGTATATCTATTTGGTTTCAGCAGTAAATGGTGGTTTACGCATTAACAGCGATGTAG
ATGTTCTAGTCGTTCGTGAATCATAGTTTACCTCAATTAACCTCGAAAAAACTAACAGAAA
GACTAATGACTATATCAGGAAAGATTGGAAATACGGATTCTGTTAGACCACTTGAAGTTA
CGGTTATAAATAGGAGTGAAGTTGTCCCTTGGCAATATCCTCCAAAAAGAGAATTTATAT
ACGGTGAGTGGCTCAGGGGTGAATTTGAGAATGGACAAATTCAGGAACCAAGCTATGATC
CTGATTTGGCTATTGTTTTAGCACAAAGCAAGAAAGAATAGTATTTCTCTATTTGGTCTTG
ATTCTTCAAGTATACTTGTCTCCGTACCTTTGACAGATATTCGAAGAGCAATTAAGGATT
CTTTGCCAGAATAATTGAGGGGATAAAAAGGTGATGAGCGTAATGTAATTTTAACCCCTAG
CTCGAATGTGGCAAACAGTGACTACTGGTGAATTAACCTCGAAAAGATGTGCTGCAGAAAT
GGGCTATACCTCTTTTACCTAAAGAGCATGTAACCTTTACTGGATATAGCTAGAAAAAGGCT
ATCGGGGAGAGTGTGATGATAAGTGGGAAGGACTATATCAAAGGTGAAAAGCACTCGTTA
AGTATATGAAAAATTCTATAGAACTTCTCTCAATTAGGCTAATTTTATTGCAATAACAG
GTGCTTACTTTTTAAACTACTGATTTATTGATAAATATTGAACAATTTTGGGAAGAATA
AAGCGTCTCTTGTGAAATTAGAGAACGCTTTATTACTTTAATTTAGGTACC

Figure 6.29: Sequence of spectinomycin-resistance cassette. Sequence starts as read from the M13 forward primer.

GAAGTTATGGAAATAAGACTTAGAAGCAAACCTTAAGAGTGTGTTGATAGTGCAGTATCTT
AAAATTTTGTATAATAGGAATTGAAGTTAAATTAGATGCTAAAAATTTGTAATTAAGAAG
GAGTGATTACATGAAACAAAAATATAAAATATTCTCAAACTTTTTAACGAGTGAAAAAGT
ACTCAACCAAATAATAAAAACAATTGAATTTAAAAGAAACCGATACCGTTTACGAAATTTGG
AACAGGTAAAGGGCATTAAACGACGAAACTGGCTAAAATAAGTAAACAGGTAACGTCTAT
TGAATTAGACAGTCATCTATTCAACTTATCGTCAGAAAAATTAAACTGAATACTCGTGT
CACTTTAATTCACCAAGATATTCTACAGTTTCAATTCCCTAACAAAACAGAGGTATAAAAT
TGTTGGGAGTATTCCTTACCATTAAAGCACACAAAATTATTAAAAAAGTGGTTTTTTGAAAAG
CCATGCGTCTGACATCTATCTGATTGTTGAAGAAGGATTCTACAAGCGTACCTTGGATAT
TCACCGAACACTAGGGTTGCTCTTGCACACTCAAGTCTCGATTACGCAATTTGCTTAAGCT
GCCAGCGGAATGCTTTTCATCCTAAACCAAAGTAAACAGTGTCTTAATAAACTTACCCG
CCATGCCACAGATGTTCCAGATAAATATTGGAAGCTATATACGTAATTTGTTTCAAAATG
GGTCAATCGAGAATATCGTCAACTGTTTACTAAAAATCAGTTTTCATCAAGCAATGAAACA
CGCCAAAGTAAACAATTTAAGTACCGTTACTTATGAGCAAGTATTGTCTATTTTAAATAG
TTATCTATTATTTAACGGGAGGAAATAATTCTATGAGTCGCTTTTGTAAATTTGGAAAGT
TACACGTTACTAAAGGGAATGTAGATAAATATTAGGTATACTACTGACAGCTTCCAAGG
AGCTAAAGAGGTCCCTAGACTCTAGACCCGGGGATCTCTGCAGTCGGGAAGATCTGGTAA
TGACTCTCTAGCTTGGAGCATCAAATAAAACGAAAGGCTCAGTCGAAAAGACTGGGCCTTT
CGTTTTATCTGTTGTTTGTTCGGTAC

Figure 6.30: Sequence of erythromycin-resistance cassette. Sequence starts as read from M13 forward primer.

6.2.3 Sequence of *plcR* knock-out constructs

```
AGCGTCATATAGATTTTACTTCATTTTTTCGACAAAAAATTTGTTATAGTAGGATTAGGTTATCGGTCTAAATCT
GGATAACTTTACCACCTAATAGTTGTGATTACTCCATTTTTATCTACTTTTATAATGAGATCTTGATCATATACTT
TATAGTTTTTTATAAGTTTTGTGCAAGATGAAATTCGGTTTTGATTTTTCTTTATCGGTAGGTTGAAATCTACATTTT
TTCAGTTGTTACTTGCTCTTGTTGAGCCTTAGCCCCAGTTACCTCACCTTTTAAATACTTTTTTGCAATATTTTC
TTTTATATCATTTTTGAGGTTGTGTTAATTTCCAAATTGTTAAGCTAGGCTGAGCAATTTCAACTTTTACTTCATT
TTTCCTAATTCTTGGGTGTGGATAGTTTTTGGCGATAAAGGATAAAAAAGACCGAGTGTAATGGAAATATGGGCA
AGTTTTCTGTAATTTATCTATAATACTCCTAATCTATTATTGGATGTGAGATGAATTCATGAAAAATTTGCCGA
ATTTTATATATATTATGCATTATTTTCATATCAAAAATTGTGCAATTCACATTATTGTAGTGGTATGACAACTCGA
AAAATTAGATTGTTATAGTGGGATGGTGAGTAAGTAGGTACCCGGGGATCCTCTAGAGTCGACCTGCAGGCATGC
AAGCTTGGCGTAATCATGGTCATAGCTGTTTCTGTGTGAAATTTGTTATCCGCTCACAATTCACACACAACATACG
AGCCGGAAGCATAAAGTGTAAGCCTGGGGTGCCTAATGAGTGAGCTAACTCACATTAATTGCGTTGCGCTCACT
GCCGTTTTAGTCGAAACTGTCGTGCAGCTGCATATGATCGCACGCGCRGGGAGAGCGGTTGCGTATTGGGCGC
TCTTCCGCTTCTCGCT
```

Figure 6.31: Sequence of pUC19_*plcR*upstream clone insert. Sequence starts as read from M13forward primer.

```
GGAWGCGTMTATAGATTTTACTTCATTTTTTCGACAAAAAATTTGTTATAGTAGGATTAGGTTATCGGSCTAAAT
CTGGATAACTTTACCACCTAATAGTTGTGATTACTCCATTTTTATCTACTTTTATAATGAGATCTTGATCATATAC
TTTATAGTTTTTTATAAGTTTTGTGCAAGATGAAATTCGGTTTTGATTTTTCTTTATCGGTAGGTTGAAATCTACAT
TTTTTCAGTTGTTACTTGCTCTTGKTGAGCCTTAGCCCCAGTTACCTCACCTTTTAAATACTTTTTTGCAATATTT
TCTTTTATATCATTTTTGAGGKTGTGTTAATTTCCAAATTGTTAAGCTAGGCTGAGCAATTTCAACTTTTACTTCA
TTTTTCCTAATTCTTGGGTGTGGATAGTTTTTGGCGATAAAGGATAAAAAAGACCGAGTGKAAATGGAAATATGGG
CAAGTTTTCTGTAATTTATCTATAATACTCCTAATCTATTATTGGATGTGAGATGAATTCATGAAAAATTTGCC
GAATTTTATATATATTATGCATTATTTTCATATCAAAAATTGTGCAATTCACATTATTGTAGTGGTATGACAACTC
GAAAAATTAGATTGTTATAGTGGGATGGTGAGTAAGTAGGTACCCGGGATYCGCMAATATGCMATAATTGSMTAAG
ATACGGATGGRTTTTTCMTGATATATTTAAAGAAAAAAAATGCGGGTGATGGAATATGAAAAAACTACTTATTGG
TAGTCTGTTAACGTTAGCAATGGCAKGGGGTATTTTATTAGGAGATACAGCTTTAGAGAAAAACCAAGTAATTTTC
TCATAATGATCAAGAAGTACAATTAGCTTTCAGATGTACCTTTTGAATATTAAAAAAAACAACCGTCTTACTTAGAC
GGTTGTTTTTTGTGGAGTAACCTCCAAACGCTTTTACTARAACGGGCTTACTAATAAAAGAAATCCTTGAATGTGGT
CACAGTTTTGCTCATATAAACTTCCATTGTCTTTCGTTTTCTACMCTTCTGCGATACTTCTAAATTAGTTCTTTGA
TAGTGTAAATATGAAGAAAWATCGCTTCTCTAAAGACTAGTGTATCGCAAATAATCTCGAGCATTTTTATGATATGA
TATTTGTAATAGCTAAGACTATACAGTCAAGTCATCATGAAATGATACGRATTGAGCTGTYAGTTTGCACCTACG
ATGATTTGGTAATGCCRTCGACTGCAGGCATGCAGCTTGTATCWGGCWAGCKTTCCTGKTGATGATCGCTCATC
CACACATCGACGGACTAGGTATCTGGGGTCTAAGTGACTATCCATATTGCGTGCTATGACCTTCCACATGGCACC
GTGCTGTCACKGACTA
```

Figure 6.32: Sequence of pUC19_*plcR*upstream_*plcR*downstream clone insert. Sequence starts as read from M13forward primer.

```
TAGAGTCGACCTGCAGGCATGCAAGCTTCTATATCAGCAAGTTGTTTGTGCGCAGTTTTAGTTGGAGTTGAAAT
AATAGTATTAACGGCTGTTTTCTGTTTTTGGGGTAGGACTTGTTTTTTGTACAGGCGGCTCATTAGGATCTACAAT
ATGAGTAAATGAAACAGTACCTTGGTTTTCACTAAACCATGTGGTGGAACACTAATAACTTGAACCTGAAAAAGA
TATAGTTGCTGCTTCAGTAGGATCCAATGTGCCTACTGTTATACCTGTGGAAGGGTTGTATTTGGCTGTGAAAT
CCCGTTAATAGTCACGCTATTTGGAATGAAAGTAGTTCCATTTGGAATAGGGTCTGTCAGGACGATATTAGTAGC
AGGAACAGTTCGGTTATTTTGTAAACTAATGGTATACTATGGAGATCTGTATAATAAAAGAAATAATTATTAATCTG
TAGACAAATTGTGAAAGGATGTACTTAAACGCTAACGGTCAGCTTTATTGAAACAGTAATTTAAGTATATKTCCAA
TCTAGGGTAAGTAAATTGAGTATCAATATAAACTTTATATGAACATAATCAACGAGGTGAAATCATGAGCAATTT
GATTAACGGAAAAATACCAAATCAAGCGATTCAAACATTAATAATCGTAAAAAGATTTATTTGGAAGTTCAATAGT
TGGAGTATATCTATTTGGTTCAGCAGTAAATGGTGGTTTACGCATTAACAGCGATGTAGATGTTCTAGTCGTCGT
GAATCATAGTTTACCTCAATTAACCTGAAAAAACTAACAGAAAGACTAATGACTATATCAGGAAAGATTGGAAA
TACGGATTCTGTTAGACCACTTGAAGTTACGGTTATAAATAGGAGTGAAGTTGTCCCTTGGCAATATCCTCCAAA
AAGAGAATTTATATACGGTGAGTGGCTCAGGGGTGAATTTGAGAATGGACAAATTCACGAACCAAGCTATGATCC
TGATTTGGCTATTGTTTTAGCACAAAGCAAGAAAGAATAGTATTTCTCTATTTGGTCTGATCTTCAAGTATACT
TGTCTCCGTACCTTTGACAGATATTCGAAGAGCAATTAAGKATTCTTTTGGCAGAACTAATTGAGGGGATAAAGG
```

TGATGAGCGTAATGTAATTTTAACCCTAGCTCGAATGTGGCAAACAGTGACTACTGGTGAAATTACCTCGAAAGA
TGTCGCTGCAGAATGGGCTATACCTCTTTTACCTAAAGAGCATGTAACCTTACTGGATATAGCTAGAAAAGGCTA
TCGGGGAGAGTGTGATGATAAGTGGGAAGGACTATATTCAAAAGGTGAAAGCACTCGTTAAGTATATGAAAAATTC
TATAGAAACTTCTCTCAATTAGGCTAATTTTATTGCAATAACAGGTGCTTACTTTTAAAACTACTGATTTATTGA
TAAATATTGAACAATTTTGGAGAAAAGAATAAAGCGTCCTCTTGTGAAATTAGAGAACGCTTTATTACTTTAATT
TAGTAATGATGTCACCAATATTCACAATTTGCTGGTTTGCACCTTTTCGTTGGATTAATAATAGTAGCATTAAATTT
GTGTTTCAACTAAATTACTTGTAGAGTTTCGATTAATTGGTGGTTGATT

Figure 6.33: Sequence of pUC19_plcRupstream_plcRdownstream_spectinomycin clone insert. Sequence starts as read from M13forward primer.